Spring 2016

ELECTROCHEMICAL CHARACTERIZATION OF XANTHATE CHEMISORPTION ON COPPER AND ENARGITE

Tyler Broden
Montana Tech of the University of Montana

ELECTROCHEMICAL CHARACTERIZATION OF XANTHATE CHEMISORPTION ON COPPER AND ENARGITE

by

Tyler Broden

A thesis submitted in partial fulfillment of the requirements for the degree of

Master of Science in Metallurgical/Mineral Processing Engineering

Montana Tech

2016

Abstract

The electrochemical reactions of copper and enargite (Cu_3AsS_4) were studied in the absence and presence of xanthate by cyclic voltammetry (C.V.) using electrodes fashioned from pure copper wire obtained from the Metallurgical and Materials Engineering Department, and an enargite mineral sample obtained from the Orphan Girl mine in Butte, MT. Voltammograms were produced in buffer solutions of pH values ranging from 7-12. Electrochemical reactions were discerned by comparing E_H-pH diagrams calculated from thermodynamics using StabCal, a computer program developed by Dr. Huang at Montana Tech. The chemisorption of xanthate on the surface of copper was observed but not on enargite. On the other hand, surface precipitation of copper xanthate was observed on both surfaces.

Keywords: cyclic voltammetry, E_H, pH, enargite, arsenic

Dedication

I would like to thank my family for all their love and support. Without their constant support I could not have gone this far with my education. My mother, father, grandmas and grandpas, sister and brother have been my rocks, my support group. They have always been so proud of me and my accomplishments that I could never let them down, so I kept going with my school work and I thank you for the drive you have given me. I love you.

I dedicate this thesis to my grandfather, Bill Kempa, who passed away on December 29th, 2012. I had hoped that he would at least have seen me graduate and go on to my first fulltime job. He was one of the greatest men I ever knew.

Acknowledgements

First of all I would like to thank Dr. Courtney Young. Six years ago he showed my family and I around the labs of Montana Tech's Metallurgical and Materials Engineering Department and inspired me to attend school here. Without his support and guidance I would not have become a Master's student. His constant input and advice allowed me to go forward with my research and get through the stumbling blocks that I ran into.

To Nick Gow, I would like to personally say "Thank you", for taking me under his wing as a fellow graduate student, and educating me in the theory of cyclic voltammetry. His previous research in this field, along with his study of the mineral enargite allowed me to not start from scratch, but delve right into research.

To Dr.'s, Downey, Gleason and James, I would like to express my sincere gratitude for assisting with data interpretation, helping me prepare for my defense, being on my committee, and editing my thesis.

To Dr. Huang, I thank you so very much for assisting me with StabCal. Without your tireless efforts and constant support, I do not believe I would have been able to finish my data interpretation or my thesis on time. Thank you.

To the Metallurgy staff, including Dr.'s Meier, Sudhakar, Twidwell, and Griffiths, and Karen Holland, I would like to express my appreciation for my education and the opportunity to be a metallurgist. Your input and classes have given me the tools I need to succeed in the field and in life, and I thank you.

Table of Contents

List of Tables

List of Figures

List of Equations

Glossary of Terms

Term	Definition
Arsenic	Element #33 which is of environmental and toxicological concern.
Collector	Heterpolar molecule that adsorbs from solution to the solid surface causing it to become hydrophobic
Copper	Element #29 which exists naturally as a native metal as well as simple to complex oxides, hydroxides, carbonates silicates and sulfides. It has marketable value, and is used primarily for electrical conductivity.
Cyclic Voltammetry	Measure of the current caused by applying a potential or voltage to induce Redox reactions of an electrode under controlled conditions.
E_H	Measure of potential in volts for a chemical species to undergo reduction by attaining electrons or undergo oxidation by reducing electrons.
Enargite	A copper arsenic sulfide with composition Cu_3AsS_4.
Flotation	Separation of valuable minerals from gangue due to differences in hydrophobicity and accomplished via the introduction of air bubbles into a slurry.
Hydrophobicity	Surface state that does not allow water to orient at; can be naturally occurring but is often induced with collectors
Modifier	A reagent that aids collector interaction with a surface (activator) or prevents it (depressant); pH modifiers are most common because they can activate one surface and depress another
Penalty Element	Any element present as itself or in a compound that is detrimental to the environment. The presence of this element will result in a fine from the smelter if present above a set level.
pH	Measure of the logarithmic activity of the hydrogen ion in solution.
Redox	Reduction-Oxidation.
SHE	Standard Hydrogen Electrode; a reference scale in which hydrogen gas evolution from hydrogen ions in solutions is set at 0 volts under STP conditions.
STP	Standard Temperature (25°C) and Pressure (1atm).

Xanthate	A collector with a reactive carbon-disulfide headgroup connected to an oxygen atom and an inert organic tail. Varying in adsorption length, normally ranging from methyl to hexyl

1. Literature Review

Enargite (Cu_3AsS_4) is an arsenic-bearing mineral of possible economic worth due to the presence of copper in its structure. Because it also contains arsenic, it is toxic and therefore can be a threat to the environment. Thus, the removal of enargite from an operation may be worth significant economic as well as toxicological value, assuming it is present in large amounts.

Enargite is one of the more common sulfides encountered in gold and copper deposits. The presence of arsenic in mineral concentrates reduces the value of the concentrate by presenting environmental hazards as well as noxious hazards that must be handled at a smelter. Concentrates that contain less than 0.2% by mass of arsenic can be sent to a smelter without penalty (Greenfacts, 2011); however, pure enargite is 19% by weight arsenic and is heavily penalized or diluted for processing. Tailings can be disposed of to the environment, but preference is to remove it completely because it oxidizes readily to form soluble arsenite and arsenate (Fornasiero, Fullston, Li & Ralston, 2001). Exposure of tailings and ores/deposits in mining operations to water makes enargite removal important. Otherwise, waste waters, particularly acid rock drainage, will result, requiring treatment before they can be discharged.

Lethal doses of acute arsenic exposure are usually greater than 99 milligrams in the average adult. Prolonged exposure to arsenic may produce chronic effects such as lung cancer, skin cancer, liver cancer, or even pigmentation damage to the skin (Greenfacts, 2011). Due to the damage caused by low levels of exposure, arsenic is a hazard in mining operations and the surrounding environment, if released.

Due to the harmful environmental and toxicological characteristics of arsenic, it is usually undesired in refinery and smelter concentrate. The removal of arsenic-bearing minerals by flotation has the potential to be extremely beneficial. The flotation parameters such as E_H/pulp

potential, pH, feed rate, and reagent usage may all affect the overall efficiency of the separation. To maximize the efficiency of separation, knowing the ideal parameters is vital.

An E_H – pH diagram, like the one seen in **Figure 1**, shows the possible transitions that may occur for arsenic. The diagram shows the possible redox reactions that may occur. For example, at pH 13 and an E_H value of -0.5 Volts, arsenate (AsO_4^{3-}) is shown to be a stable species. Its formation from arsenic metal is shown below:

Equation 1:

$$As + 4H_2O = AsO_4^{3-} + 8H^+ + 5e^-$$

Equation 1: Arsenic Oxidation

However, the information from an E_H – pH diagram may not be enough to fully predict how a system will function in an operation because these diagrams are calculated from thermodynamics, which assumes equilibrium that may not be attained in the short time frames in flotation. In this regard, it is important to realize that the kinetics of flotation are critical but diagrams like this, nevertheless, help with redox understanding. Thus, particular species and conditions may not be obtained in the process.

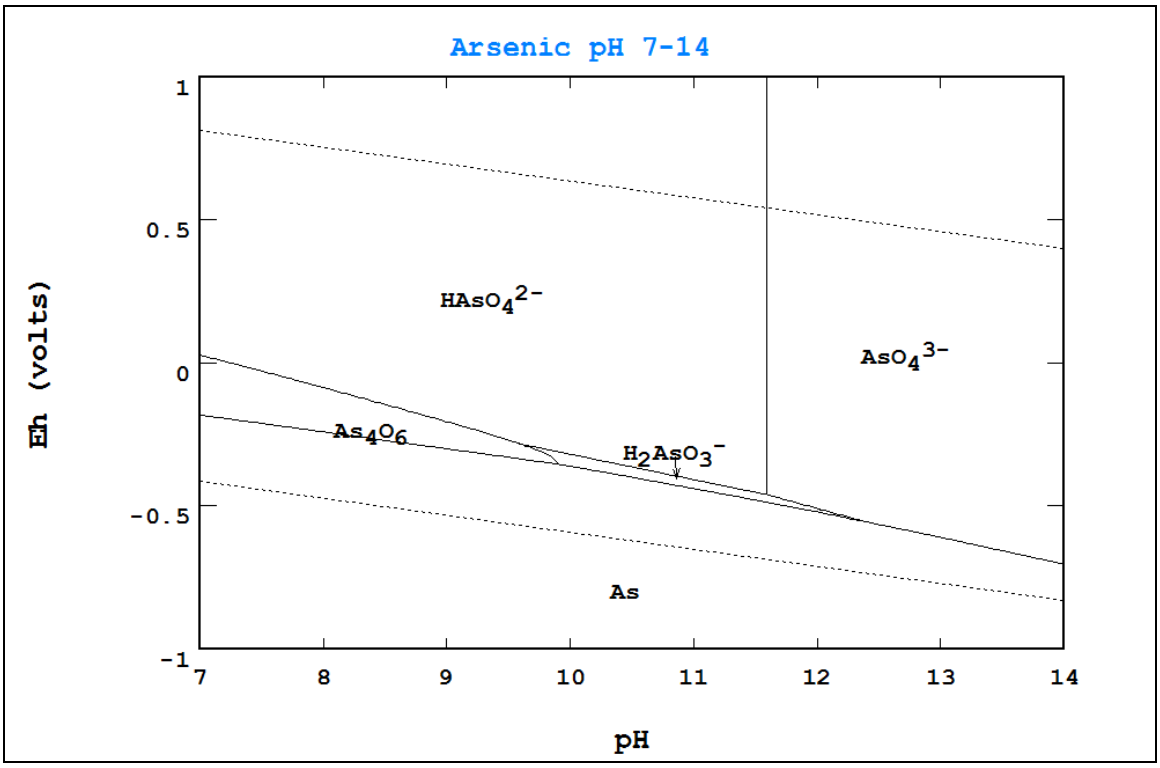

Figure 1: E_H-pH Diagram of 1M Arsenic Water System.

1.1. Flotation

Froth flotation is the most widely used in mining particle and ion separation technique. Its success is based on hydrophobicity and is affected by numerous parameters, including, but not limited to: hydrophobicity, particle size, mineralogy, % solids, density, pH and concentration of reagents such as collectors and pH modifiers. By making the particles hydrophobic, air bubbles will adhere to and carry the particles into froth, leaving behind the hydrophilic particles. In direct flotation, valuable metals report to the froth, are recovered as a concentrate, and can be either processed further to increase the purity or dried to yield final product. Oppositely, the gangue minerals, being hydrophilic, remain in the flotation cell and eventually report to the tails. They may be further treated, recirculated in the system, or disposed of according to grade, depending on the process. By comparison, in reverse flotation, the gangue minerals are rendered

hydrophobic and the valuable minerals remain hydrophilic. In either case, the presence of penalty elements such as arsenic will have to be monitored in both the con and the tails.

Figure 2 shows the components of a typical continuous flotation lab cell. The stationary standpipe allows air to be drawn or forced down its length and into the slurry. It also contains the shaft which turns and rotates the impeller to agitate the slurry and break the air stream into bubbles. The air inlet valve controls the air flow to the slurry. Bubbles, thus generated, rise through the slurry and collide with particles, attaching to those that are hydrophobic, eventually forming froth at the surface of the slurry. Hydrophilic particles can short circuit into the froth in which case wash water may be added to push them back into the slurry.

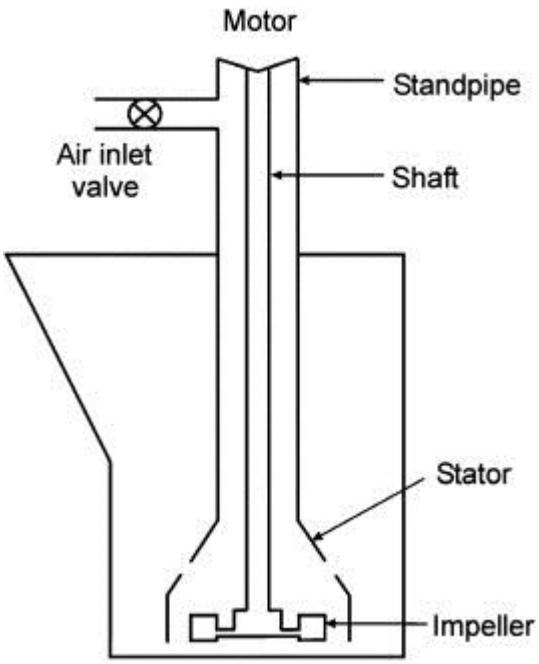

Figure 2: Lab Flotation Cell (Koh & Schwarz, 2007)

Several minerals like talc and elemental sulfur are naturally hydrophobic. However, most minerals require hydrophobicity to be induced. Induced hydrophobicity is accomplished by coating their surface with oil. Nearly 150 years ago, this was done for sulfide minerals using

bulk-oil flotation. In this case, hydrophobic or oolophilic sulfide minerals would preferentially wet by oil and thereby transfer to the oil phase. Today, reagents called collectors serve this purpose, essentially forming a "layer of oil" upon adsorption. Collectors are heteropolar molecules, having a reactive inorganic polar head group and an inert organic non-polar tail. To work, the head group must adsorb chemically or physically to the mineral surface, or precipitate out on the surface. These processes cause the organic tail to protrude from the surface into the solution. If enough collector molecules interact in this manner, the protruding tails acts like an oil coating and therefore induces hydrophobicity. If adsorption occurs because of a physical bond, it is referred to as physisorption. If it is a chemical bond, it is called chemisorption. If the surface solubilizes even slightly, it may react with the collector and surface to precipitate out. To be effective, collectors must be selective for the mineral to adsorb or precipitate out. Furthermore, collectors should interact only at the solid/liquid interface.

In the case of arsenic sulfides and sulfide minerals in general, xanthate is the most effective collector used to make them hydrophobic. It was the first collector invented (Cytec, 2010), and possesses carbon disulfide as its head group and ranges from methyl to hexyl for the organic tail. The two are connected through an oxygen-epoxide link. Because the head group is anionic, potassium or sodium are present as cations to balance the charge. If precious metals are associated with resulting concentrates, further treatment such as fine grinding and flotation may be used to prepare them for pyrometallurgical smelting or hydrometallurgical leaching. If precious metals are absent, or they are present in economically insufficient amounts, the material will be considered gangue and disposed of properly as tailings.

A flotation system has three components: chemicals, operation, and equipment. Aside from collectors, chemical components consist of frothers, activators, depressants, and pH modifiers.

The operational components consist of feed rate, mineralogy, particle size, particle density, % solids, and temperature. The equipment components consist of cell design, agitation, air flow in forms such as N_2, CH_4, O_2-enriched etc., cell bank configuration, and cell bank control.

Frothers are also heteropolar chemicals but in this case, preferentially adsorb at the liquid/air interface. They are used to stabilize the froth and accomplish this by lowering the surface tension of the water. Although a frother increases the wettability and therefore decreases the degree of hydrophobicity of particles, its impact is minimal unless the frother is also active at the solid/liquid interface and/or used in excessive concentrations. Frothers are usually of low-molecular weight and are either alcohols or short chain polymers of oxygen bonded to hydrocarbons. The froth does not get pulled into the agitated slurry and is therefore stable, at least long enough, to report to the launder where it can then break (Cytec, 2010).

1.2. Elemental Molecular Characteristics

1.2.1. Arsenic

Arsenic is a crystalline solid but is not stable naturally. It is predominantly found substituted for metals in sulfide minerals. Examples include realgar (AsS), Orpiment (As_2S_3), arsenopyrite ($FeAsS_2$), tennantite ($Cu_{12}As_4S_{13}$), and enargite (Cu_3AsS_4). It also exists as oxides like arsenolite (As_2O_3) and even a metal-like state such as domeykite (Cu_3As). Arsenic bearing minerals emit arsenic trioxide gas of when heated in excess air, as shown in **Equation 2** (Lenntech, 2011)**.**

$$As_2S_{3(g)} + 9/2O_{2(g)} = AsO_{3(g)} + 3SO_{2(g)}$$

Equation 2: Arsenic Trioxide Formation

Because arsenic is highly volatile as an oxide, this reaction predominates in smelting processes (Mihajlovic, Strbac, Zivkovic, Kovacevic, & Stehernik, 2007).When off gases cool, the As_2O_3 condenses and must be captured, typically by electrostatic precipitators or in a baghouse. Arsenic exposure may result in the death of plant and animal life, reduce the ability of plants to photosynthesize, and diminish the ability of animals to reproduce. The amount and duration of arsenic exposure determines the effects observed due to its presence (Greenfacts, 2011).

The presence of arsenic in a copper concentrate generates penalty costs for a mine site if the ore is sent to a smelter (Haga, et. al, 2012). Arsenic is also one of the most common of the toxic impurities found in copper concentrates, and the smelter has to treat the ore to prevent any toxicological problems on site, and prevent any possible exposure of arsenic to the environment, whether in solid, liquid or gas form.

Arsenic-bearing sulfide minerals are readily floatable with xanthate due to the presence of metals like copper in their structures (Castro, et. al, 2003). However, arsenic-only sulfides such as realgar (AsS) can also be floated using xanthate. Castro et. al. (2003) determined that dixanthogen and arsenic (III) xanthate formed on the mineral surface to induce hydrophobicity and thereby allow for their successful flotation.

Due to the hydrophobic tendency of arsenic minerals, selective flotation can be enhanced by the pre-oxidation of slurries using oxidizing agents (Ma & Bruckard, 2009). The process causes sulfide oxidation to elemental sulfur which is naturally hydrophobic and made more hydrophobic with xanthate. It also renders non-arsenic bearing minerals hydrophilic by forming oxide and hydroxide layers on their surfaces preventing xanthate interaction. Hydrophobicity is

accomplished by controlling the pH and oxidation of the slurry. It has therefore been recognized that E_H and pH diagrams can be used to improve flotation.

1.2.2. Copper

Copper is a metal used in many processes due to its electrical conductivity and its ability to alloy with other metals. It can readily form an oxide above pH 4 and, the higher the pH, the lower the potential, as seen in **Figure 3**.

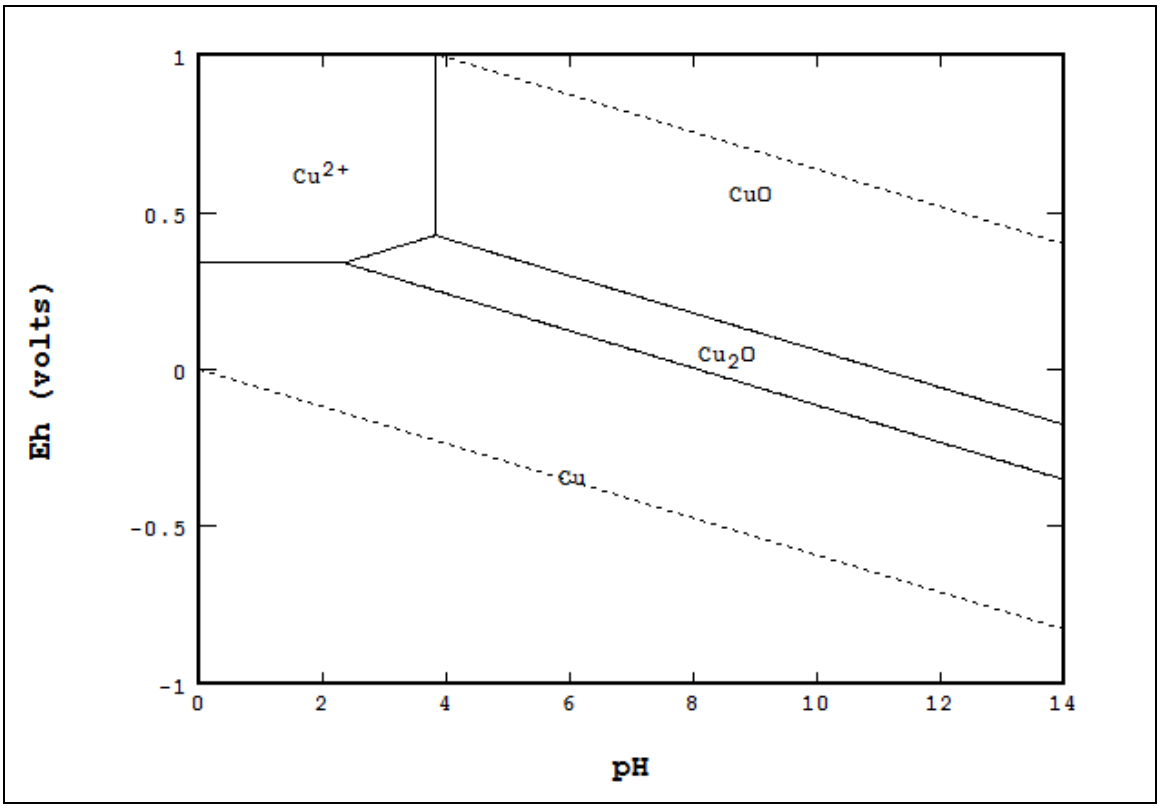

Figure 3: E_H-pH Diagram of Copper-Water System. 1M Cu Concentration.

Many copper sulfides are associated with arsenic because they often form together or are close to one another geologically (Haga, et. Al, 2012). The presence of arsenic with copper decreases the economic worth of the copper because of the environmental and toxicological hazards, due to the costs needed to manage associated health and safety issues.

One copper mineral that presents such problems is enargite (Cu_3AsS_4). It is essentially equivalent to covellite (CuS) with arsenic substituting for every fourth copper. Copper is associated with sulfur and arsenic atoms in the enargite structure (Velasquez, et al., 2000). It normally is collected with copper flotation concentrates as a nuisance mineral, typically with chalcopyrite ($CuFeS_2$) and bornite (Cu_5FeS_6) as the main minerals. However, it can be processed to form its own concentrate as well. Enargite flotation is possible due to the use of xanthate collectors, which appear to work best by targeting exposed copper atoms at the surfaces. The flotation of enargite results in a high arsenic concentration that require subsequent extractive processing to lower arsenic amounts thereby yielding a pure copper sulfide product. As long as arsenic can be treated, the flotation of enargite can be a process of significant economic worth.

1.2.3. Sulfur

When exposed to water, sulfur will oxidize due to its chemical affinity for oxygen. Such oxidation leads to the formation of sulf-oxy compounds such as sulfate (SO_4^{2-}), but can be very slow due to sulfur's natural hydrdophobicity.

Oxidation is a problem in some respects because an oxidized surface may not allow for flotation if an oxide/hydroxide coating results; the oxide coating will not allow xanthate to attach to the surface. However, it is also possible for enargite and other sulfide minerals to oxidize to elemental sulfur and thereby develop hydrophobicity, in which case xanthate may not be needed.

Another problem with sulfide minerals is that, in the presence of air and water, there is a high probability that the minerals will oxidize in the long term and result in acid rock drainage (A.R.D.) and toxic-metal release. It is a naturally occurring process and typically yields water under pH 5. Sulfide as pyrite is one of the main causes of A.R.D. (Skousen, 2011). A.R.D is

common in coal mining, but is also associated with metal mining. Thus, the removal of sulfide minerals, particularly pyrite from an operation can also be of great environmental importance.

1.2.4. Enargite

Enargite (Cu_3AsS_4) is a copper bearing mineral that is problematic in many of the gold-copper mines due to the presence of arsenic in the mineral structure (Guo and Yen, 2002). The enargite structure is based on an orthorhombic coordination derived from the structure of wurtzite (Posfai and Sundberg, 1998). An orthorhombic face centered system, as shown in **Figure 4**, is a crystal structure in which all interior angles are 90°, and the length of the base, width and height are all distinct, such that the dimensions a, b, and c are not equal (Richerson, 2006).

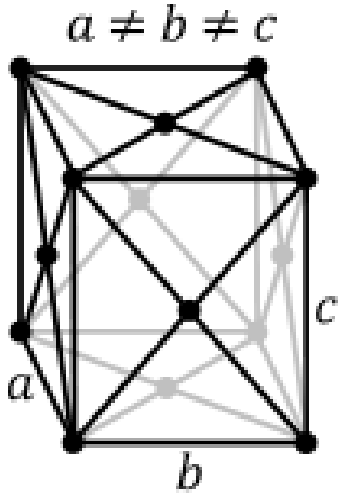

Figure 4: Orthorhombic Face Centered Cubic Crystal Structure (Wikipedia, 2007)

The tetrahedral arrangement of atoms is favored because the electron pairs are at 109.5° angles making them ideally spaced, giving the largest bond angles and hence the greatest distance between atoms (Gilbert, et. al, 2004). An example of the tetrahedral arrangement is given in **Figure 5**.

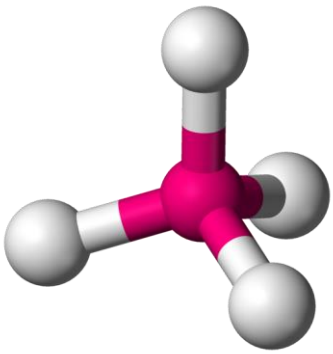

Figure 5: Tetrahedral Arrangement (Wikipedia, 2006)

The tetrahedral arrangement of atoms can be found in various compounds, one of which is wurtzite, as shown in **Figure 6.** The sulfur atoms (lighter in color) surround the metal atoms (darker in color) of zinc and iron (Gilbert, et. al, 2004).

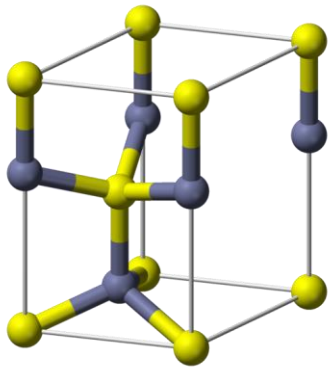

Figure 6: Wurtzite Structure (Wikipedia, 2011)

In enargite, each of the copper and arsenic atoms are surrounded by four sulfur atoms and each have covalent bonds. There are three times as many copper atoms as there are arsenic atoms. **Figure 7** shows the crystal structure of enargite depicted by Pauporte and Schuhmann in their study of enargite.

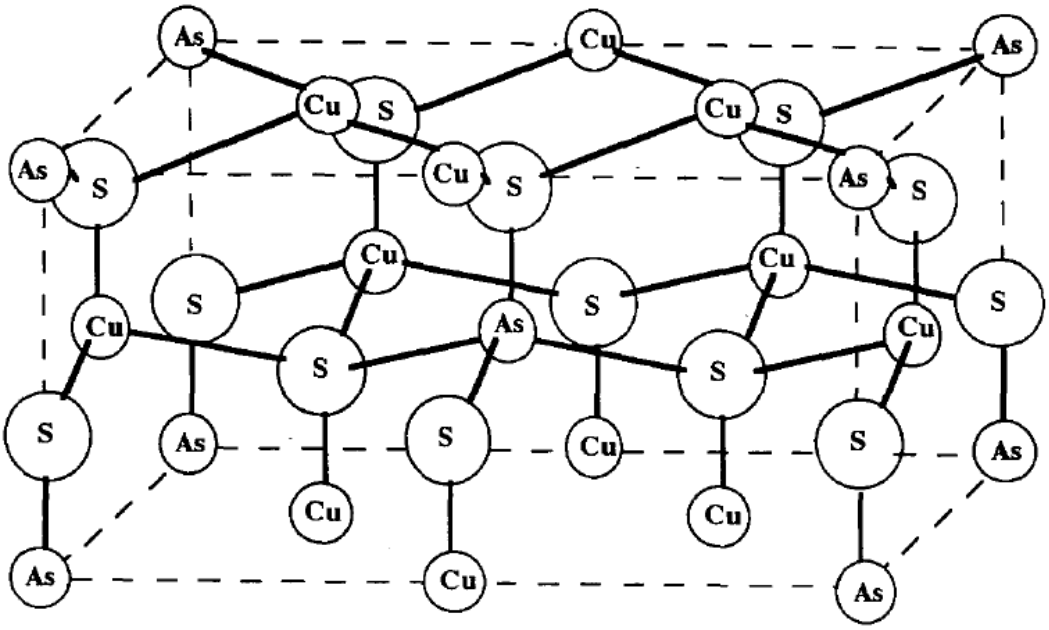

Figure 7: Enargite Crystal Structure (Pauporte and Schuhmann, 1996)

Enargite has a molar mass of 393.82 g/mol, a known melting temperature of 944 Kelvin (Seal, et. al, 1996), a standard enthalpy of -42.78 kcal/mol, and an entropy of 85.17 cal/degree K (Kantar, 2002). Its dissolution occurs in the presence of ferric iron according to **Equation 3:**

$$Cu_3AsS_4 + 11Fe^{3+} + 4H_2O = 3Cu^{2+} + AsO_4^{3-} + 4S^o + 8H^+ + 11Fe^{2+}$$ **Equation 3: Enargite Degradation**

Although this reaction shows the formation of elemental sulfur, it helps to understand how A.R.D. can cause arsenic to go into solution. It is the same as "ferric leaching" and the result of Fe^{3+}/Fe^{2+} redox couple due to iron's ability to undergo easily electron oxidation and reduction. It can also be enhanced by the presence of bacteria, which help speed up the oxidation of arsenic. The bacteria, referred to as extremophiles, can survive despite the toxic environment (Fantauzzi et. al , 2009). Hence, exposure of enargite to acid environments, particularly in the presence of extremophiles, would dissolve both copper and arsenic necessitating their removal, perhaps to recover the copper for economic gain and the arsenic for water treatment.

Enargite has been separated from various copper sulfides by using the differences in their tendencies to create oxide layers. Low levels of oxide layer formation of minerals can help in flotation by promoting the adsorption of collectors. In instances of high oxygen exposure, a physical barrier of oxides or hydroxides prevents the adsorption of collectors. Enargite was separated from chalcocite by using hydrogen peroxide (H_2O_2) as an oxidizing agent. The introduction of hydrogen peroxide controlled the potential of the solution and allowed the collector to adsorb onto the enargite and float, while the chalcocite was depressed. The depression of the chalcocite occurred because the hydrogen peroxide formed a hydroxide layer on the chalcocite and prevented adsorption of any collector on the surface (Senior et al. 2006). Thus, it was found that by understanding the properties of enargite, selective flotation may be performed. Consequently, as shown earlier for the binary water systems of arsenic and copper, E_H and pH will be similarly important (Greenfacts, 2011).

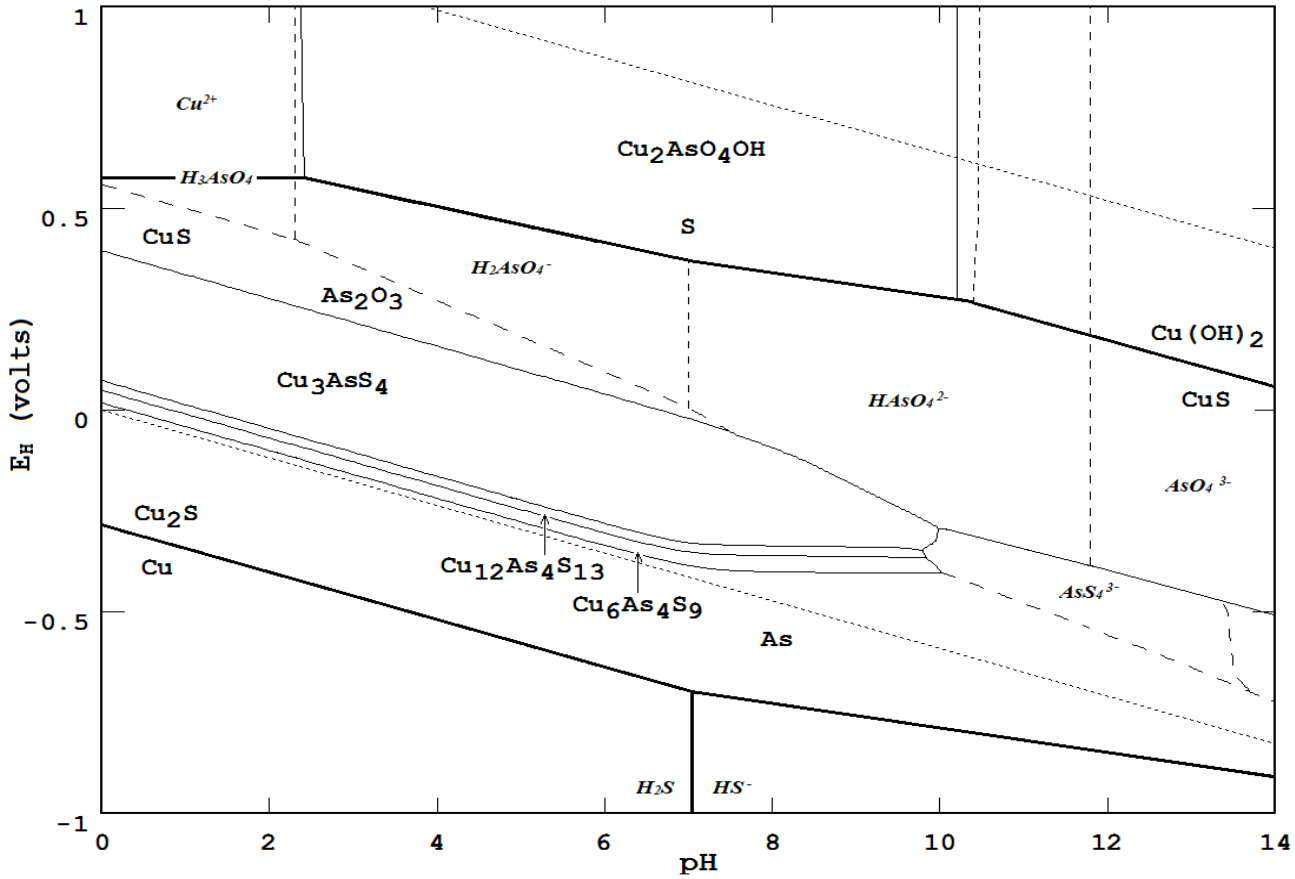

Figure 8 : Complete Updated E_H-pH Diagram for the Cu-As-S system, [Cu]=0.075M, [As]=0.025M, [S]=0.1M. Sulfur oxidation is limited to elemental sulfur. (Gow, Young and Huang)

When exposed to a pH range of 0 to 4, enargite can decompose to Cu_2S via the following reaction (Ferron and Wang, 2003):

$$3Cu_3AsS_4 + 6H_2O = AsS_4 + As_2S_2 + 3Cu_2S + 3HCuO_2^- + 3HS^- + 6H^+$$ **Equation 4: Cu_2S Formation**

In acidic conditions where H^+ is present, a layer of As_2O_3 may form on the surface. **Equation 5** was taken from an SGS survey explaining the oxidation of enargite (Ferron and Wang, 2003).

$$4Cu_3AsS_4 + 3O_2 = 12CuS + 2As_2O_3 + 4S$$ **Equation 5: CuS Formation**

In the presence of oxygen, Cu_2O or CuO may form on the enargite surface by reactions similar to the following two equations (Cordova R. et. al, 1996).

$$Cu_3AsS_4 + 3O_2 + 3H_2O = AsS_4 + 3CuO + 3H_2O_2$$ **Equation 6: CuO Formation**

$$Cu_3AsS_4 + 3O_2 + 6OH^- = AsS_4 + 3HCuO_2^- + 3HO_2^-$$ **Equation 7: CuO_2^- Formation**

At potentials greater than 0.5 Volts between pH 1 and pH 9, enargite reaches a wide zone of stability of cupric arsenate $Cu_3(AsO_4)_2$ due to the formation of an arsenic oxide surface layer (Castro and Baltierra, 2005). The behavior of enargite at these upper potentials has been studied by various authors. Flotation studies have been conducted using different collectors in acidic conditions as well as alkaline conditions and include those with PAX as the collector often using voltammetry to help discern the electrochemical reactions.

From these previous studies, an understanding of enargite flotation was obtained but was not complete. This study investigates the effects of PAX onto both a copper and an enargite surface at higher pH values. Voltammetry will be used so the effect of E_H can be measured. Through the use of E_H-pH diagrams, the surface reactions of copper and enargite by themselves, as well as copper and enargite in the presence of PAX will be characterized. The oxidation and reduction of copper and enargite on the surface due to the addition of PAX will be seen through the exchange of electrons in the system, and the potentials yielding collector adherence will be recorded and presented to give a baseline of preliminary tests for flotation.

1.3. Previous Investigations of Enargite Flotation

Numerous investigations and studies have been conducted on the enargite system. Pyrometallurgical, hydrometallurgical and electrometallurgical techniques have been examined

separately, and in conjuntion with one another, in the hopes of finding a solution to the problems associated with this mineral. The presence of oxygen, low and high pH modifiers, complexing agents, potential-controlling reagents, and various flotation chemicals have been studied. This review focuses on those that involve flotation with an emphasis on xanthate chemistry in the absence and presence of potential control. Periodic reference to studies on enargite electrochemistry are given even though they may have been done for hydrometallurgical or environmental purposes; in essence, these studies are about floation, just in the absence of xanthate.

Table I: Previous Enargite Flotation Pulp Potentials

Author	pH	Collector	pulp potential (V)
Castro and Honores 2005	8	N/A	> -0.075
Castro and Honores 2003	11	N/A	> -0.025
Ma and Bruckard 2009	10.5	PEX	0.15 to 0.27
Kantar 2002	10.5	PEX	0.15 to 0.27
Guo and Yen 2002	10	PAX	0.00 to 0.25
Guy and Bruckard 2006	11	N/A	-0.125 or 0.29
Castro and Honores 2001	8	N/A	-0.15 to -0.05

Previous attempts at pulp-potential control of enargite flotation are listed in **Table** . In the study conducted by Ma and Bruckard, the flotation of enargite was found to be strongly dependent on the pulp potential. At pH 10.5 and in the presence of ethyl xanthate, enargite was found to have a recovery of 98% when the potential was kept between 0.15 and 0.27 Volts. They attributed the phenomenon to copper oxide formation, noting that at 5×10^{-3} M, copper xanthate oxidizes to copper oxide at 0.40 Volts. They further noted that formation of sulfur layers would have rendered the enargite more readily floatable due its natural hydrophobicity but the presence

of copper oxide could negate that and simultaneously prevent copper xanthate and dixanthagen from forming on the surface of enargite. Such a layer would prevent flotation of enargite, which agrees with Allison et al. (1972), Leja et al. (1963), as well as Haga et al. (2012) as discussed next.

As indicated in **Figure 7**, a typical enargite crystal structure would ideally have copper exposed on every face. Copper being exposed on every face would allow for xanthate to adsorb onto a copper atom. If, however, copper is not the exposed atom, arsenic and/or sulfur are the exposed atoms so a sulfur oxide or arsenic oxide layer will likely form on the surface.

Haga et al. (2012) found that enargite may be selectively floated from pyrite (FeS_2) and chalcopyrite ($CuFeS_2$). They used PAX as the collector and Methyl Isobutyl-Carbinol (MIBC) as the frother and adjusted the pH between 4 and 11, allowing flotation of 5, 10, and 15 minutes. In their single mineral studies, they found enargite recoveries reached a minimum of 50% at pH 7 but maximum at pH 4 and 80% at pH 11. Using the same parameters at pH 4 on mixed ores, it was observed that selectivity over the other minerals occurred. They attributed the selectivity to enargite yielding elemental sulfur and/or arsenic sulfide and thereby having an enhanced hydrophobicity on top of that established by just copper xanthate. However, based on the E_H-pH diagram in **Figure 8** (Gow et al. 2014), it is not likely that arsenic sulfide plays a role since it is not stable under the conditions indicated.

In a flotation study of enargite conducted by Centin Kantar (2002), enargite was not flotable under reducing conditions, but was found to be naturally flotable under oxidizing conditions. The pH of the system was varied, and the effect of collector was studied. He discovered that, in conditions less than pH 5.5, elemental sulfur formed on the mineral surface of enargite, as depicted in **Equation 8:**

$$Cu_3AsS_4 + 4H_2O = 3CuS + H_2AsO_4^{2-} + S^o + 6H^+ + 5e^-$$

Equation 8: Elemental Sulfur Formation

This reaction agrees with **Figure 8** (Gow et al., 2014). Kantar (2002) also determined that the hydrophobicity of enargite increased with increasing potential and attributed it to increased sulfur formation.

By comparison, under alkaline and oxidizing conditions, Kantar (2002) found enargite yielded CuO and Cu_2O, which decreased its flotability. He concluded that this was due to the lack of the formation of elemental sulfur as depicted in **Equation 9**: albeit it in disagreement with **Figure 8**:

$$Cu_3AsS_4 + 23H_2O = 3CuO + HAsO_4^{2-} + 4SO_4^{2-} + 45H^+ + 35e^-$$

Equation 9: CuO Layer Formation

However, in the presence of PEX, Kantar (2002) obtained the same results as Ma and Bruckard, (2009) with enargite flotation being maximum at low pH between 5 and 6 but decreased at increasing pH because elemental sulfur became absent. Interestingly, he also found flotation to be best between potentials of 0.15 and 0.27 volts, which was attributed to copper xanthate but, unlike Ma and Bruckard (2009), also dixanthogen.

Guo and Yen (2005) investigated the selective flotation of enargite and chalcopyrite in copper concentrate by examining the effect of potential. When the potential of this system was greater than 0.4 Volts, chalcopyrite was depressed, and selective flotation of enargite did occur. From their polarizaiton studies, they concluded that electrical conductivity differences between the two minerals rendered chalcopyrite easier to oxidize at higher pulp potentials, thereby depressing it and floating enargite.

Guo and Yen (2002) additionally found that, when Potassium Amyl Xanthate was added to the solution and the potential was 0.2 Volts, more than 97% of the enargite was recovered in

the concentrate along with about 20% of the chalcopyrite. They found the best separation occurred when the potential of the system was 0.6 Volts and attributed enargite having greater flotability and chalcopyrite being easier to oxidize due to differences in their electrical conductivity. Because of the higher potentials involved, they theorized that elemental sulfur and dixanthogen were responsible in comparison to collectorless flotation tests conducted without PAX.

In another study, Senior et al. (2006) developed a three-stage flotation circuit to separate the four copper minerals in Tampakan deposit in the Phillipines: enargite, chalcopyrite, chalcocite (Cu_2S), and cuprite (Cu_2O). In the first stage, chalcocite and cuprite floated in the presence of xanthate at pH 11 and E_H of -0.125 volts, with cuprite floating due to CuX formation and chalcocite to elemental sulfur. By making the conditions slightly more oxidizing, cuprite no longer floated in the second stage due to the oxidation of cuprous xanthate via:

$$CuX + H_2O = CuO + X^- + 2H^+ + e^-$$

Equation 10: Cuprous Xanthate Decomposition

Similar conditions were used to separate enargite from chalcopyrite ($CuFeS_2$) in the third stage. In this case, enargite floated due to elemental sulfur but chalcopyrite remained hydrophyllic presumably due to its oxidation to CuO. They also noted that enargite could be selectively floated from the other copper minerals at pH 11 if the E_H was increased to 0.29 volts. Higher potentials caused all the minerals to be depressed which would concur with the use of H_2O_2 (Fullston et al. 1999) and O_2 (Ma and Bruckard, 2009; Kantor, 2002) as flotation reagents as well.

In a later study, Guo and Yen (2005) also found that enargite did not float at a potential less than 0.0 Volts, and did not float if the potential was greater than 0.35 Volts. Below 0.0

Volts, neither mineral formed an oxide layer on the surface, so PAX could adsorb onto both surfaces. Above 0.35 Volts, both mineral surfaces begin to form oxide layers, as predicted by their E_H-pH diagrams, which would block the adsorption of PAX onto either surface. Between 0.0 and 0.35 Volts, however, the selective flotability of enargite increased as the potential was increased due to the formation of an oxide layer on the chalcopyrite surface.

The adsorption of sulfur-bearing collectors onto the surface of a sulfur mineral is an electrochemical process. One such example is the reaction between copper metal and xanthate to produce dixanthogen. A xanthate compound attaches to the copper ion in **Equation 11**, and then precipitates in **Equation 12** to form dixanthogen and cuprous xanthate (Poling, 1976):

$$4X^- + 2Cu^{2+} = Cu_2X_4$$

Equation 11: Xanthate with Copper Ion

$$Cu_2X_4 = X_2 + 2CuX$$

Equation 12: Dixanthogen and Cuprous Xanthate

This phenomena was observed by Guo and Yen (2002) when measuring the surface potential of enargite. Their studies showed that enargite at pH 10 became hydrophobic at a pulp potential of -0.005 Volts, where xanthate began to adsorb onto the surface, and was hydrophobic through the highest tested pulp potential of 1.05 Volts. The hydrophobicity of enargite was due to the xanthate adhering to the surface of the enargite. When PAX was administered and adhered to the surface of the enargite, as determined by UV spectroscopy, the xanthate ions prevented the oxidation of the surface of the enargite by covering the surface in a monolayer of xanthate ions and hence not allowing an oxide layer to form. They observed that during negative scan potentials with PAX, dixanthogen began to be produced on the surface of the enargite. The decomposition of xanthate can be seen via **Equation 13.** The formation of dixanthogen, which

will form on the electrode surface, is shown in **Equation 14.** The electrode surface was examined with UV Spectroscopy to confirm this formation.

$$ROCSSK + H_2O = ROH + KOH + CS_2$$

Equation 13: Xanthate Decomposition

$$2X^- = X_2 + 2e^-$$

Equation 14: Dixanthogen Formation

It was also found that, if the pulp potential was higher than 0.25 Volts, enargite could be separated from chalcocite and chalcopyrite, since these minerals would be depressed under these potentials. The depression of chalcocite and chalcopyrite is due to these copper sulfides forming an oxide layer on the surface which blocks the adsorption of PAX.

Guo and Yen (2002) concluded that, at higher concentrations, there was a greater potential range of dixanthogen adsorbing onto the enargite surface. Guo and Yen also found that, at a potential higher than 0.4 V, the amount of dixanthogen on the surface of the enargite was greater at pH 7 than at pH 10. The large amount of dixanthogen was due to the hydroxide product film present at pH 10, causing a decrease in the dixanthogen adsorption on the enargite surface. The dixanthogen adsorption required a cathodic polarization voltage to be applied to the electrode to remove the dixanthogen from the surface. They found that, at upper potentials, there would be a large decrease in the amount of dixanthogen because there would be oxidation products, such as arsenic oxides, being produced on the surface of enargite. It was extremely difficult to remove the dixanthogen from the enargite surface, since a very low potential (as low as -0.6V) was required to reduce the dixanthogen, which results in a wide range of possible pulp potentials at which enargite would float. If there was already dixanthogen on the surface of the enargite, the potential range at which flotation may occur was found to be -0.4 to 1.05 Volts.

Dixanthogen on the surface would allow for separation from enargite, or further concentrating to occur.

2. Theory

2.1. Cyclic Voltammetry

Cyclic Voltammetry is used to study electro-active species through the observation of redox reactions at the surface of conductive materials. Typically, the technique is a three-electrode system requiring a working electrode (WE) of the material, a reference electrode (RE), and a counter electrode (CE). There is also a cell containing the solution of interest, a potentiostat to apply voltage between the working and reference electrodes as well as measure current between working and counter electrodes, and a computer program to generate the voltammograms.

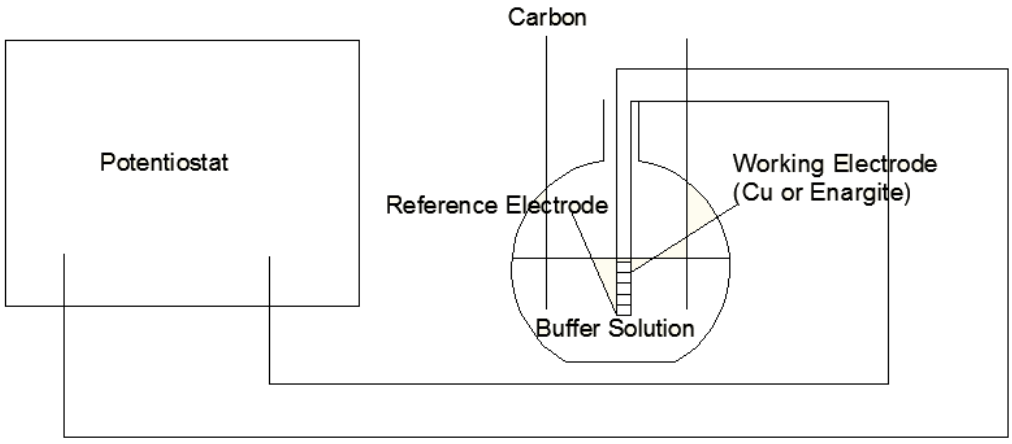

Figure 9 : Potentiostat Setup

The reference electrode, such as the standard calomel Ag/AgCl saturated KCl electrode (+197mV vs. SHE) used in this study, measures the current generated by applied potential to the working electrode (enargite in this study) in pH buffer solutions with or without stirring. When a voltage or potential (E_H) is applied between the counter electrode and working electrode, the working electrode may respond by undergoing redox reactions and thereby generating a current. Oxidation reactions yield positive current and reduction reactions yield negative current. By scanning the potential and plotting it as a function of the current, a voltammogram will be

produced. Redox reactions are identified through the potential that they initiate at and by the amount of current in the machine. Furthermore, because redox reactions are often pH-dependent, the solutions are usually buffered to control the pH. In this regard, redox reactions can be more easily identified. For the purposes this study, pH and the E_H values can mimic the conditions in a flotation cell and specific pH and E_H conditions determine where hydrophobicity occurs. The conditions would be sought to obtain flotation or avoided to prevent it.

In CV, the current increases as the potential becomes increasingly positive or negative since there is a directly proportional relationship between voltage and current, however, when redox reactions occur and even go to completion, the availability of the working electrode can become depleted and/or its resistance increased due to the formation of insulating products. In addition, the electrochemical reaction may switch from chemical control to diffusion control, where current becomes constant. In the other case, the electrode availability decreases along with current resulting in a peak on the voltammogram. Because it is a cyclic process of applying a voltage, either increasing or decreasing, the current peaks that are generated in one direction are usually observed in the other but in the reverse order.

CV is used to determine the redox reactions at the working electrode surface. The application of voltage between electrodes generates a species during the forward scan cycle and then during the reverse scan cycle regenerates the original material. The proposed regeneration assumes the redox reactions are reversible; however, this may not always be the case. For example, if a reaction yields an aqueous species and it either diffuses away into the bulk of the solution or stirring is used, the species will not be present to react in reverse. It is important to understand that, for oxidation reactions, electrons flow away from the working electrode (and current is

positive) and for reduction reactions, they flow into the working electrode from solution (and current is negative).

For this study, copper and then enargite (Cu_3AsS_4) were the working electrodes, Ag/AgCl was the reference electrode, Carbon was the counter electrode, and various buffers were used to control the solution pH. Potassium Amyl Xanthate (PAX) was added to the system to simulate flotation conditions. By controlling the pH at 7, 8, 9, 10, 11, or 12, the only variable in the system was the applied potential since stirring was not conducted. The initial scan generated peaks on the voltammograms that were characteristic of the interaction between the mineral and the buffer solution. Upon the addition of PAX, any additional peaks generated are characteristic of the interaction between the copper or enargite surface and PAX at the given pH value. In this regard, the conditions for copper and enargite flotation with PAX can be identified.

2.2. Fourier Transform Infrared Spectroscopy

Fourier Transformation Infrared (FTIR) Spectroscopy refers to the detection and measurement of infrared radiation after it interacts with molecular vibrations in order to identify, characterize and/or quantify them. The Infrared (IR) spectrum occurs at wavenumbers from 100 cm^{-1} to 10,000 cm^{-1}. Due to variations in optical properties, a single FTIR Spectrometer is not capable of detecting all values in this range and, in this regard, is divided into three regions with the Near Infrared (NIR) at 4,000 to 10,000 cm^{-1}, the Mid Infrared (MIR) at 400 to 4,000 cm^{-1}, and the Far Infrared (FIR) at 100 to 400 cm^{-1}.

Most FTIR spectrometers operate in the MIR range, and most are used to collect spectra with energy distribution as a function of wavenumber. Energy is usually relative to a background and expressed in either %Transmittance or Absorbance. The instrument splits the radiation into two beams, each of which is to be passed through the sample. One beam is of a fixed beam length,

and the other is of a variable length, determined by a mirror that is translated back and forth a set distance within the instrument. The two different beams produce an interferogram with variations in intensities due to constructive and destructive interference. Following Fourier transformation of the interferogram, the resulting spectra shows peaks at wavenumbers where energy absorbances occur. Ultimately, the peaks correspond to the vibrations of molecular bonds and include scissoring, wagging, in-plane or out-of-plane bending, and asymmetrical and symmetrical stretches. The spectra are then characterized by comparison of the peak values present in the FTIR library so that the vibrating atoms can be determined, characterized and/or quantified. Depending on the distance that the mirror moves, the FTIR also has high resolution and is faster than the dispersive techniques due to the passage of the entire radiation range through the sample compared to slits.

Compounds, depending on their molecular size and content, can have multiple unique band values in the IR spectra, due to the interaction of the IR radiation with the vibration of the atoms in a compound. If atoms are rearranged so that different bonds result, particular peaks will be repeated where vibrations are the same but may be slightly shifted depending on their molecular environment. In this regard, a carbon single bonded to a hydrogen atom resulting in a stretching interaction may be present over several wavelength ranges but will be different, for example, for cyclohexane compared to normal hexane.

3. Experimental Objectives

3.1. Voltammetry

The purpose of this study was to observe the effects of pH and PAX on the redox chemistry of the copper-water system and enargite-water systems. By cycling a voltage to the working electrode of copper or enargite, current will be generated that is specific to each. The software records current as the response signal to the applied voltage (Kissinger & Heineman, 1983), generates a voltammogram unique to the working electrode. Enargite yields a different voltammogram than copper due to the presence of sulfur and arsenic in its structure, but could have similar features due to the presence of copper. The generation of these voltammograms at various pH values shows the effects that pH, E_H and the addition of PAX has on the electrochemistry of the working electrode. Furthermore, when a collector such as PAX is added to the system, differences in voltammograms in the absence and presence of collector will indicate the conditions where the electrode becomes hydrophobic. Analysis of the peaks will also indicate how they become hydrophobic, as discussed at the end of Chapter 1.

3.2. Separation

By finding peaks on the voltammagrams that are unique to enargite and to the collector and enargite system, it is possible to find an optimal flotation range based on the pulp potential. The voltammograms in this process will show the redox reactions that occur on the surface of the working electrodes of enargite and copper, as examined separately. The surface reactions at the tested pH values will also show the effect that pH has on the system of copper and that of enargite. With this information, the pH and E_H parameters of a flotation system can be established, and the redox reactions that will occur in the system can be predicted. Using this

information, the ideal flotation parameters can be estimated, and the redox reactions within a flotation cell controlled.

4. Methodology

4.1. Specimens

High purity copper wire was purchased at a local hardware store. It was 0.51 mm in diameter and had dual purpose for this study. First, it was used as the copper working electrode in that portion of the research. Second, it was used as the connection to the enargite mineral specimen as it was fashioned into a working electrode. The enargite was provided by J&M Minerals in Butte, MT and came from the Orphan Girl Mine in Butte, MT. The elemental compositions of both the copper wire and the enargite were determined using a LEO scanning electron microscope and energy dispersive X-ray spectrometer (SEM/EDX) equipped with Mineral Liberation Analysis (MLA) software.

4.1.1. SEM Imaging

A Scanning Electron Microscope (SEM) was used to obtain compositional information about the specimens. An SEM has a microscope column that sits above the specimen stage. In this column, an electron gun fires a beam of electrons at a mounted specimen. Electrons in the SEM undergo two types of collisions from the sample atoms. The first is elastic, where back scatter electrons are produced as the electrons from the beam are deflected by the atoms of the specimen laterally. The second type is inelastic, which results in secondary electron generation. The beam electrons propagate through the atomic layers, and electrons from the outer atomic shell are ejected due to sufficient energy transferred to them from the beam electrons. When an inner shell atom is ejected, an outer shell electron moves to the inner shell to satisfy the vacancy, and emits an electron due to the change in energy state.

The energy of the X-ray depends on the element being analyzed. For example, the X-ray signal is a series of characteristic peaks in the EDX display, such as the copper wire spectrum in **Figure 10**.

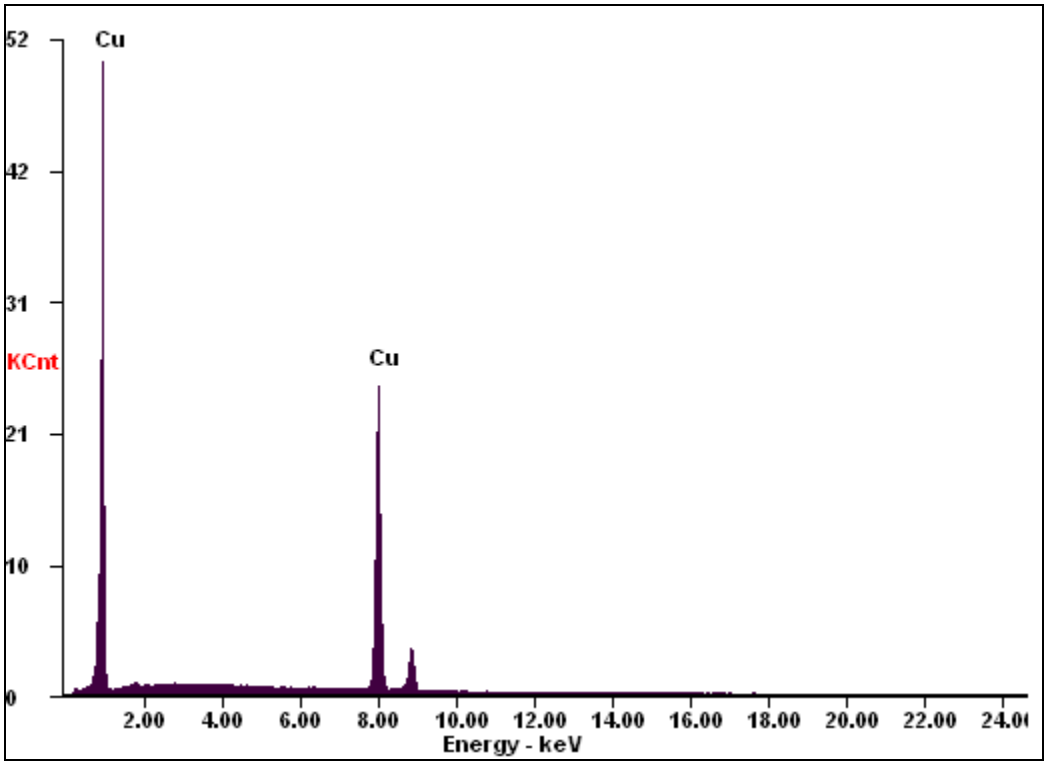

Figure 10: EDX Spectrum of Copper Wire

The amount of each element can be determined on a weight percent basis and tabulated to show the composition.**Table II** shows such a composition of the copper wire specimen.

Table II: Composition of Copper Wire

Element	Wt%	At%
CuK	100.00	100.00
Matrix	Correction	ZAF

A section of enargite was cut, ground and polished in preparation for the SEM analysis. As with the copper wire, the enargite was bombarded with electrons from the SEM electron gun,

and the resulting X-rays were detected and analyzed using the EDX software. **Figure 11** shows the energy dispersive spectrum generated by the enargite.

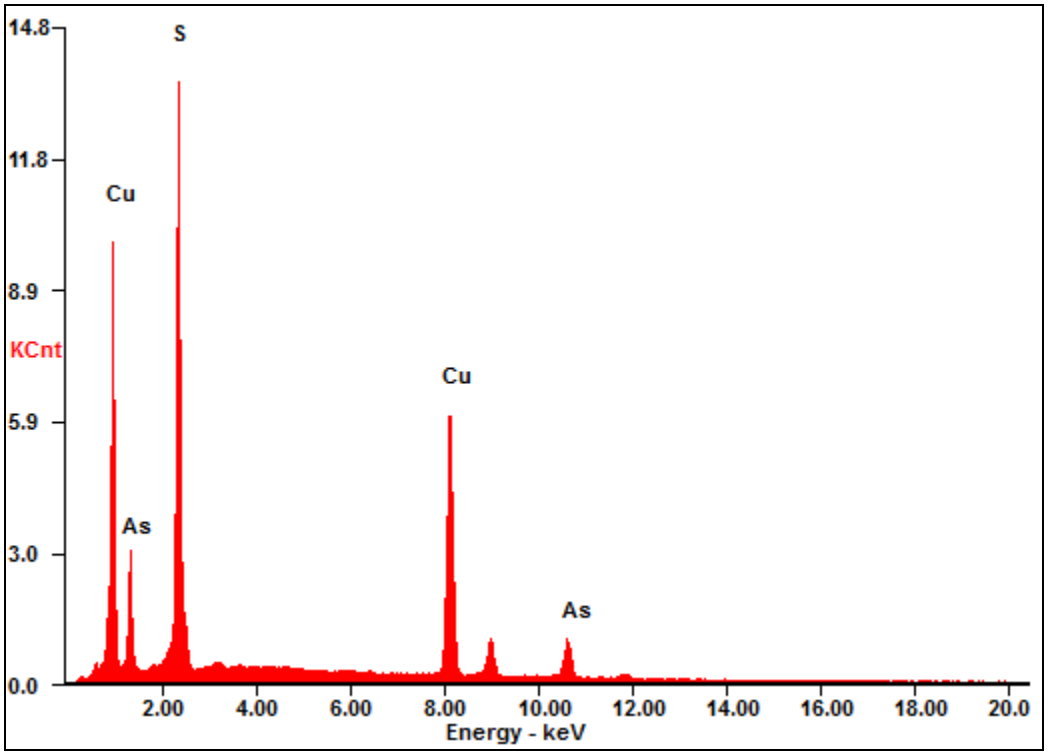

Figure 11: EDX Spectrum of Enargite

The analysis of enargite is in agreement with the formula of enargite Cu_3AsS_4, where sulfur makes up half of the atoms present, copper over a third, and the rest is arsenic, as shown in

Table **III**. Composition of the enargite sample as determined by the EDX spectrum and program can be seen in

Table **III**, and the theoretical composition of enargite is shown in **Table IV**. A slight difference in weight and atomic percentages can be seen and is due to standardless analysis used

by the equipment. However, for experimental purposes, the theoretical and actual compositions of enargite are close enough to consider the sample relatively pure enargite.

Table III: Actual Composition of Enargite Sample as Determined by MLA

Element	Wt %	At %
SK	32.69	50.10
CuK	49.01	37.90
AsK	18.30	12.00

Table IV: Theoretical Composition of Enargite

Element	Wt %	At %
S	32.57	50.00
Cu	48.41	37.50
As	19.02	12.50

4.2. Electrodes

The standard calomel electrode (Ag/AgCl) was used as the reference electrode. Measured voltages were compared to the standard hydrogen electrode (SHE) by adding 0.197 volts.

The copper wire electrode was made from copper wire measuring 48 cm in length. It was wound around the reference electrode thirteen times, with approximately 16 cm immersed in the solution within the voltammetric cell.

The enargite electrode was made by cutting a 1 cm^3 block of enargite and mounting it onto a piece of polyvinyl chloride (PVC) tubing with parafilm covering one end. Copper wire was attached to the backside of the enargite using Electrodag and graphite tape to ensure that it stayed in contact with the enargite. After checking for conductivity with a voltmeter, epoxy resin was poured into the tubing and allowed to set in order to seal and immobilize the enargite. The

parafilm was removed, and the sample side of the electrode was polished to evaluate the conductivity of the assembly.

4.3. pH Buffers

Test work was conducted using buffer solutions of pH 7, 8, 9, 10, 11 and 12. These pH values were chosen because, if xanthate was used in an industrial flotation circuit, lower values of pH would cause its decomposition. The buffers had a volume of 500 mL to ensure adequate volume was used in the voltammetric cell, as well as to follow the recipe of pH buffer makeup solutions. The recipe for the buffer solutions was taken out of the CRC 92nd edition of the Handbook of Chemistry and Physics (Haynes, 2011). It is assumed that these buffer solutions do not interact with the working electrodes. This assumption is usually true but necessitates doing experiments in the absence and presence of PAX to understand how PAX interacts with the electrodes. **Table V** lists the pH buffer and the chemicals required to make the buffer solution. Initially, 250 mL of 18 MΩ water were added to a volumetric flask, the chemicals were added, and then the remaining amount of water was added to bring it to volume.

Table V: pH Buffer Make-ups (Haynes, 2011)

pH	Chemical	Amount	Units
7	NaH_2PO_4	3.45	g
	0.1M NaOH	145	mL
8	$NaB_4O_7 \cdot 10H_2O$	2.38	g
	0.1 M HCl	102.5	mL
9	$NaB_4O_7 \cdot 10H_2O$	2.38	g
	0.1 M HCl	23	mL
10	$NaB_4O_7 \cdot 10H_2O$	2.38	g
	0.1 M NaOH	9.15	mL
11	K_2HPO_4	2.177	g
	0.1 M NaOH	20.5	mL
12	K_2HPO_4	2.177	g
	0.1 M NaOH	134.5	mL

4.4. Reagents

Further explanations of the function of frothers, and collectors, as well as the structure and a brief explanation of Potassium Amyl Xanthate (PAX) and Potassium Ethyl Xanthate (PEX) can be found in **Appendix 1**. The significance of both of these collectors is that they are copper collectors, and hence will adhere to the copper sites on the surface of metallic copper as well as enargite. Understanding how PAX and PEX interact with enargite could potentially lead to its selective removal.

Potassium Ethyl Xanthate was prepared by dissolving 20 grams of potassium hydroxide pellets in 200 mL of ethanol. Once the pellets were completely dissolved and the solution adequately stirred, 50 mL of this solution was mixed with 5 mL carbon disulfide (CS_2), one milliliter at a time. The equation for this overall process is **Equation 15** (Wikipedia, 2012)..

$$CH_3CH_2OH + CS_2 + KOH = CH_3CH_2OCS_2K + H_2O$$

Equation 15: PEX preparation

The mixing occurred over an ice bath to ensure that carbon disulfide gas was not emitted because, at temperatures above 112°F, carbon disulfide boils and is poisonous. The solution was then filtered and dried.

Laboratory grade potassium amyl xanthate (PAX) was used as the collector added to the pH buffer solutions for cyclic voltammetry testing. The xanthate was supplied by Montana Resources. The pellets of PAX were kept in an airtight container and stored in a fume hood to minimize contamination from the air. A $1x10^{-3}$M solution was made. In order to ensure the

quality of the PAX, the collector was analyzed using a Fourier Transform Infrared (FTIR) spectrometer.

4.5. Fourier Transform Infrared Spectroscopy

To use properly the Nicolet FTIR spectrometer in the Chemistry Department's analytical lab at Montana Tech, it was purged for fifteen minutes with nitrogen gas free of carbon dioxide and moisture as well as particulates. Typically, the nitrogen will boil off from a dewer. Once the system was purged, a background spectrum was collected. To obtain spectra of PAX and PEX, each collector was mixed with potassium bromide (KBr), ground to a powder, pressed into discs, and analyzed by transmission. In this mode, spectra are typically recorded in % Transmittance as a function of wavenumber (cm^{-1}).

Figure 12 shows the chemical compound of PAX, and **Figure 14** shows the chemical compound of PEX, both of which were used for bond characterization purposes. **Figure 13** shows the FTIR spectrum for PAX, **Figure 15** shows the FTIR spectrum for PEX, and **Figure 16** shows the two xanthate spectra overlaid FTIR spectra. The numbered peaks in the spectra are represented in **Table VI** and **Table VII**, respectively.

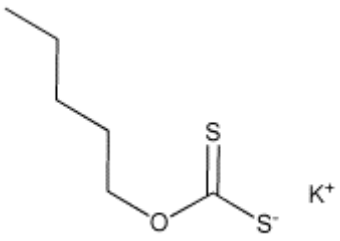

Figure 12: Structure of Potassium Amyl Xanthate (Nedichem, 2007)

The peak between 3000-3200 cm^{-1} was present in both xanthate compounds, and represent carbon-hydrogen symmetric and asymmetric stretches. Between approximately 2300-2850 cm^{-1}, numerous peaks are present, representing carbon-oxygen, carbon-hydrogen, carbon

carbon, or carbon-sulfur bonds. In **Figure 13**, peaks 30-33 are more distinct than the corresponding peaks (61-63) of the PEX compound **Figure 15**. They are more distinct in **Figure 13**, though slightly smaller. The peak collection from 1700-2000 cm^{-1} is present in both spectra, and represents carbon oxygen bonding. In **Figure 13**, however, peaks 4-8 are more sharply defined than the corresponding peaks in **Figure 15** (39-41). Several peaks depict an oxygen-hydrogen bond, which indicates that the sample is not completely dry.

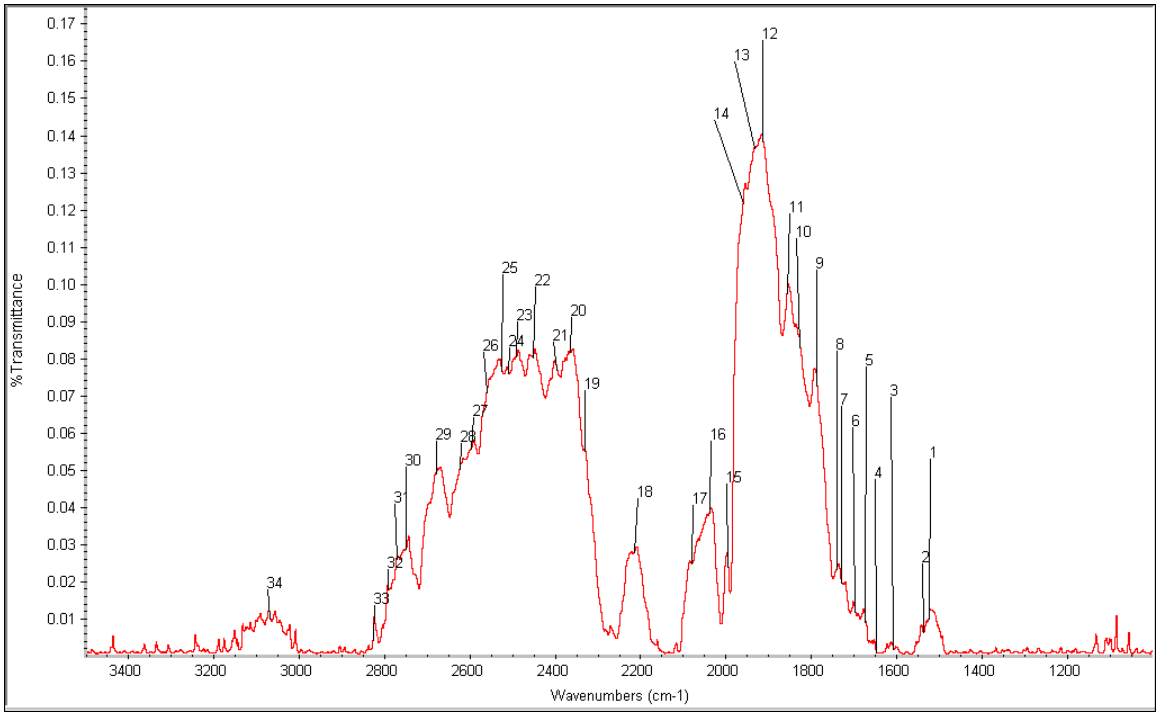

Figure 13: PAX FTIR Spectrum Showing Characteristic Peaks of PAX

Table VI: Bond Wavelengths for PAX

Peak Number	Wavelength (cm^{-1})	Bond
1	1512	C-C
2	1526	C-C
3	1542	C-O symmetrical vibrations
4	1612	C-C skeletal stretches
5	1682	C-C skeletal stretches
6	1728	C-O
7	1736	C-O
8	1787	Bridge bonded C-O
9	1852	C-O bridge
10	1893	C-O bridge
11	1911	C-O bridge
12	1998	C-O
13	2033	$C\text{-}O_2$
14	2065	C-O
15	2216	C-O
16	2335	C-O
17	2370	O-H
18	2402	O-H
19	2454	O-H
20	2489	O-H
21	2532	O-H
22	2548	O-H
23	2583	S-H
24	2610	S-H
25	2669	O-H
26	2696	O-H
27	2726	O-H
28	2745	C-H stretching
29	2772	C-H stretching
30	3000-3200	C-H stretching

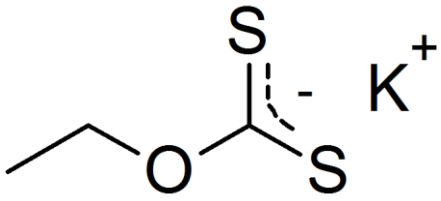

Figure 14: Structure of Potassium Ethyl Xanthate (Wikipedia, 2012)

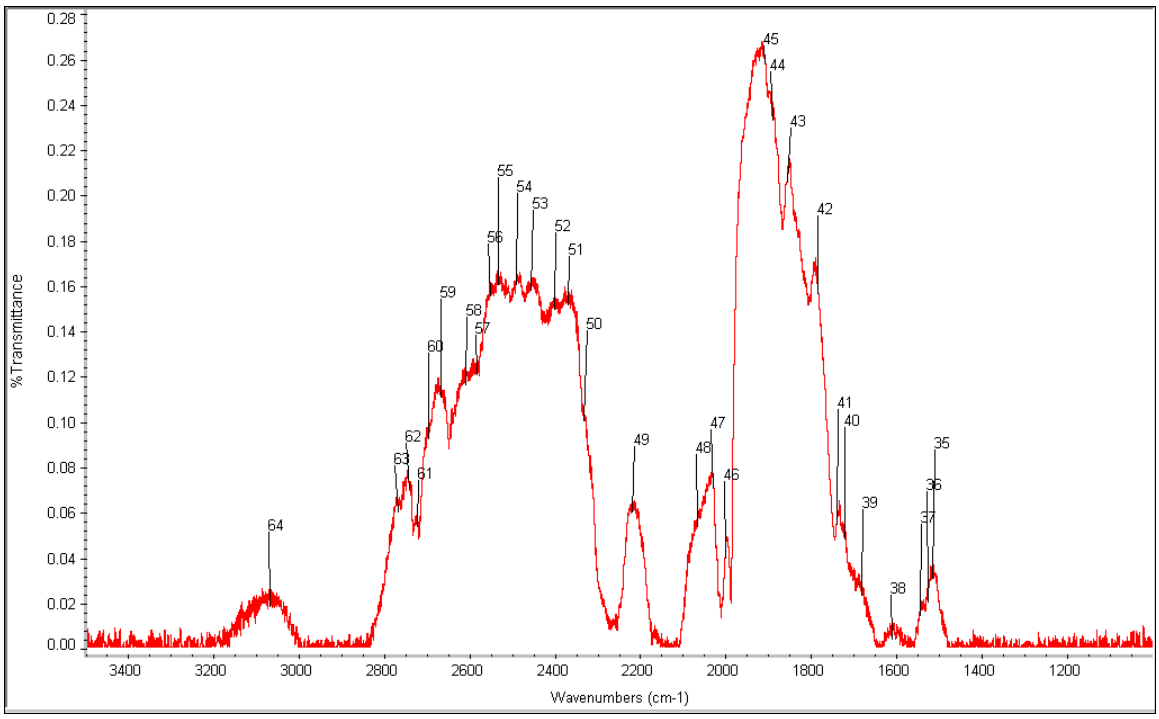

Figure 15: PEX FTIR Spectrum Showing Characteristic Peaks of PEX

Table VII: Bond Wavelengths for PEX

Peak Number	Wavelength (cm^{-1})	Bond
35	1515	C-C
36	1529	C-H bending
37	1542	C-H
38	1580-1636	C-O stretching
39	1698	C-O stretching
40	1733	C-O
41	1738	C-O
42	1790	Bridge bonded C-O
43	1849	Bridge bonded C-O
44	1893	Bridge bonded C-O
45	1914	Bridge bonded C-O
46	1998	C-O
47	2038	C-O
48	2033-2086	CO_2 vibration symmetric
49	2216	C-O
50	2362	C-O
51	2400	O-H
52	2454	O-H
53	2489	O-H
54	2529	O-H
55	2551	S-H
56	2588	S-H
57	2594	S-H
58	2613	S-H
59	2675	O-H
60	2699	O-H
61	2726	C-H stretching
62	2747	C-H stretching
63	2772	C-H stretching
64	3000-3200	C-H stretching

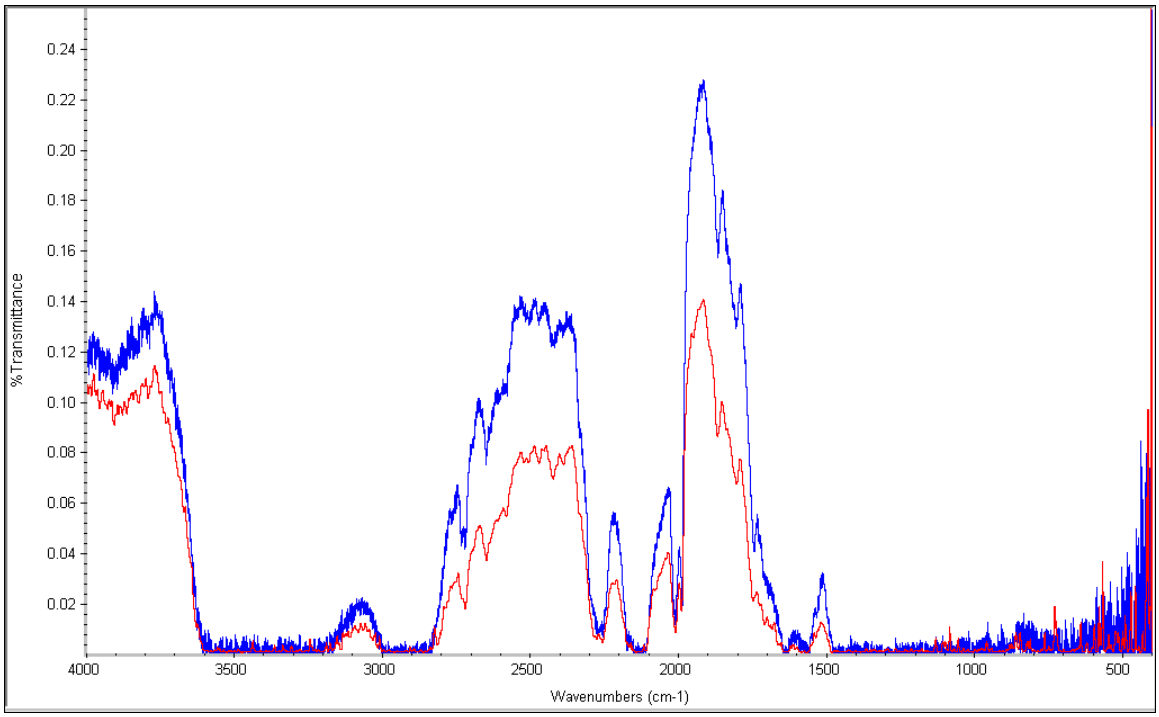

Figure 16: PAX And PEX FTIR Spectra Overlaid Showing Differences In Peaks

The spectrograph displayed the peaks for the bonds in the compound of xanthate. Each spectrograph for compounds is unique.

4.6. Cyclic Voltammetry

The pH buffer solution was placed in the voltammetric cell, and pure nitrogen was bubbled through the system for fifteen minutes prior to testing in order to displace free oxygen. Nitrogen gas from a cylinder provided by Nalco was purified by passing it through heated copper in a tube furnace thereby removing remnant O_2, CO_2 and H_2O from the gas. The addition of the nitrogen reduces the equilibrium concentration of oxygen present and removes all dissolved oxygen (Ohmi, 1993).

The working enargite electrode was taped to the reference electrode (in the case of the copper electrode, the copper wire was wound around the reference electrode) in order to minimize the distance between the working and reference electrodes. Minimizing the distance

between the working and reference electrode ensured that the two electrodes were minimally influenced by the surrounding medium, thereby making the IR drop small. A fresh surface of electrode was generated by polishing the surface of the electrode with 400 grit sand paper to ensure that no residual compounds from the previous test remained on the electrode surface.

After purging the system, the electrodes were immersed in the solution, and the voltage was applied. The potential was held constant at the beginning of each test for 10 minutes to allow equilibrium to be reached and electron flow to be fully established. Then an anodic scan was conducted from the starting potential to a negative potential. Upon reaching the user-set lower potential, the scan was swept back in the positive direction, past the starting potential, until it reached the user-set upper potential. The scan then went back in the negative direction until it reached the starting potential. This process was one cycle.

Upon completion of the buffer solutions testing at the six pH values for both electrodes, 5mL of the xanthate solution were added to the cell. The solution was mixed and once again purged of any free oxygen by using pure nitrogen bubbled into the system.

Upon completion of the test work, resulting voltammagrams were analyzed with the help of E_H-pH diagrams generated with StabCal to determine possible redox reactions from the onset of current flow as observed for each specimen. Such ‘onsets’ are often observed as peaks. The appearance of new “onsets” or peaks when PAX or PEX are present, would suggest conditions at which the specimens become hydrophobic.

5. Results

5.1. Isotherm of Copper Wire at pH 7

The amount of PAX on the copper electrode surface was determined by integrating the charge that was passed cathodically in the absence and presence of PAX. The copper wire and reference electrode were immersed in the buffer solution, and the initial potential was -200 mV vs. S.H.E. The potential was held four minutes and then a scan was conducted at 20 mV/sec to a final potential of -550 mV. Upon completion of the scan, the potential was raised 20 mV, and the procedure was repeated. Ten additional tests were performed this way, at potentials of -180, -160, -140, -120, -100, -80, -60, -40, and -20 mV. **Figure 17** shows the copper wire in the absence of PAX results and the graph shows no activity at any of the potentials.

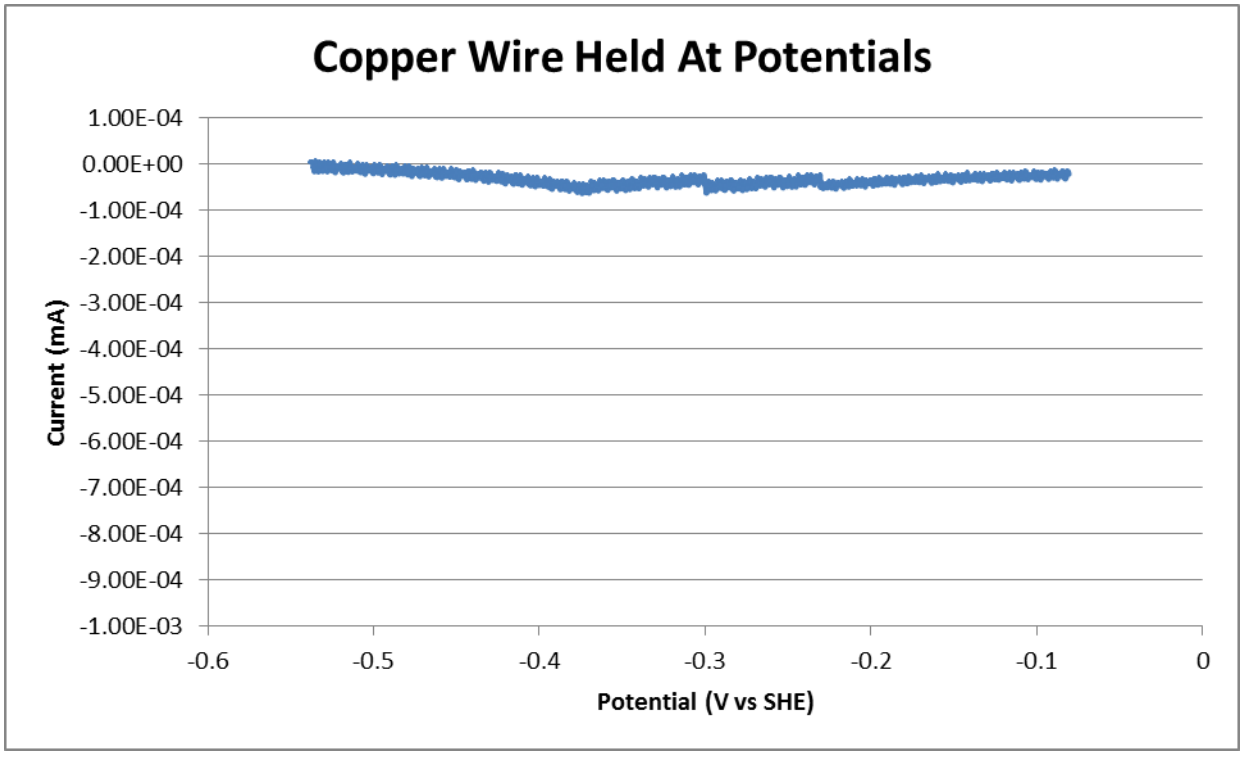

Figure 17: Copper Wire Held at Potentials in pH 7 Buffer Solution. Cathodic Voltammogram in the Absence of PAX After Equilibrating for 4 Minutes at Various Starting Potentials

The lack of peaks is indicative of no electrochemical reactions occurring between the copper wire and the buffer solution, as was expected. A concentration of $1x10^{-5}$M PAX was then added to the system, and the same procedure was used. Peaks developed with their magnitude dependent on initial potential. When the largest magnitude peak repeated identically, it was assumed that a monolayer of chemisorbed xanthate on copper had been achieved and the procedure was stopped. The voltammetric results from these tests are shown in **Figure 18**.

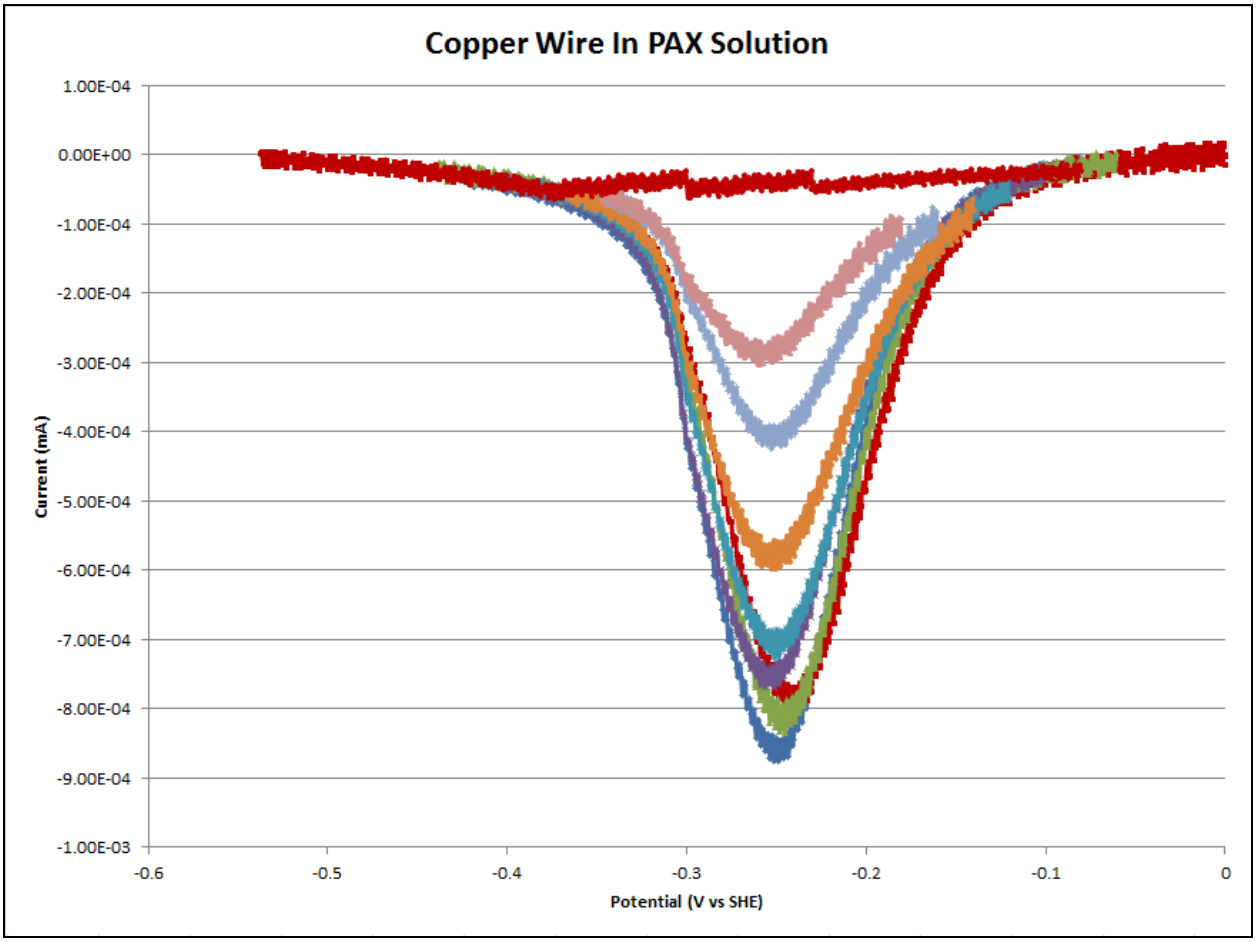

Figure 18: Cathodic Voltammagrams of Copper in the Presence of 1 x 10^{-5} M PAX at pH 7 after Equilibrating for 4 Minutes at Various Starting Potentials

Areas under the curves of both the copper wire with and without xanthate were found using Simpson's Rule (Thomas Jr., et. al, 2007). The difference of these respective areas was determined and assumed to be due to xanthate chemisorption onto copper. By ratioing each area

to the largest area where monolayer coverage occurred, surface coverage of chemisorbed xanthate as a function of potential would result (see **Figure 19)**.

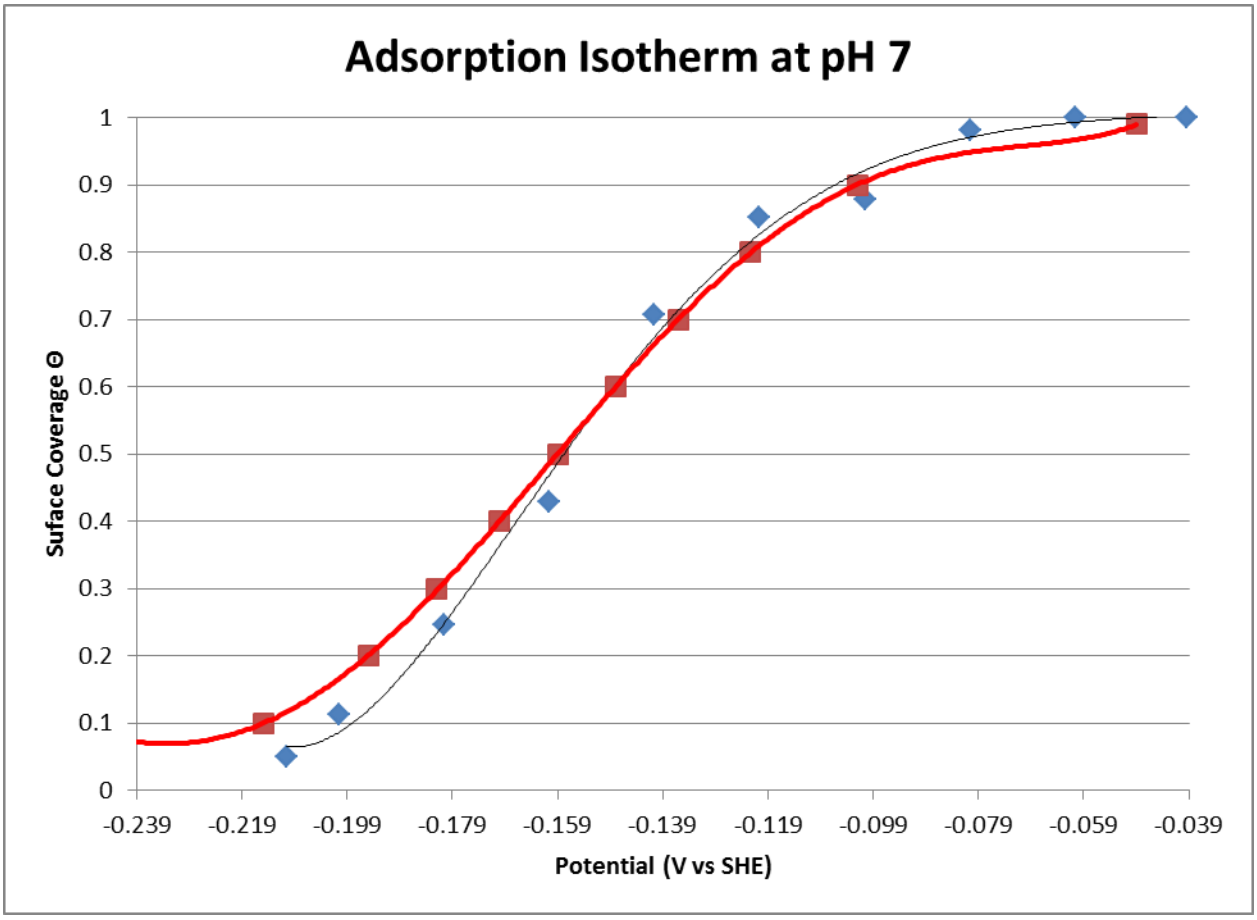

Figure 19: Adsorption Isotherm of PAX onto Copper (blue), with 100% Surface Coverage at a Potential of -0.04V. At pH 7 According to Gow, Young, Huang, Hope, & Takasaki, 2008, this is where Cu_2O is stable. Bold red line is calculated Frumkin Isotherm of same parameters

The Frumkin model (Huang & Young, 1996) can now be used for modelling the adsorption of xanthate onto the surface of copper. In **Equation 16**, θ is the surface coverage expressed as a decimal (i.e. 0.5 would be 50% surface coverage), a_A is the concentration of the xanthate, E is the applied voltage (SHE), T is the temperature in Kelvin, R is the universal gas constant, F is Faraday's constant, and the parameters to be estimated are g, K and ϒ; where ϒ is the electrosorption valency, and g and K are constants.

Figure 19 shows both the derived isotherm from the Frumkin equation (shown in bold and red), and the isotherm found in this experiment (blue data points and curve). As will be shown, the measured isotherm matches well with the derived isotherm.

$$\left[\frac{\theta}{1-\theta}\right]e^{g\theta} = Ka_A e^{\frac{\Upsilon FE}{RT}}$$

Equation 16: Frumkin Equation

The estimated slope ($\frac{d\theta}{dE}$) of the isotherm at half monolayer coverage is 9.231, the reciprocal of the slope ($\frac{dE}{d\theta}$) is 0.108, and θ = 0.5. The electrosorption valency (Υ) can now be solved for by taking the natural log of **Equation 16** and re-arranging it to solve for Υ:

$$\frac{\Upsilon FE}{RT} = \ln\left(\frac{\theta}{1-\theta}\right) + g\theta - \ln(K) - \ln(a)$$

Equation 17: Natural log of Frumkin Equation

And then $\frac{dE}{d(\log a)} = \frac{-RTlog(10)}{\Upsilon F}$ since the other terms are constants and equal zero upon differentiation. Then $\frac{-RTlog(10)}{F}$ = 0.059 since all terms are known constants. If multiple concentrations of xanthate were added to the system, a plot similar to **Figure 21** could then be generated, and a graph of potential vs log(concentration) could be derived. The $\frac{dE}{d(\log a)}$ term would be the slope in such a plot. This value was found to be -0.0493 using xanthate in a copper system (H.-H. Huang), assuming the same slope, Υ = 1.2.

Next, the value of g can be found when θ = 0.5 using **Equation 16** and solving for E to yield:

$$E = \frac{RT}{\Upsilon F}(\ln\left(\frac{\theta}{1-\theta}\right) + g\theta - \ln(k) - \ln(a))$$

Taking the partial derivative of this with respect to θ would equal:

$$\frac{\partial E}{\partial \theta} = \frac{\partial(\frac{RT}{\Upsilon F}\left(\ln\left(\frac{\theta}{1-\theta}\right) + g\theta\right))}{\partial \theta}$$

Which then simplifies to:

$$\frac{\partial E}{\partial \theta} = \frac{RT}{\Upsilon F}\left(\frac{1}{\theta} + \frac{1}{1-\theta} + g\right)$$

And when θ = 0.5, then

$$\frac{\partial E}{\partial \theta} = \frac{RT}{\Upsilon F}(4 + g)$$

Now $\frac{\partial E}{\partial \theta}$ = is 0.108, so rearranging and solving for g yields g=1.0596938, or g is about 1.06

Returning to **Equation 17** and re-arranging with respect to K yields:

$$K = \exp(\frac{-\Upsilon FE}{RT} + \ln\left(\frac{\theta}{1-\theta}\right) + g\theta - \ln(a))$$

At θ = 0.5, $a_A = 1x10^{-5}$, and E = -0.159V, K was found to be 2.853E+08. Woods, Young and Yoon calculated Υ to be 1.2, g to be 0 and K to be 5.30E+11 for Potassium Ethyl Xanthate on copper. Thus, the Frumkin Isotherm plotted was:

$$\left[\frac{\theta}{1-\theta}\right]e^{1.06\theta} = 2.853 * 10^8 a_A e^{\frac{1.2FE}{RT}}$$

Table VIII compares the estimated voltage of monolayer coverage at 25%, 50%, and 75% from the surface coverage equation from **Figure 19** to the deriving voltage from the Frumkin Isotherm equation at the same adsorption values. As can be seen in **Table VIII**, the derived isotherm matches the Frumkin Equation estimates for monolayer surface coverage very well. The potentials found represent the adsorption of xanthate onto the surface of the copper. These values were plotted on the copper-xanthate E_H-pH diagram, seen in **Figure 20**. The X term represents Xanthate.

Table VIII: Isotherm vs Frumkin Values of Monolayer Coverage

Coverage	Isotherm Values	Frumkin Values	Variance
25%	-0.179	-0.188	4.79%
50%	-0.158	-0.159	0.63%
75%	-0.129	-0.130	0.77%

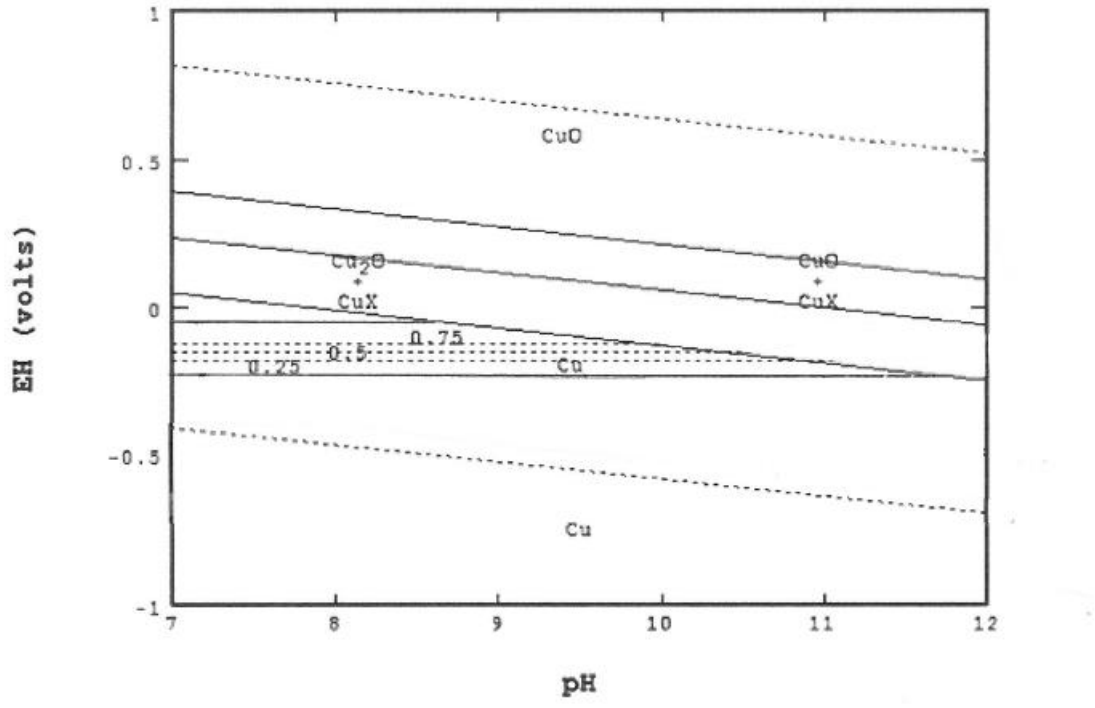

Figure 20: EH-pH diagram of 25%, 50% and 75% monolayer coverage of 10^{-5} M PAX on Copper

Using this graph, the surface reactions occurring on the copper wire and on the surface of the copper can be characterized. It is important to note that this diagram could apply if the enargite reduces to metallic copper at these potentials.

A similar study of the chalcocite-xanthate system was done by Young, et. al, (1991). In their study, they derived isotherm equations that generated a Surface Coverage vs. Potential graph, similar to the one just determined. In their work, done at pH 9.2, they assumed that, at equilibrium with copper xanthate, the coverage of chemisorbed xanthate also reached a monolayer. Their plot can be seen in **Figure 21**.

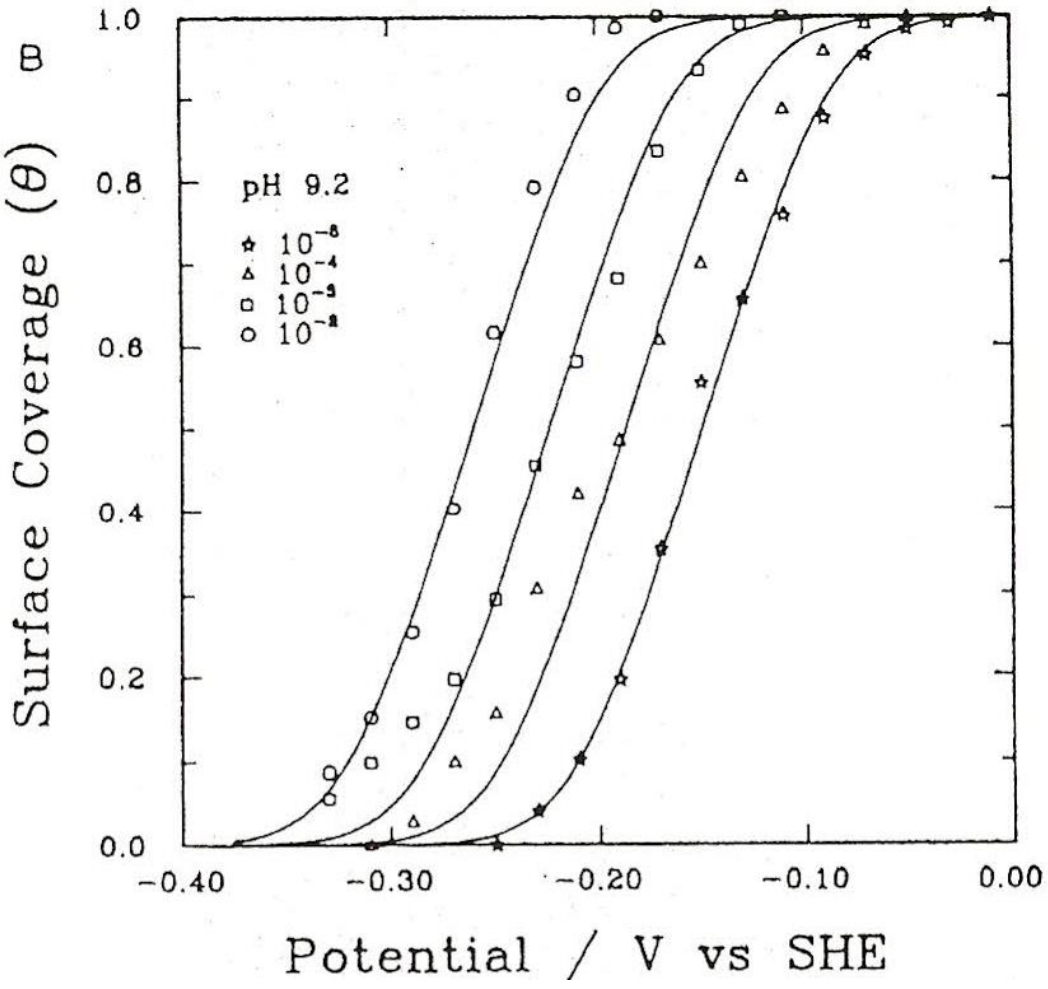

Figure 21 : Potential dependence of coverage of chemisorbed xanthate on chalcocite in pH 9.2 with various concentrations of ethyl xanthate (mol dm^{-3}). The solid lines are the derived isotherms.

Using the data generated from their chalcocite-xanthate flotation and rest potential studies, Woods, et. al, (1991) were able to generate E_H-pH diagrams based on the thermodynamic data found at flotation pulp potentials. **Figure 22** shows the E_H-pH diagram for the Copper/Water/Ethyl Xanthate system, at the same concentrate as in this study.

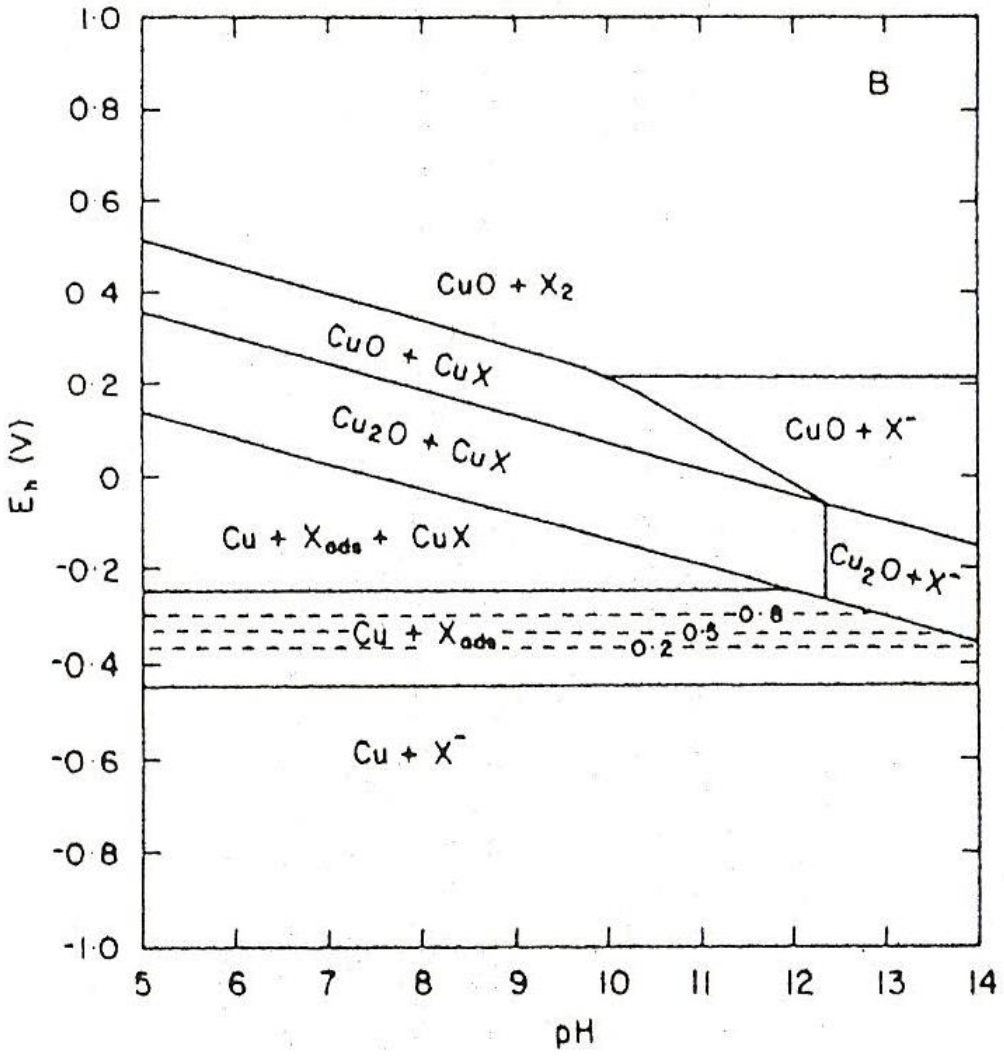

Figure 22 : E_H-pH Diagram for the Copper/Water/Ethyl Xanthate System for an Initial Xanthate Concentration of 10^{-5} mol dm^{-3}. Dashed Lines are Fractional Surface Coverages as Indicated

Figure 23 shows the same concentrate of ethyl xanthate, this time without sulfur-oxygen anions. Also, $Cu_{2-x}S$ stoichiometries are considered, and are identified in the acid region.

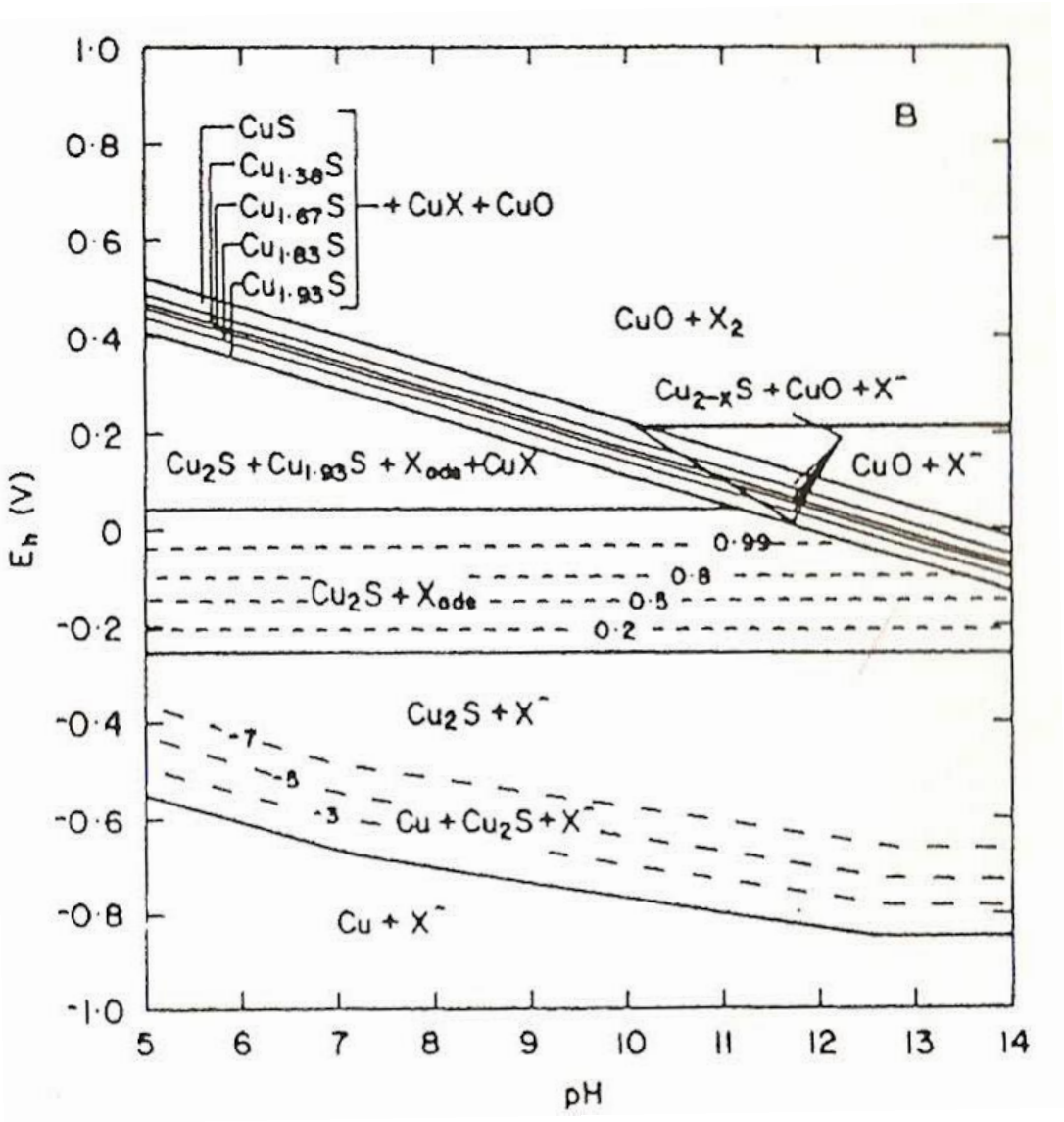

Figure 23 : EH-pH Diagram for the Chalcocite/Water/Ethyl Xanthate System for an Initial Xanthate Concentration of 10^{-5} mol dm^{-3}. Sulfur-oxygen Anions not considered. Species Labelled $Cu_{2-x}S$ cover the same range of stoichiometries identified in the acid regions. Dashed lines are fractional surface coverages as indicated.

5.2. Voltammetric Results

Abbreviated results of this voltammetric study are shown below. For a complete compendium of the experiments, the voltammagrams generated, and the reactions characterized, see Appendix B.

5.2.1. Copper Wire

A copper wire was the first of the electrodes tested. Experiments in the absence and presence of PAX were performed at pH 7, 8, 9, 10, 11, and 12 with each showing the characteristic peaks of a copper wire. At pH 7, 8 and 9 in the absence of PAX, there are two peaks present in the voltammagram;, and at pH 10, 11, and 12 also in the absence of PAX, there are four peaks present in the voltammagrams. Such peaks show how readily the copper wire can form an oxide layer on its surface. Typically, in the presence of PAX, at least one additional peak is observed.

The following voltammagrams, in addition to those present in **Appendix B**, are presented in pairs. The first voltammagram shows the electrode in just the buffer solution with tables showing proposed reactions of the system. A second voltammagram represents the electrode in the buffer with PAX in the system. Subsequent tables list additional reactions but only those involving PAX. Reactions from the previous tables are assumed to still occur, but are excluded for simplicity. The identification of the reactions are often aided by modeling the potential and pH at which reactions occur with respective E_H-pH diagrams.

Figure 24 shows the voltammagram of the copper wire at pH 7. As previously described, there are two peaks present, representing a pair of Redox reactions. **Table IX** shows the

reactions that are likely occurring. Each peak begin at approximately the same potential implying that the reactions are reversible.

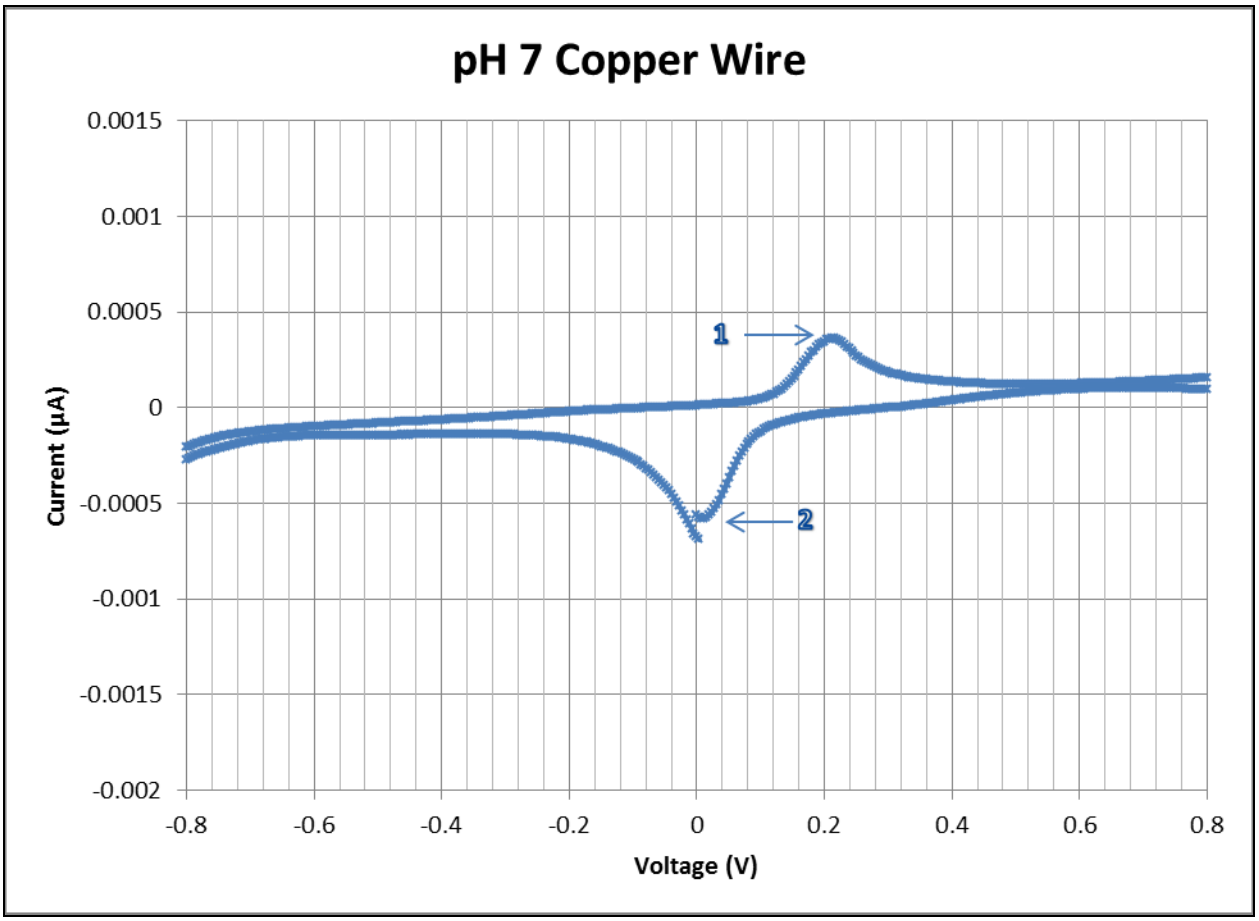

Figure 24: pH 7 Copper Wire Voltammagram

Table IX: pH 7 Copper Wire System Reactions

Peak	E_H Value (V)	Reaction
1	0.04 to 0.27	$Cu° + H_2O + = CuOH + H^+ + e^-$
2	0.22 to -0.15	$CuOH + H^+ + e^- = Cu° + H_2O$

Upon completion of this test, a concentration of 1 x 10^{-5} M of PAX was added to the buffer solution. **Figure 25** shows the resulting voltammagram, which indicates the appearance of new peaks, one of which is barely noticeable. It is important to note that hydrophobic films can passivate the surface and cause peaks to shift; oxidation peaks to higher potentials and reduction peaks to lower potentials.

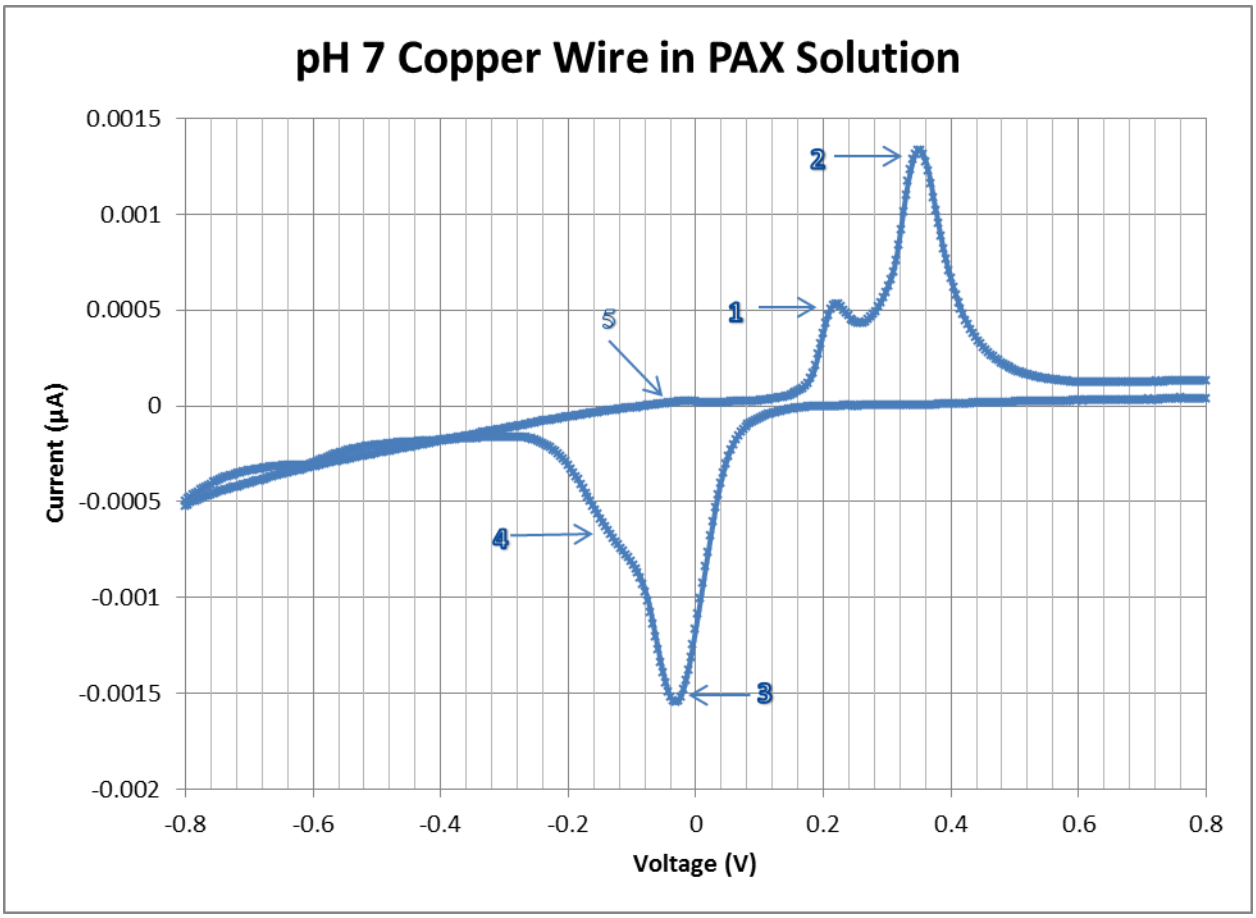

Figure 25: pH 7 Copper Wire in PAX Solution

Peaks 1 and 3 appear to be similar to those obtained without PAX. Peaks 2 and 4 must be due solely to PAX reacting with a film of CuOH/Cu_2O created with the copper surface reacting with water. The first peak shows the xanthate forming copper xanthate, while the fourth peak shows the xanthate coming off the copper surface. A second reaction shows the possible

formation of dixanthogen, and the third reaction is the reverse of this formation. The fifth peak is the formation of adsorbed xanthate, calculated and shown in the previous isotherm. As noted in **Table X,** this reaction appears at approximately -0.14V, which compares well to **Figure 19.**

Table X: pH 7 Copper Wire in PAX Reactions

Peak	Eh Value (V)	Reaction
1	0.14 to 0.23	$Cu° + X^- = CuX + e^-$
2	0.23 to 0.51	$CuX + 2OH^- = Cu(OH)_2 + 1/2X_2 + 2e^-$
3	0.09 to -0.14	$Cu(OH)_2 + 1/2X_2 + 2e^- = CuX + 2OH^-$
4	-0.18 to -0.22	$CuX + e^- = Cu° + X^-$
5	-0.14 to 0.08	$X^- = X_{ads} + e^-$

Two previous peaks are still present, but are shifted due to the surface being hydrophobic as a result of the presence of CuX and/or X_{ads}. In this regard, the hydrophobic surface does not react until significant underpotentials are able to allow for reaction back to metallic copper.

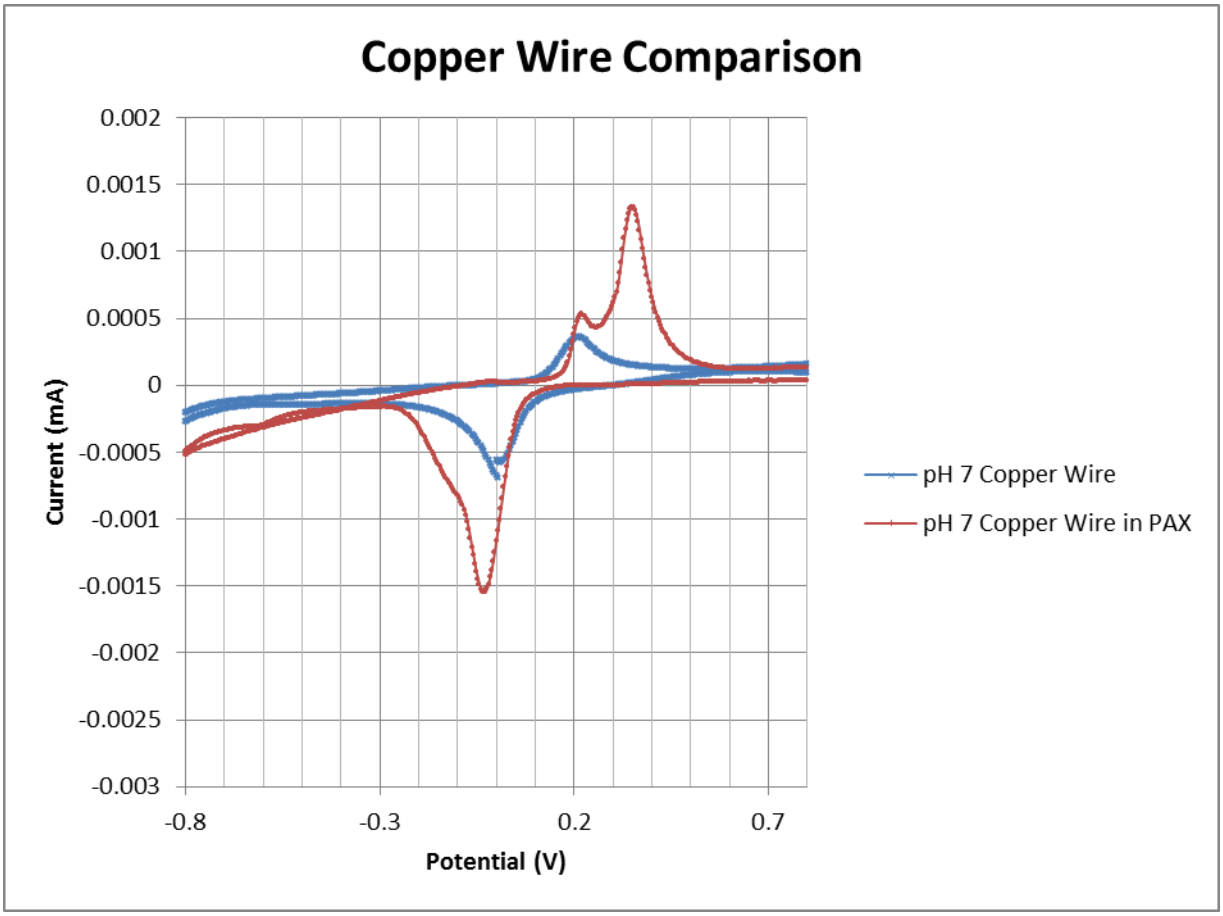

Figure 26: pH 7 Overlay Comparison of Copper

Figure 26 shows the voltammagram of the copper wire in the buffer solution with and without xanthate. The peaks from the copper wire in the buffer solution are shown as the curve with smaller peaks, while the PAX system yielded the larger peaks. The peaks of the PAX system match the copper wire system almost exactly, except for a slight shift to higher potentials. It is noted that the peaks in the presence of xanthate become narrower and higher. The negative peaks represent the desorption of xanthate from the copper surface.

The tests conducted at pH 12 are shown in **Figure 27** and **Figure 28**. The four peaks shown in **Figure 27** are characteristic of the copper wire reactions.

Table XI: pH 12 Copper Wire

Peak	E_H Value (V)	Reaction
1	-0.14 to 0.10	$Cu° + OH^- = CuOH + e^-$
2	0.12 to 0.25	$CuOH + OH^- = Cu(OH)_2 + e^-$
3	0.00 to -0.14	$Cu(OH)_2 + e^- = CuOH + OH^-$
4	-0.30 to -0.70	$CuOH + e^- = Cu°+ OH^-$

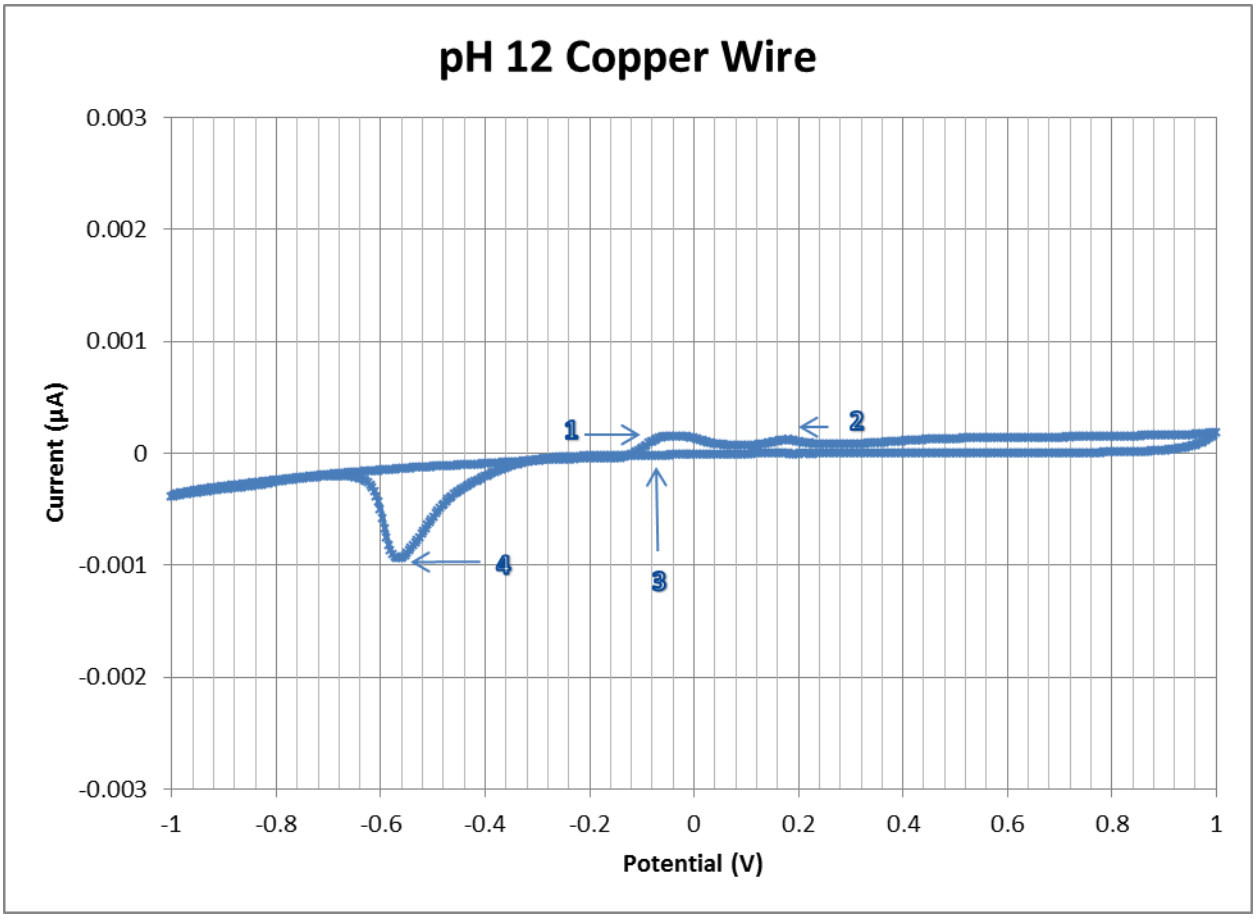

Figure 27: pH 12 Copper Wire Voltammagram

There are more peaks in the pH 12 system than were present at pH 7, due to the shift in copper oxide regions from the E_H-pH diagram. Copper can form an oxide layer more readily at greater pH values. At pH 12, CuOH readily oxidizes on the surface to $Cu(OH)_2$. At pH 7, CuOH does not readily precipitate as $Cu(OH)_2$, hence the singular set of peaks on the pH 7 voltammagram of copper wire.

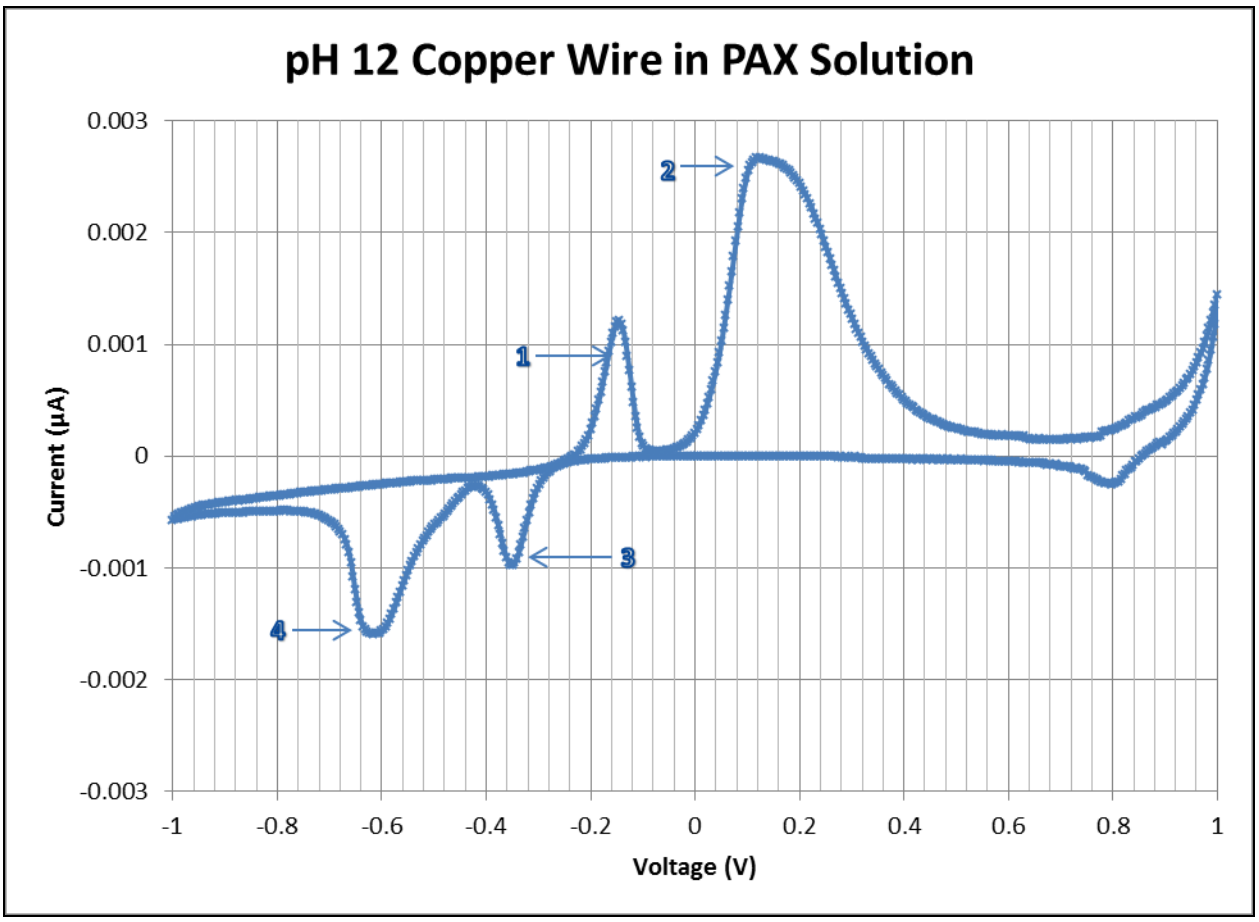

Figure 28: pH 12 Copper Wire in PAX Voltammagram

Figure 28 shows the voltammagram for copper in 10^{-5}M PAX solution. The peaks from the copper wire are present in the xanthate voltammagram with copper, but are once again amplified due to the adsorption of xanthate onto the copper surface. The reactions at peaks 1 and 2 appear to be the same as observed at pH 7 but shifted to lower potentials because of the pH being 12. Peaks 3 and 4 are also the same but are significantly shifted due to underpotentials needed to overcome the hydrophobicity. **Table XII** shows the deduced reactions based on the E_H-pH diagram of the Copper/Amyl Xanthate system.

Table XII: Copper Wire in PAX Reactions

Peak	E_H Value	Reaction
1	-0.23 to -0.03	$Cu^0 + X^- = CuX + e^-$
2	-0.03 to 0.55	$CuX + 2OH^- = Cu(OH)_2 + 1/2X_2 + 2e^-$
3	-0.19 to -0.39	$2e^- + Cu(OH)_2 + 1/2X_2 = CuX + 2OH^-$
4	-0.41 to -0.78	$CuX + e^- = Cu^0 + X^-$

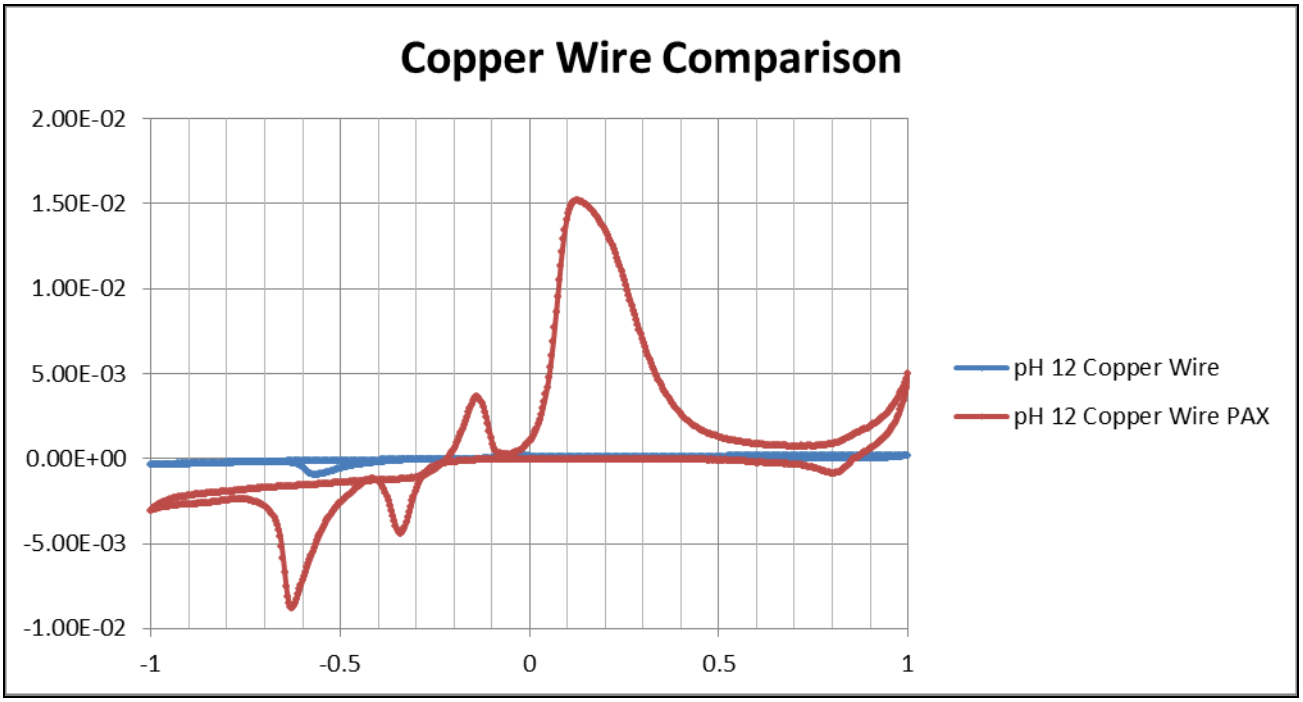

Figure 29: pH 12 Overlay Comparison of Copper Wire in the Absence and Presence of 10^{-5}M PAX

Figure 29 shows the voltammagrams of the copper wire at pH 12 in the absence and presence of PAX. The addition of the xanthate to the system caused the copper peaks to shift an average of -0.35 Volts, or the equivalent of -0.07V/pH, as shown in **Table XIII** by taking:

$$\frac{Average\ Voltage\ Difference}{pH\ Difference} = \frac{0.36}{pH\ 12-7}.$$

The slope is close to the expected value of -0.06V/pH because redox reactions show one e^- per H^+ being involved.

Table XIII: Voltage Shift Due To pH Change

No PAX	Peak 1	Peak 2
pH 12	-0.16	-0.32
pH 7	0.08	0.12
Difference	0.24	0.48
EH/pH	.048	.096
Average	.072	

The second peak of the xanthate system is large and broad, presumed to be due to the kinetics of the system as well as the changing surface conductivity. Two chemical reactions are occurring (see**Table XIV**) almost simultaneously. The copper (I) oxide reaction has not yet completed before the copper (II) oxide reaction begins to occur, which in turn registers as one large peak on the voltammagram.

It was initially presumed that PAX adsorbed onto the surface of the copper. It is evident that the reactions viewed were the oxidation and reduction reactions of copper with oxygen. Thus, the presumed monolayer of chemisorbed xanthate did not occur, but rather was representative of a passivating copper oxide film.

Table XIV: Voltage Shift Due To pH Change With Xanthate

With PAX	Peak 1	Peak 2	Peak 3	Peak 4
pH 12	-0.24	-0.06	-0.24	-0.42
pH 7	0.12	-0.26	0.12	-0.08
Difference	0.36	0.32	0.36	0.34
E_H/pH	0.07	0.06	0.07	0.06
Average	.065			

5.2.2. Enargite

Upon completion of the copper wire testing, the enargite electrode was tested at the same pH values, both with and without PAX. Voltammagrams at pH 7 and pH 12 are again presented. A compilation of voltammagrams collected at other pH buffers can be found in the Appendices. Results at pH 8, 9 and 10 are similar to pH 7, whereas pH 11 is similar to pH 12. It is important to note again that peaks shift in the absence of xanthate are likely pH dependent; whereas those in the presence can additionally be affected by hydrophobicity.

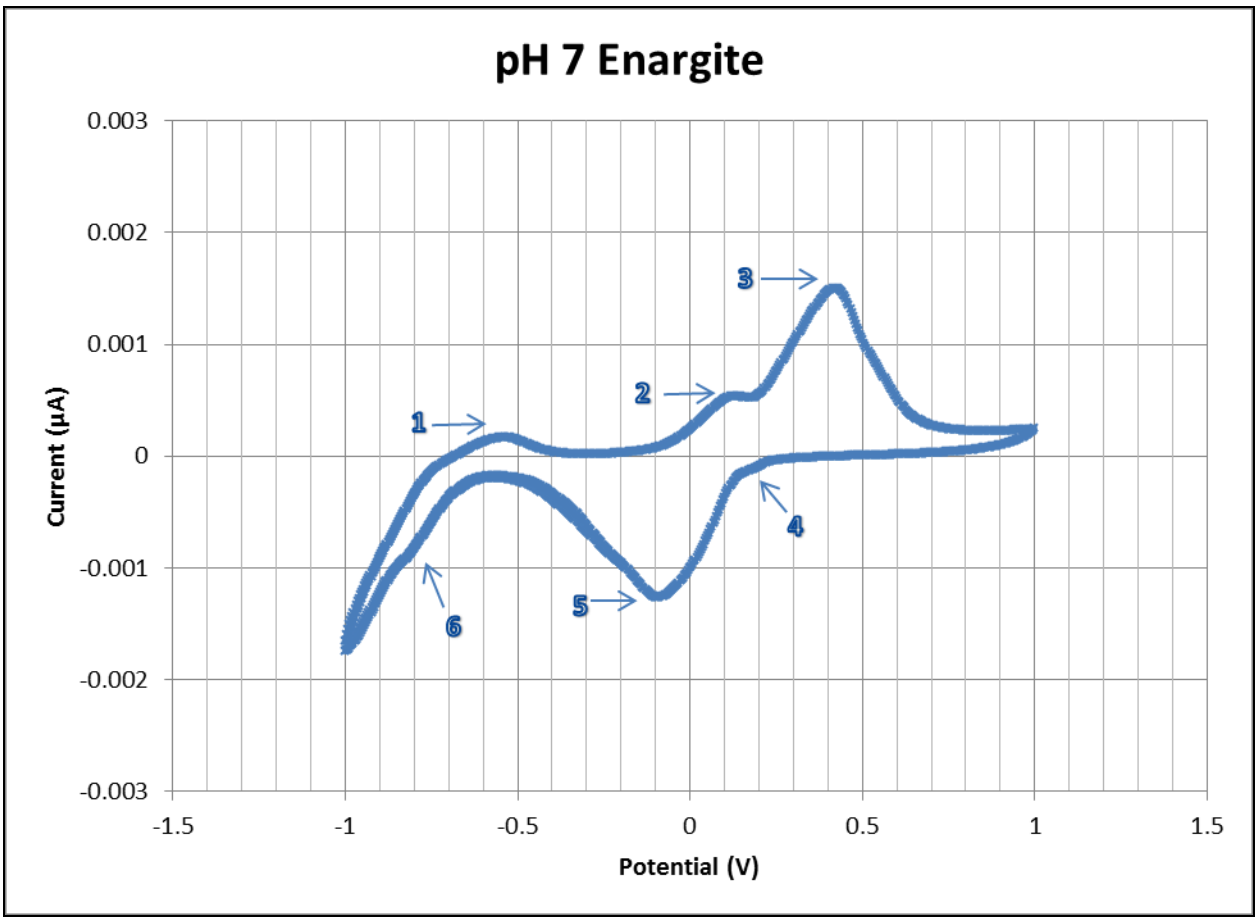

Figure 30: pH 7 Enargite Voltammagram

Table XV : pH 7 Enargite Reactions

Peak	E_H Value (V)	Reaction
2	0.05 to 0.20	$Cu_3AsS_4 + 3H_2O = 3CuS + H_3AsO_3 + S^o + 3H^+ + 3e^-$
3	0.20 to 0.65	$2CuS + HAsO_4^{2-} + H_2O = Cu_2As_4OH + 2S^o + 2H^+ + 4e^-$
4	0.24 to 0.13	$Cu_2As_4OH + 2S^o + 2H^+ + 4e^- = 2CuS + HAsO_4^{2-} + H_2O$
5	0.13 to -0.45	$3CuS + H_3AsO_3 + S^o + 3H^+ + 3e^- = Cu_3AsS_4 + 3H_2O$
6	-0.74 to -0.87	$Cu_3AsS_4 = (Cu_{12}As_4S_2/Cu_6As_4S_9) = 3/2Cu_2S + As^o + 5/2HS^- + 5/2H^+ + 5e^-$
1	-0.60 to -0.40	$3/2Cu_2S + As^o + 5/2HS^- + 5/2H^+ + 5e^- = (Cu_{12}As_4S_2/Cu_6As_4S_9) = Cu_3AsS_4$

Figure 30 shows the voltammagram of enargite at pH 7. The six peaks labeled are characteristic of enargite at pH 7 (Gow et al., 2015; Gow, 2015). Peak 2 corresponds to enargite oxidation to covellite (CuS) and elemental sulfur (S^o) as well as either arsenite (H_3AsO_3) or arsenate ($HAsO_4^{2-}$). Olivenite (Cu_2AsO_4OH) forms at higher potentials giving rise to Peak 3. These reactions are reversed (peaks 4 and 5) to reproduce enargite. Further reduction yields peak 6 corresponding to a series of reactions in which tennantite ($Cu_{12}As_4S_{13}$) and sinnerite ($Cu_6As_4S_9$) form along with chalcocite (Cu_2S) and bisulfide (HS^-). When the potential is reversed, these products react to reform enargite (peak 1). These reactions are depicted in **Table XV** and can be seen by the E_H-pH diagram in **Figure 31** from Gow et al. (2015) and Gow (2015).

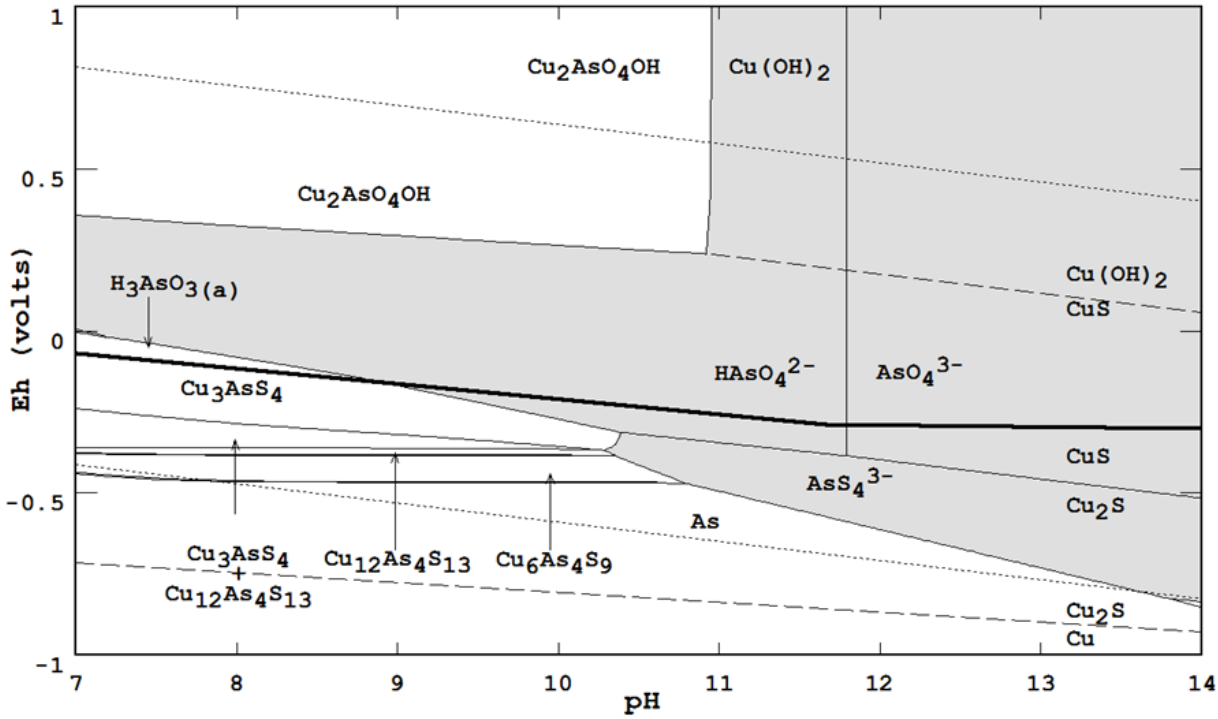

Figure 31 : E_H-pH Diagram of Enargite (Gow et al., 2015; Gow, 2015)

Figure 31 shows the species of copper, arsenic and sulfur between pH 7-14. As shown in the E_H-pH diagram, elemental sulfur forms above the solid line. In this study, no sulfoxy species such as sulfate (SO_4^{2-}) were considered. Hence, the bold solid line denotes the equilibrium between elemental sulfur (S^o) and sulfide (S^{2-}, HS^-, and H_2S) with S^o stable above the line.

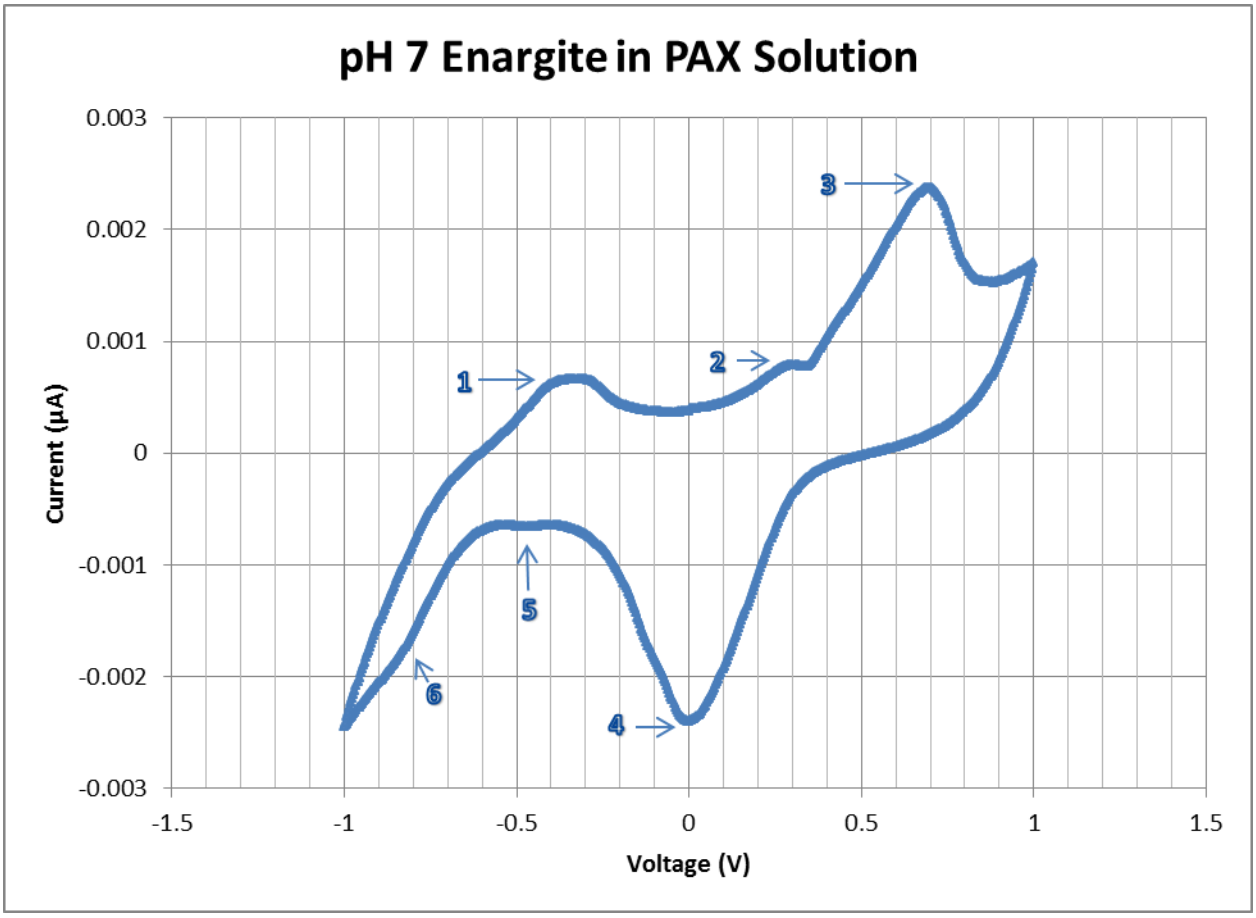

Figure 32: pH 7 Enargite in 10^{-5} M PAX Solution

Figure 32 depicts the voltammagrams of enargite obtained in the presence of PAX at pH 7. It appears that the peaks are the same six peaks but close examination indicates that they are slightly shifted, presumably due to PAX forming a hydrophobic coating on the surface. There is no evidence that X_{ads} forms because no new peaks are observed, particularly between peaks 1 and 2 where it would be expected.

Figure 30 and **Figure 32** are compared in **Figure 33**. Clearly, the presence of xanthate enhances the reactions depicted in **Table XV.** This is attributed to CuX formation and increases the amount of various products such as covellite. Hence, **Table XVI** is similar to **Table XV** with the exception of CuX.

Table XVI : pH 7 Enargite in PAX Reactions

Peak	E_H Value (V)	Reaction
2	0.00 to 0.33	$Cu_3AsS_4 + X^- + 3H_2O = CuX + 2CuS + H_3AsO_3 + 2S^o + 3H^+ + 4e^-$
3	0.33 to 0.75	$CuS + X^- = CuX + S^o + e^-$
4	0.50 to -0.30	$CuX + S^o + e^- = CuS + X^-$
5	-0.40 to -0.60	$CuX + 2CuS + H_3AsO_3 + 2S^o + 3H^+ + 4e^- = Cu_3AsS_4 + X^- + 3H_2O$
6	-0.70 to -0.90	$Cu_3AsS_4 = (Cu_{12}As_4S_2/Cu_6As_4S_9) = 3/2Cu_2S + As^o + 5/2HS^- + 5/2H^+ + 5e^-$
1	-0.60 to -0.15	$3/2Cu_2S + As^o + 5/2HS^- + 5/2H^+ + 5e^- = (Cu_{12}As_4S_2/Cu_6As_4S_9) = Cu_3AsS_4$

Figure 33 shows the overlaid diagram of enargite and enargite in PAX.

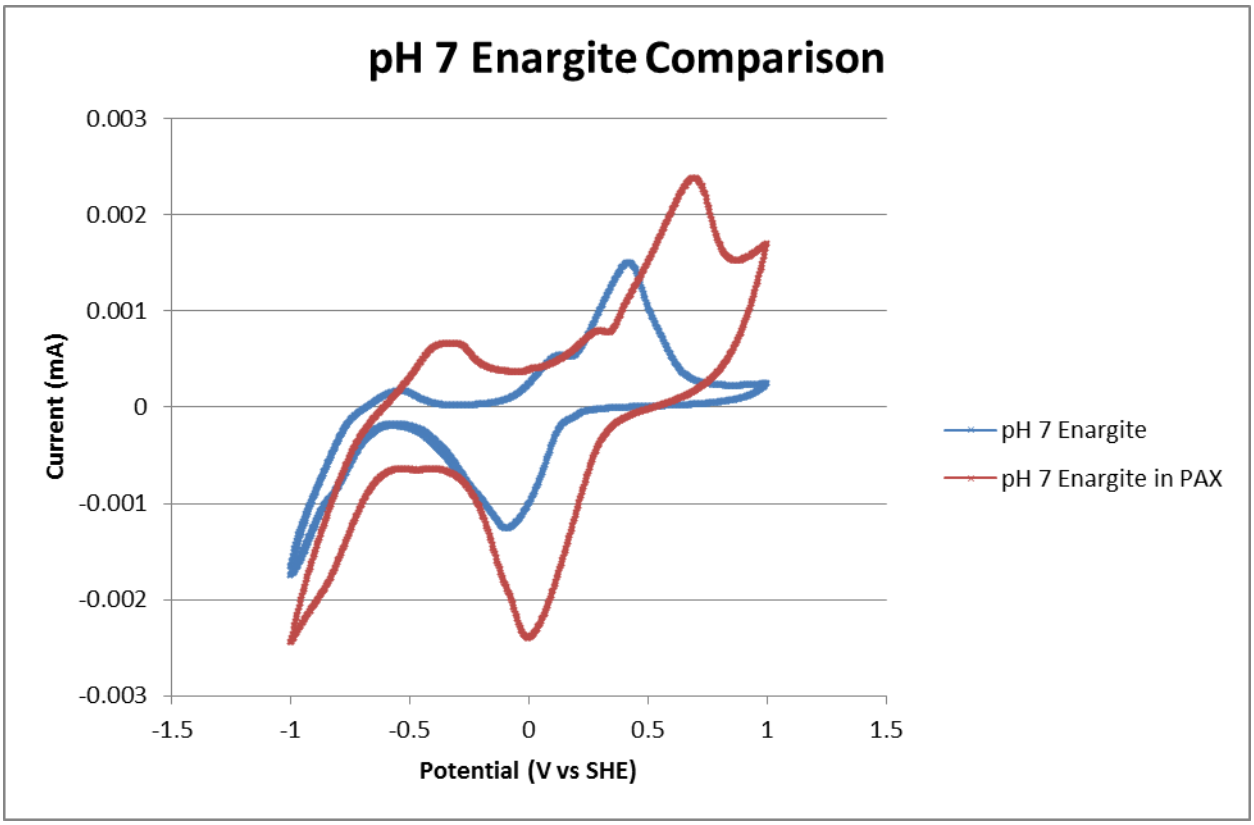

Figure 33: pH 7 Overlay Comparison of Enargite

Therefore, according to the voltammetry at pH 7, CuX does not form unless the E_H exceeds 0 mV. **Figure 31** shows this coincides with CuS stability and would be in agreement with the reactions proposed in **Table XVI**, particularly peak 2.

Table XVII : pH 12 Enargite

Peak	E_H Value (V)	Reaction
2	-0.38 to -0.15	$Cu_2S + 1/2AsS_4^{3-} + 2H_2O = 2CuS + 1/2AsO_4^{3-} + S^o + 4H^+ + 4e^-$
3	-0.09 to 0.40	$AsS_4^{3-} + 4H_2O = AsO_4^{3-} + 4S^o + 8H^+ + 8e^-$
4	0.55 to 0.64	$CuS + 2H_2O = Cu(OH)_2 + S^o + 2H^+ + 2e^-$
5	-0.19 to -0.69	$CuS + 3/2AsO_4^{3-} + 6S^o + 14H^+ + Cu(OH)_2 + 14e^- = Cu_2S + 3/2AsS_4^{3-} + 8\ H_2O$
6	-0.85 to -0.95	$AsS_4^{3-} + 4H^+ + 5e^- = As^o + 4HS^-$
1	-0.70 to -0.50	$As^o + 4HS^- = AsS_4^{3-} + 4H^+ + 5e^-$

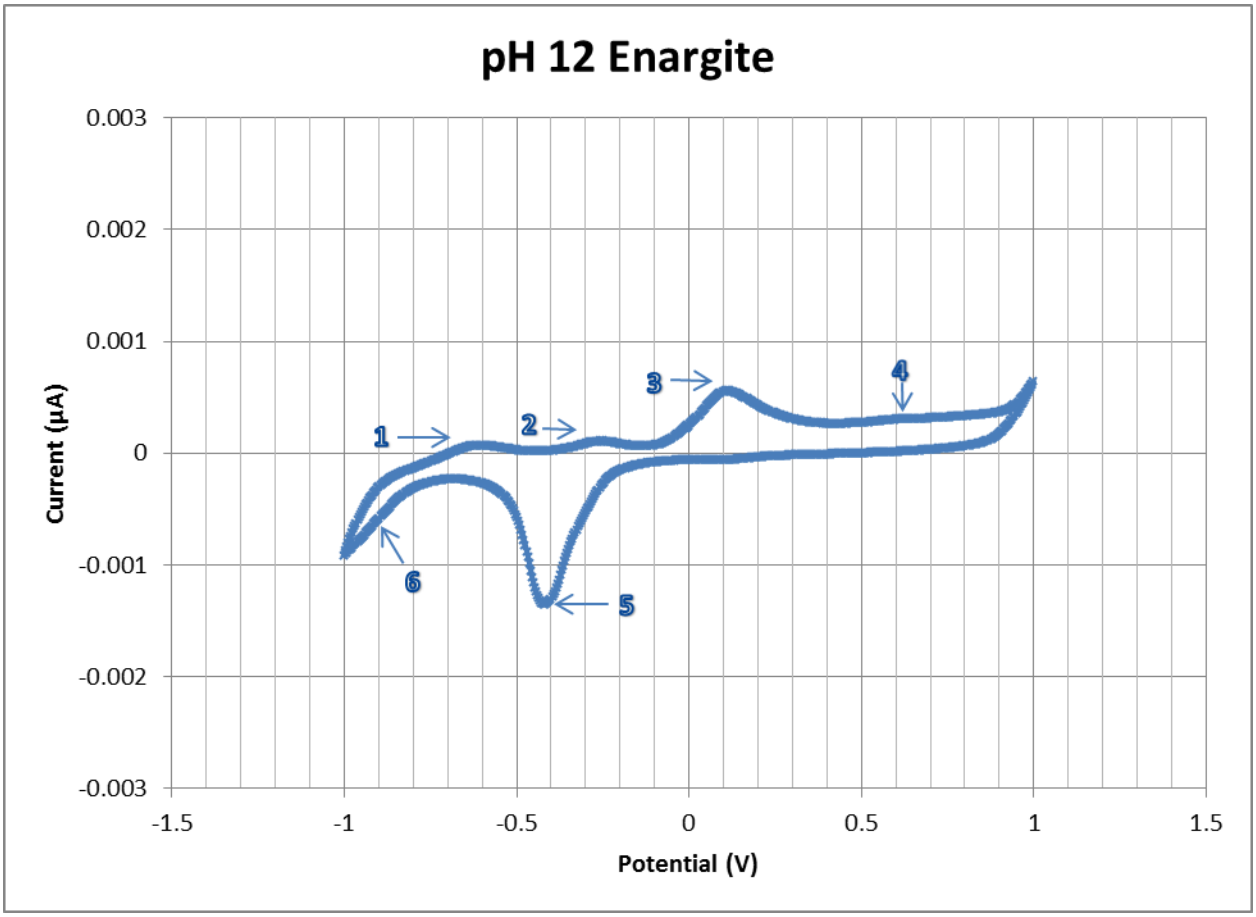

Figure 34 : pH 12 Enargite Voltammagram

Figure 34 shows the voltammagram obtained for enargite at pH 12 in the absence of PAX. The results compare well with **Figure 31.** To begin, enargite is not stable at this pH and likely decomposes, as interpreted from **Figure 31**.

$$Cu_3AsS_4 + 3OH^- + 3e^- = Cu_2S + CuS + 1/2AsS_4^{3-} + 1/2AsO_3^{3-} + 3/2H_2O$$

Equation 18: Enargite Decomposition

Figure 31 suggests this reaction occurs at pH > 10.5. However, resulting chalcocite (Cu_2S) oxidizes to covellite (CuS) as depicted in **Table XVII** giving rise to peak 2. Peak 4 is then caused by covellite oxidizing to cupric hydroxide ($Cu(OH)_2$) and elemental sulfur (S^o). Peak 3 is the redox equilibrium between thioarsenate (AsS_4^{3-}) and arsenate (AsO_4^{3-}). Because cupric hydroxide passivates the surface, the reverse of peaks 2-4 are observed simultaneously as peak 5. Peak 6 results from the equilibrium of arsenic (As^o) and thioarsenate (AsS_4^{3-}) and is reversed as Peak 1.

Figure 35 shows the voltammagram obtained for enargite at pH 12 in the presence of PAX. Proposed reactions are shown in **Table XVIII**. As occurred at pH 7, xanthate enhances the reactions, particularly those causing peaks 3 and 4 and consequently peak 5. Likewise, it is attributed to CuX formation. Peak 3 initiates near 0 mV and is attributed to covellite (CuS), the same as peak 3 at pH 7. This reaction is pH-independent and therefore depicted in **Figure 36** as a horizontal line near 0 mV. **Table XVIII** shows the reactions at each peak seen in **Figure 35.**

Table XVIII : pH 12 Enargite in PAX Reactions

Peak	E_H Value (V)	Reaction
2	-0.21 to 0.00	$Cu_2S + 1/2AsS_4^{3-} + 2H_2O = 2CuS + 1/2AsO_4^{3-} + S^o + 4H^+ + 4e^-$
3	0.15 to 0.56	$CuS + X^- = CuX + S^o + e^-$
4	0.56 to 0.95	$CuX + 2OH^- = Cu(OH)_2 + X^- + e^-$
5	-0.05 to -0.65	$CuS + 1/2AsO_4^{3-} + 2S^o + Cu(OH)_2 + 4H^+ + 6e^- = Cu_2S + 1/2AsS_4^{3-} + 2H_2O + 2OH^-$
6	-0.85 to -0.95	$AsS_4^{3-} + 4H^+ + 5e^- = As^o + 4HS^-$
1	-0.60 to -0.25	$As^o + 4HS^- = AsS_4^{3-} + 4H^+ + 5e^-$

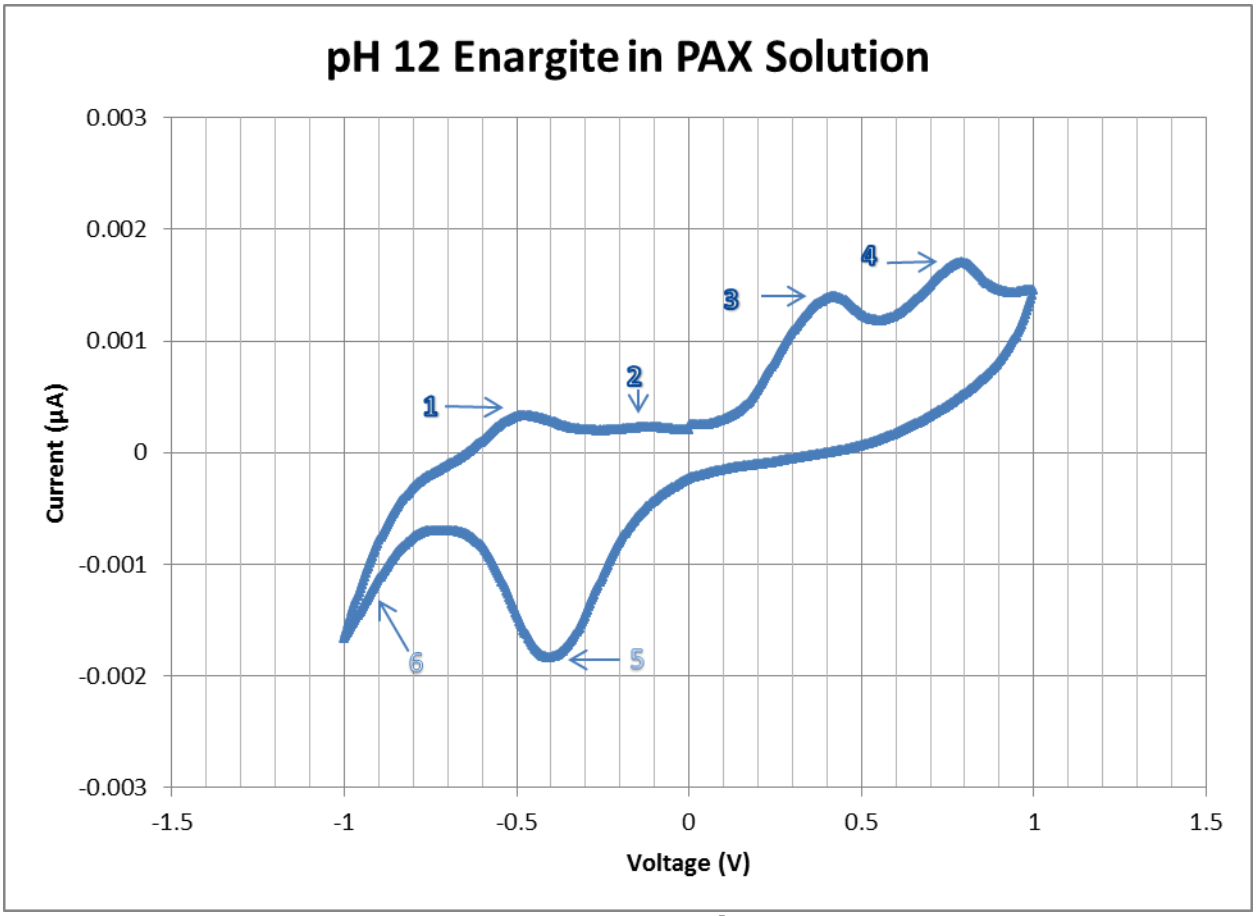

Figure 35 : pH 12 Enargite in 10^{-5}M PAX solution

The purpose of this study was to determine if xanthate chemisorbs in the enargite-xanthate system. As already noted, X_{ads} was not observed on enargite at pH 7. For metallic copper, it was observed at pH 7 and not pH 12. It makes sense to conclude that X_{ads} does not

occur on enargite at pH 12. Furthermore, based on another perspective, enargite is not stable above pH 10.5. Under these conditions, chalcocite and covellite are stable. Woods et al. (1991) showed Potassium Ethyl Xanthate chemisorbed (see **Figure 23**) on chalcocite so it is reasonable to conclude Potassium Amyl Xanthate likely would as well. A detailed analysis of the voltammagrams obtained at other pH values, however, do not indicate the presence of new peaks just below 0 mV, particularly at pH 11. It is reasonable to conclude that the formation of thioarsenate (AsS_4^{3-}), arsenate (AsO_4^{3-}) and/or arsenite (AsO_3^{3-}) prevents it from occurring, much like a depressant. In this regard, the E_H – pH diagram shown in **Figure 36** for the PAX-enargite system appears to be accurate.

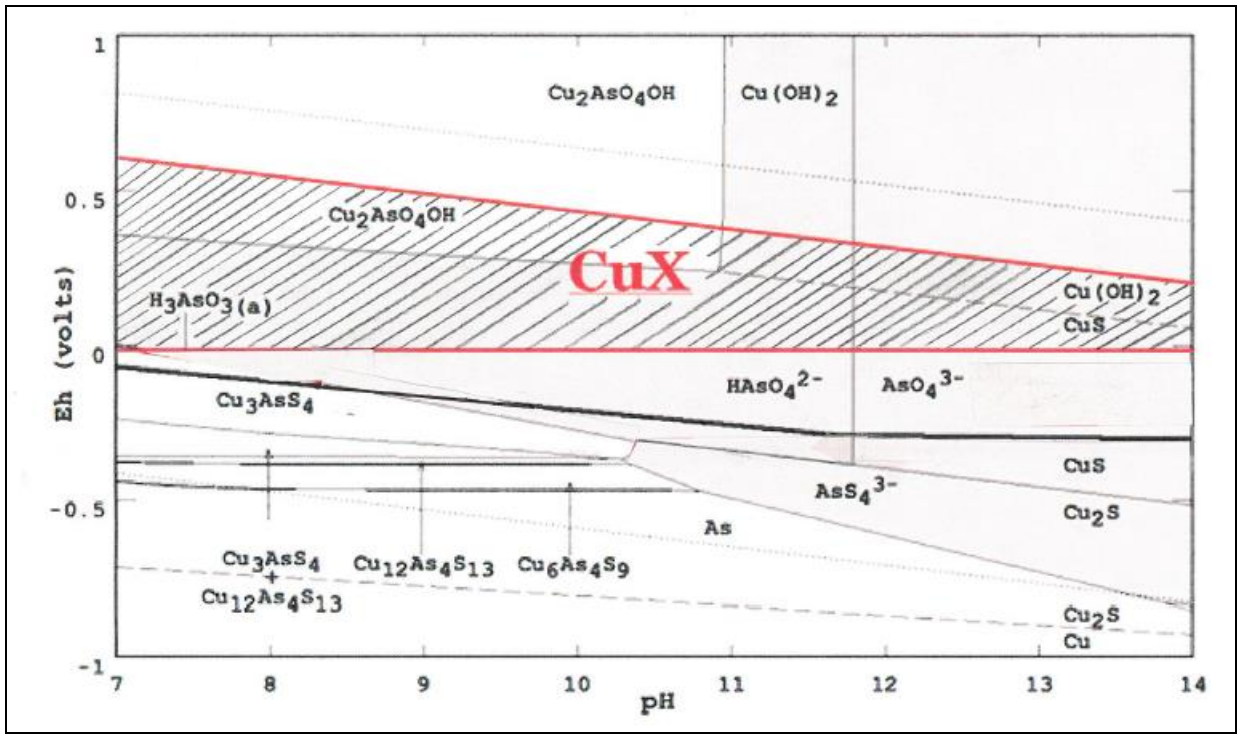

Figure 36 : E_H-pH Diagram of Enargite with Xanthate

5.3. Theoretical Flotation Values

As has been shown from the E_H-pH study, as well as the development of the isotherm at pH 7, the flotation of copper using PAX is possible in the range of pH 7-12, at an E_H of approximately -0.25, which is the potential at which the reaction seen in **Equation 19** occurs.

$$X^- = X_{ads} + e^- \qquad \textbf{Equation 19: Xanthate Chemisorption}$$

This represents the xanthate adsorption reaction onto the copper surface. As the E_H decreases, however, the possible flotation decreases, because the region of stability of xanthate chemisorption decreases. The potential becomes increasingly critical as the pH is increased because the potential must be controlled more finely in order not to cross into the region where CuOH forms on the E_H-pH diagram.

Regardless of this fact, it is evident through all performed experiments that copper can be floated between pH 7-12. All diagrams of copper exhibit peaks indicative of xanthate adsorption. The pH and E_H of xanthate adsorption is shown in **Table XIX**. As shown earlier in **Figure 20,** the potential range where flotation is expected to occur decreases with increasing pH.

Table XIX: Overall Xanthate Adsorption Values For Copper

pH	Cu E_H (V) Range of Formations	X_{ads} E_H (V) Range of Formations	CuX E_H (V) Range of Formations
7	-0.27 to -0.54	-.25 to -.04	-.04 to .40
8	-0.31 to -0.61	-.25 to -.04	-.04 to .34
9	-0.26 to -0.88	-.25 to -.07	-.07 to .28
10	-0.31 to -0.61	-.25 to -.13	-.13 to .22
11	0.07 to -0.75	-.25 to -.19	-.19 to .16
12	0.01 to -0.62	Not Stable	-.25 to .10

In addition to peak amplification and new peak formation, the introduction of PAX caused the shift of peak position from the original voltammagrams. **Table XX** shows the voltage that the original copper peaks were shifted upon the addition of PAX. Such results suggest that copper flotation with PAX might be best at pH 9 and 10, which is often the case in industry.

Table XX: Copper Peak Shifts Upon PAX Addition

	pH 7	pH 8	pH 9	pH 10	pH 11	pH 12
Shift (V)	-0.01	0.02	0.11	0.11	0.04	-0.07

All copper wire peaks were amplified upon the addition of PAX to the system. New peaks were present in the pH 7 system due to the adsorption of xanthate onto the surface of the copper wire, and the position of the original peaks were shifted by -0.01 Volts. In the pH 8 copper system, the original peaks were amplified because the presence of PAX adsorption peaks occurred at about the same E_H as the original copper peaks, so it appears that the peaks merged. Peaks were shifted by about 0.02 Volts. In the pH 9 copper system, several new peaks were generated due to the xanthate addition, but the original peaks were shifted significantly, by about 0.11 Volts. In the pH 10 system, the peaks were shifted by 0.11 Volts, and the peaks were amplified, but also widened. An increase in width was due to the increased amount of time required for the surface reactions to occur. At pH 11, the copper wire peaks were shifted by about 0.04 Volts. The pH 12 copper system had a great increase in magnitude and peak width, and the peak shift observed was -0.07 Volts.

Similarly for enargite, the addition of PAX to the system had peaks shifting more significantly, as shown in **Table XXI**. At pH 7, the enargite system did not have any new peaks present. The largest peak shifted by 0.29 Volts upon PAX addition, and all of the peaks were amplified. At a pH of 8, the enargite system was only slightly shifted upon the addition of PAX, and no new peaks were observed; whereas at pH 9, the system was amplified upon the addition of PAX, and the greatest peak was shifted by 0.31 Volts. The pH 10 system showed a shift of 0.21 Volts of the greatest peak, and the peaks were amplified by the addition of PAX. Similarly, pH 11 system underwent the greatest peak shift of 0.37 Volts and also had peak broadening. Likewise, at pH 12 the enargite system had a shift of 0.31 Volts. All of these effects were

observed when xanthate was added to the enargite system, but as previously stated, X_{ads} was not observed on enargite at pH 7. Enargite is also unstable above pH 10.5. Therefore, despite the observance of shifted peaks in the enargite-xanthate system, it is reasonable to conclude that Potassium Amyl Xanthate does not chemisorb onto the enargite surface.

Table XXI: Enargite Peak Shifts Upon PAX Addition

	pH 7	pH 8	pH 9	pH 10	pH 11	pH 12
Shift (V)	0.29	-0.10	0.31	0.21	0.37	0.31

However, if the enargite-PAX system is analyzed like that of the copper-PAX system as shown in **Table XXI**, one can see from **Table XXII** that the dramatic peak shifts observed for enargite may not be due to CuX formation but rather to the presence of sulfur in the system, more specifically, to the formation of elemental sulfur (S^o). As such, its presence could lead to flotation without a collector; suggesting that enargite flotation with PAX is induced by both CuX and S^o, which depends on the potential of the system.

Table XXII - Overall Xanthate Adsorption Values For Enargite

pH	X_{ads} E_H (V) Range of Formations	CuX E_H (V) Range of Formations	S^oE_H (V) Range of Formations
7	Not Stable	-.04 to .40	> = -.04
8	Not Stable	-.04 to .34	> = -.09
9	Not Stable	-.04 to .28	> = -.14
10	Not Stable	-.04 to .22	> = -.19
11	Not Stable	-.04 to .16	> = -.25
12	Not Stable	-.04 to .10	> = -.30
13	Not Stable	-.04 to .04	> = -.30
14	Not Stable	-.04 to -.02	> = -.30

6. Conclusions

6.1. Previous work

Ma and Bruckard (2009) found in their research that the flotation of enargite depends on pulp potential. Haga, Tongamp and Shibayama (2012) found that enargite was flotable at pH 11in the presence of PAX. Centin Kantar (2002) found that as the potential is increased, a copper oxide layer may form on the surface of enargite. The copper oxide layer that may form is seen in the E_H-pH diagram of enargite; and, in this case, would be expected to prevent xanthate from adsorbing onto the surface of the enargite.

6.2. Copper Results

An isotherm of copper at pH 7 was found by integrating the area under voltammetric curves and using ratios of each curve to the largest curve, assumed to be the monolayer. The ratio of these curves to the overall curve allowed for the generation of an isotherm, showing the surface coverage of the copper with xanthate. The generated isotherm matched extremely well with the Frumkin Isotherm, as derived in Chapter 5. Thus, it was demonstrated that xanthate adsorbs onto copper.

6.3. Enargite Results

Previous authors found that the flotation of enargite using xanthate collector is possible. The collector used in this study was Potassium Amyl Xanthate (PAX). Xanthate should adsorb onto enargite, thereby forming either chemisorbed xanthate or copper xanthate precipitate, either of which allow for flotation. The hindrance of the flotation comes from the formation of a copper oxide surface layer at oxidizing potentials, or nothing at reducing potentials. The formation of copper oxide occurs above specific E_H values that differ across the pH region, as shown in **Figure 20** and **Figure 36.** If kept below the CuOH formation line, the adsorption of xanthate

should occur. However, chemisorbed xanthate was only observed on metallic copper, and not on enargite.

6.4. Further Test Work

Further evaluation of copper could be extremely beneficial to the mineral processing industry. Isotherms for copper using PEX have been found at pH 6.8 and 9.2 in a study by Dr. Courtney Young, and at pH 12 presented in this study. The generation of copper isotherms at pH values 8, 10, 11 and 12 using PEX, and the generation of copper isotherms using PAX at pH values 8, 9, 10, 11, and 12 would give much information on the copper system using these collectors. The isotherm data would also allow for better flotation recovery predictions by controlling the E_H values to yield optimum recovery. Micro-flotation tests of enargite at the previously mentioned values with the collectors listed would also be beneficial to the mineral processing community.

In addition, a voltammetric study of enargite using the collector PEX at the parameters of this study would be beneficial to the mineral processing industry, specifically to the operations using PEX as the collector. PAX was determined to have a stability range of -0.06mv to -0.22mV. In research performed by Woods, Young and Yoon, PEX was determined to have a stability range of -0.25 to -0.45 mV. Such stability range leads to an interesting observation that the length of the hydrocarbon chain of the xanthate (ethyl, butyl, propyl, amyl) may not only change the potential range in which that the xanthate can chemisorb in, but it may also cause a shift in the range of chemisorption. Follow up research could include the examination of the xanthate chemisorbed regions of stability changing which xanthate hydrocarbon was used (PAX, PEX, SIPX, etc). Assuming a linear change in potential correlating to the length of the hydrocarbon, **Table XXIII** is a prediction of the potential ranges shifting due to chain length.

Table XXIII-Potential Range Corresponding to Hydrocarbon Chain Length

Hydrocarbon	Potential Range (mV)
Ethyl	-0.25 to -0.45
Propyl	-0.18 to -0.36
Butyl	-0.12 to -0.30
Amyl	-0.06 to -0.22

Additionally, several other tests could have been performed that would have added to this study, including;

- An enargite sample could be obtained, in addition to copper, so micro-flotation tests could be conducted
- Further analysis using Raman spectroscopy would be useful to show spectro-electrochemical results
- Testing enargite voltammetrically using the previously listed xanthates to systematically study effects of hydrocarbon chain length

Bibliography

Allied Corrosion Industries Inc. *Cathodic Protection System Design for TDF-L Reactor/Wash Station*. Marietta: Cathodic Protection System Design for TDF-L Reactor/Wash Station, 2000.

Allison, S. A., et al. "A determination of the products of reaction betweer various sulfide minerals and aqueous xanthate solution, and a correlation of the products with electrode rest potentials." *Metallurgical Transactions* (1972): 2613-2618.

Asbjornsson, J., et al. "Electrochemical and Surface Analytical Studies of Enargite in Acid Solution." *Journal of The Electrochemical Society* (2004): E250-E256.

ASTM. "Standard Practice of Conventions Applicable to Electrochemical Measurements in Corrosion Testing." *ASTM: Designation: G 3-89*. May 1994.

Balaz, P., et al. "Influence of mechanical activation on the alkaline leaching of enargite concentrate." *Hydrometallurgy* (2000): 205-216.

Balaz, Peter and Marcela Achimovicova. "Mechano-chemical leaching in hydrometallurgy of complex sulphides." *Hydrometallurgy* (2006): 60-68.

Brenntag Canada Inc. *Material Safety Data Sheet Potassium Amyl Xanthate, Solid*. 17 June 2009. 10 February 2013. <http://reviewboard.ca/upload/project_document/EA0809-004_MSDS_for_Potassium_Amyl_Xanthate_1328896837.PDF>.

Castro, S. H. and L. Baltierra. "Study of the surface properties of enargite as a function of pH." *Int. J. Miner. Process.* (2005): 104-115.

Castro, S. H., L. Baltierra and C. Hernandez. "Redox Conditions in the Selective Flotation of Enargite." Doyle, F. M., G. H. Kelsall and R. Woods. *Electrochemistry in Mineral and Metal Processing VI*. Pennington: The Electrolchemical Society, Inc., 2003. 27-36. 10

February 2013. <http://books.google.com/books?id=LKLCIfs4jP4C&pg=PA32&lpg=PA32&dq=arsenic+floatability&source=bl&ots=syVztqzj5-&sig=R7Iz4veLpNx7b8OJDcXiukkJHsw&hl=en&sa=X&ei=OwAYUeuTHe_LigK6hYH4DA&ved=0CFcQ6AEwCA#v=onepage&q=arsenic%20floatability&f=false>.

Chemistry, The Royal Society of. *Infrared Spectroscopy*. n.d. 27 January 2013. <http://media.rsc.org/Modern%20chemical%20techniques/MCT3%20Infrared.pdf>.

Cook, Nigel J. and Stephen L. Chryssoulis. "Concentrations of "invisible gold" in the common sulfides." *Canadian Mineralogist* (1990): 1-16.

Cordova, R., et al. "An electrochemical study of enargite in aqueous solutions by transient techniques." Woods, R., F. M. Doyle and P. Richardson. *Electrochemistry in Mineral and Metal Processing IV*. Pennington: The Electrochemical Society Proceedings Series, 1996. 356.

Cordova, R., H. Gomez and R. Schrebler. "An Electrochemical Study of Enargite in Aqueous Solutions by Transient Techniques." *Electrochemical Proceedings* (2005): 356-367.

Corporation, Nicolet Instrument. *Nicolet TQ*. Madison: Nicolet Instrument Corporation, 2000.

CSIRO. "Arsenic bubbles ease copper troubles." 2 February 2006. *Media Release.* 8 November 2011. <http://www.csiro.au/news/psl.148.htm>.

Cytec. *Mining Chemicals Handbook*. 2010.

Elsener, Bernhard, et al. "Electrochemical and XPS surface analytical studies on the reactivity of enargite." *Eur. J. Mineral* (2007): 353-361.

Fantauzzi, M., et al. "An XPS analytical approach to elucidating the microbially mediated enargite oxidative dissolution." *Anal Bioanal Chem* (2009): 1931-1941.

—. "The surface of enargite after exposure to acidic ferric solutions: an XPS/XAES study." *Surf. Interface Ana.* (2007): 908-915.

Ferron, C. J. and Q Wang. "Copper Arsenide Minerals as a Sustainable Feedstock for the Copper Company." *SGS Mineral Services: Technical Bulletin*. SGS, 2003. 11 February 2013. <http://www.sgs.com/~/media/Global/Documents/Technical%20Documents/SGS-MIN-WA330-Copper-arsenide-minerals-EN-11.pdf>.

Filippou, Dimitrios, Pascale St-Germain and Tassos Grammatikopoulos. "Recovery of Metal Values From Copper-Arsenic Minerals and Other Related Resources." *Mineral Processing & Extractive Metall. Rev.* (2007): 247-298.

Fornasiero, D., et al. "Separation of enargite and tennantite from non-arsenic copper sulfide minerals by selective oxidation or dissolution." *Int.J. Miner. Process* (2001): 109-119.

Forssberg, K. S. Eric, Britt-Marie Antti and Bertil I. Palsson. "Computer-assisted calculations of thermodynamic equilibria in the chalcopyrite-ethyl xanthate system." Rome: The Institution of Mining and Metallurgy, 1984. 251-264.

Fullston, D, D. Fornasiero and J. Ralston. "Oxidation of Synthetic and Natural Samples of Enargite and Tennantite: 2. X-ray Photoelectron Spectroscopic Study." Langmuir. American Chemical Society, 1999. 4530-4536.

Fullston, D., D. Fornasiero and J. Ralston. "Oxidation of Synthetic and Natural Samples of Enargite and Tennantite: 1. Dissolution and Zeta Potential Study." Langmuir. American Chemical Society, 1999. 4524-4529.

Fullston, Damian, Daniel Fornasiero and John Ralston. "Zeta potential study of the oxidation of copper sulfide minerals." *Colloids and Surfaces* (1999): 113-121.

Gardner, J. R. and R. Woods. "The use of a particulate bed electrode for the electrochemical investigation of metal and sulphide flotation." *Aust. J. Chem.* (1973): 1635-44.

Gaudin, A. M. and Reinhardt Schuhmann, Jr. *The Action of Potassium n-Amyl Xanthate on Chalcocite*. Study. Butte, 1935.

Gilbert, Thomas R., Rein V. Kirss and Geoffrey Davies. *Chemistry The Science in Context*. New York: W.W. Norton & Company, 2004.

Glagovich, Neil. *Infrared Spectroscopy*. 27 July 2007. 28 January 2013. <http://www.chemistry.ccsu.edu/glagovich/teaching/316/ir/table.html>.

Goldstein, Joseph, et al. *Scanning Electron Microscopy and X-ray Microanalysis*. New York: Kluwer Academic/Plenum Publishers, 2003.

Gow, R. N., et al. "Electrochemistry of Enargite: Reactivity in Alkaline Solutions." 2008.

Greenfacts. "Scientific Facts on Arsenic." 2011. *GreenFacts.* 8 November 2011. <http://www.greenfacts.org/en/arsenic/index.htm>.

Guo, H and W. T. Yen. "Selective flotation of enargite from chalcopyrite by electrochemical control." *Minerals Engineering* (2005): 605-612.

Guo, H. and W.-T. Yen. "Surface Potential And Wettability of Enargite in Potassium Amyl Xanthate Solution." *Minerals Engineering* 2 April 2002: 405-414.

Gupta, Mark Zachary. "An investigation into the leaching of enargite under atmospheric conditions." Kingston, May 2010.

Haga, K, W Tongamp and A Shibayama. "Separation of Enargite from Cu-Concentrate." *IMPC* (2012): 1871-1881.

Haynes, W. *CRC Handbook of Chemistry and Physics*. CRC Press, 2011.

Heavy Metal Toxicity. 2013. 6 February 2013. <http://www.patientsmedical.com/healthaz/heavymetaltoxicity/default.aspx>.

Henao, J. A., G. Diaz de Delgado and J. M. Delgado. "Single-Crystal Structure Refinement of Enargite [Cu3AsS4]." *Materials Research Bulletin* (1994): 1121-1127.

Huang, H. H. and J. D. Miller. "Kinetics and Thermochemistry of Amyl Xanthate Adsorption by Pyrite and Marcasite." *International Society of Mineral Processing* (1978): 241-266.

Huang, Hsin Hsiung and Courtney A. Young. "Mass-Balanced Calculations of Eh-pH Diagrams Using Stabcal." *Electrochemical Proceedings*. Pennington: The Electrochemical Society, 1996. 227-238.

Kantar, Cetin. "Colloids and Surfaces." 18 April 2002. *Science Direct.* 30 October 2011. <http://www.sciencedirect.com/science/article/pii/S0927775702001978>.

Khoshdast, Hamid and Abbas Sam. "Flotation Frothers: Review of Their Classifications, Properties and Preparation." *The Open Mineral Processing Journal* (2011): 25-44.

Kim, Dong Su, Sung Eun Kuh and Kwang Soon Moon. "Characteristics of Xanthates Related to Hydrocarbon Chain Length." *Geosystem Eng.* (2000): 30-34.

Kissinger, Peter T. and William R. Heineman. "Cyclic Voltammetry." *Journal of Chemical Education* (1983): 702-706.

Knight, Jerry E. "A Thermochemical Study of Alunite, Enargite, Luzonite, and Tennantite Deposits." *Economic Geology* (1977): 1321-1336.

Koh, P.T.L. and M. P. Schwarz. *CFD model of a self-aerating flotation cell*. 2007. November 2012. <http://www.google.com/imgres?q=flotation+cells&start=199&um=1&hl=en&sa=N&biw=1280&bih=865&tbm=isch&tbnid=W60JSCffpAnQMM:&imgrefurl=http://www.scie

ncedirect.com/science/article/pii/S0301751607001767&docid=548pokXFfRb3_M&imgurl=http://ars.sciencedirect.com/>.

Lab, Science. "Carbon Disulfide." n.d. *Material Safety Data Sheet.* <https://www.sciencelab.com/msds.php?msdsId=9927125>.

Leja, J., L. H. Little and G. W. Poling. "Xanthate adsorption studies using infrared spectroscopy." *Trans. Inst. Min. Metall.* (1963): 407.

Lenntech. "Arsenic." 2011. *Lenntech.* 8 November 2011. <http://www.lenntech.com/periodic/elements/as.htm>.

LTD, Process Technologies Australia PTY. "Arsenic-containing copper concentrates." Deloraine: Newmont, November 2008.

Ma, X. and W. J. Bruckard. "Rejection of arsenic minerals in sulfide flotation - A literature review." 18 July 2009. *Science Direct.* 14 March 2012. <http://www.sciencedirect.com/science/article/pii/S0301751609001483>.

Macdonald, Digby D. "Cyclic Voltammetry of Copper Metal in Lithium Hydroxide Solution at Elevated Temperatures." *Journal of the Electrochemical Society* (1974): 651-656.

Mihajlovic, Ivan, et al. "A potential method for arsenic removal from copper concentrates." *Minerals Engineering* (2007): 26-33.

Muller, A. and R. Blachnik. "Reactivity in the system copper-arsenic-sulfur I. The formation of Cu3AsS4, enagite." *Thermochimica Acta* (2002): 153-171.

Nadkarni, R. M. and C. L. Kusik. "Hydrometallurgical Removal of arsenic from copper concentrates." (n.d.): 263-286.

NCBI. *isobutylmethylcarbinol - Compound Summary* . 28 October 2009. 10 February 2013. <http://pubchem.ncbi.nlm.nih.gov/summary/summary.cgi?cid=7910>.

Nedichem. *Sodium/Potassium butyl Xanthate*. 2007. 26 January 2013. <http://www.nedichem.com/page1/product/flre.htm>.

Newmont. n.d. 11 June 2012. <www.chem.mtu.edu/chem_eng/faculty/kawatra/Flotation_Fundamentals.pdf>.

NICNAS. *Sodium Ethyl Xanthate*. Canberra: AusInfo, 2000.

Nicolet. *Nexus 670 User's Guide*. Madison: Nicolet Instrument Corporation, 1999.

Ohmi, Tadahiro. *Ultraclean Technology Handbook*. New York: Marcel Dekker, 1993.

Pauporte, Th. and D. Schuhmann. "An electrochemical study of natural enargite under conditions relating to those used in flotation of sulphide minerals." *Colloids and Surfaces* (1996): 1-19.

Plackowski, Chris, Anh V. Nguyen and Warren J. Bruckard. "A critical review of surface properties and selective flotation of enargite in sulphide systems." *Minerals Engineering* (2012): 1-11.

Poling, G. W. "Reactions Between Thiol Reagents and Sulfphde Minerals." Fuerstenau, M. C. *Flotation*. AIME, 1976. 334-363.

Posfai, Mihaly and Margareta Sundberg. "Stacking disorder and polytypism in enargite and luzonite." *American Mineralogist* (1998): 365-372.

Posfai, Mihaly and Peter R. Buseck. "Relationships between microstructure and composition in enargite and luzonite." *American Mineralogist* (1998): 373-382.

Price, Charles C and Gardner W Stacy. "p-Nitrophenyl Sulfide." 1955. *Organic Syntheses*. 30 January 2012. <http://www.orgsyn.org/orgsyn/orgsyn/prepContent.asp?prep=CV3P0667>.

Reddy, S. Lakshmi, et al. "Optical absorption and EPR studies on enargite." n.d.

Report, Full Public. *Sodium Ehtyl Xanthate*. Canberra: Australian Government Publishing Service, 1995.

Richerson, David W. *Modern Ceramic Engineering: Properties, Processing, and Use in Design*. Boca Raton: CRC Press, 2006.

Schuhmann, D., et al. "Impedance measurements with minerals under conditions similar to those in flotation. Comparison of galena and enargite." *Electrochemical Proceedings*. n.d. 215-226.

Schumann, D., et al. "Impedance Measurements With Minerals Under Conditions Similar to Those In Flotation. Comparison Of Galena And Enargite." *Electrochemistry In Mineral And Metal Processing*. Pennington: The Electrochemical Society, 1996. 215-226.

Scully, John R. "Electrochemical." International, ASTM. *Corrosion Tests and Standards Manual*. Baltimore: ASTM International , 2005. 75-90.

Seal, II, Robert R., et al. "Heat Capacity and entropy at the temperatures 5 K to 720 K and thermal expansion from the temperatures 298 K to 573 K of synthetic enargite (Cu3AsS4)." *J. Chem. Thermodynamics* (1996): 405-412.

Senior, G. D., P. Guy and W. J. Bruckard. "The Selective Flotation of Enargite from other copper minerals-a single mineral study in relation to beneficiation of the Tampakan deposit in the Phillipines." 31 July 2006. *Science Direct.* 4 November 2011. <http://www.sciencedirect.com/science/article/pii/S0301751606001116>.

Senior, G. D., P. J. Guy and W. J. Bruckard. "The selective flotation of enargite from other copper minerals-a single mineral study in relation to beneficiation of the Tampakan deposit in the Phillipines." *International Journal of Mineral Processing* (2006): 15-26.

Silverstein, Robert M., Francis X. Webster and David J. Kiemle. *Spectrometric Identification of Organic Compounds*. Hoboken: John Wiley & Sons, 2005.

Skousen, Jeff. *Acid Mine Drainage*. 2011. 6 February 2013. <http://www.aciddrainage.com/amd.cfm>.

Somasundaran, P. and L. Zhang. "Adsorption of surfactants on minerals for wettability control in improved oil recovery processes." *Journal of Petroleum Science and Engineering* (2006): 198-212.

Tait, Stephen W. *An Introduction To Electrochemical Corrosion Testing For Practicing Scientists And Engieneers*. Racine: Pair ODocs Publications, 1994.

Technologies, Process. *Arsenic-Containing Copper Concentrates*. Deloraine: Process Technologies Australia PTY LTD, 2008.

The Dow Chemical Company. *DOW Methyl Isobutyl Carbinol*. 6 June 2009. 10 February 2013. <http://msdssearch.dow.com/PublishedLiteratureDOWCOM/dh_02bd/0901b803802bdebe.pdf?filepath=productsafety/pdfs/noreg/233-00593.pdf&fromPage=GetDoc>.

Thomas Jr., George B. , et al. *Thomas' Calculus Early Transcendentals*. Pearson, 2007.

Velasquez, P., et al. "SEM, EDX and EIS study of an electrochemically modified electrode surface of natural enargite (Cu3AsS4)." *Journal of Electroanalytical Chemistry* (2000): 87-95.

Wikipedia. *File:Orthorhombic-face-centered.svg*. 2 March 2007. 10 February 2013. <http://en.wikipedia.org/wiki/File:Orthorhombic-face-centered.svg>.

—. *File:Tetrahedral-3D-balls.png*. 12 December 2006. 10 February 2013. <http://en.wikipedia.org/wiki/File:Tetrahedral-3D-balls.png>.

—. *Potassium Ethyl Xanthate*. 8 September 2012. 13 February 2013. <http://en.wikipedia.org/wiki/Potassium_ethyl_xanthate>.

—. *Potassium Ethyl Xanthate*. 8 September 2012. http://en.wikipedia.org/wiki/Potassium_ethyl_xanthate. 20 March 2013.

—. *Wurtzite*. 27 July 2011. 10 February 2013. <http://en.wikipedia.org/wiki/Wurtzite>.

Woods, R. "The Oxidation of Ethyl Xanthate on Platinum, Gold, Copper and Galena Electrodes. Reltation to the Mechanism of Mineral Flotation." *The Journal of Physical Chemistry* (1971): 354-362.

Woods, R., C. A. Young and R. H. Yoon. "Ethyl xanthate chemisorption isotherms and Eh-pH diagrams for the copper/water/xanthate and chalcocite/water/xanthate systems." *International Journal of Mineral Processing* (1990): 17-33.

Woods, R., R. H. Yoon and C. A. Young. "Eh-pH Diagrams for Stable and Metastable Phases in the Copper-Sulfide-Water System." *International Journal of Mineral Processing* (1987): 109-120.

Young, C. A., C. Basilio and R. H. Yoon. "Thermodynamics of Chalcocite-Xanthate Interactions." *International Journal of Mineral Processing* (1991): 265-279.

Young, C. A., R. Woods and R. H. Yoon. "A voltammetric study of chalcocite oxidation to metastable copper sulfides." *Electrochemistry in Mineral and Metal Processing II* (1988).

Appendix A: General Flotation Terminology

7. Flotation Chemicals

7.1. Frother

Frothers are chemicals that adsorb at both the liquid-air and solid-liquid interfaces and affect the hydrophobicity of minerals. They are usually of low-molecular weight and contain atoms of oxygen bonded to carbon. Their purpose is to aid in creating a froth that can support minerals long enough to be pulled into the launder (Cytec, 2010). As the froth builds up, the accumulation of bubbles (the froth bed), needs to remain stable so as not to lose the floated minerals.

7.1.1. Methyl Isobutyl Carbinol (MIBC)

Methyl Isobutyl Carbinol is a frother that is commonly used in copper ore flotation. It is a colorless liquid that smells mildly like alcohol. The structure of MIBC is comprised of six carbons, an oxygen attached to an end carbon, and the remainder of the carbons surrounded by hydrogens. **Figure 37** shows the structure of MIBC. The maximum industrial dosage that MIBC may be administered in is not enough to be of a toxicological concern.

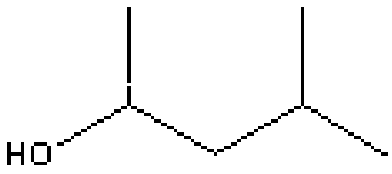

Figure 37: Mehtyl Isobutyl Carbinol (MIBC) Structure

7.2. Collectors

Collectors are a hydrocarbon chain molecule that varies in length, and whose effect of hydrophobicity varies with length. Their function is to target a specific type of mineral (e.g. copper bearing) and promote the flotation of this mineral type. When the collector is introduced to the system, the donor atom of the collector bonds directly with the metal atom on the mineral surface. The longer the hydrocarbon chain of the collector, the more hydrophobic the mineral it is bonded with will become.

7.2.1. Potassium Ethyl Xanthate

Potassium Ethyl Xanthate is a copper collector that is found in pellet form until it is about to be used, then it is solubilized in water and added to flotation cells. As shown in **Figure 38**, it is comprised of three carbons, the middle one having an oxygen bonded to it, and the end carbon having two sulfurs with an alternating single-double bond. Attached to one of the sulfur atoms is a sodium or potassium atom that breaks off in water, rendering the end of this compound anionic and ready to bond with a metal surface.

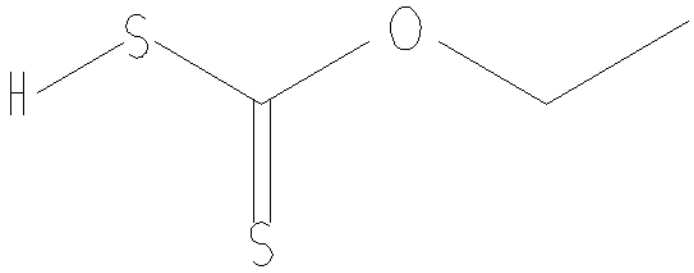

Figure 38: Potassium Ethyl Xanthate (PEX) Structure

7.2.2. Potassium Amyl Xanthate

Potassium Amyl Xanthate (PAX) was noted by Cytec as a collector "used widely in the flotation of Cu, Ni, Zn, and Au-containing iron sulfides." (Cytec, 2010). It found in pellet or

powder form before being immersed in water for use (Brenntag Canada Inc., 2009). As shown in **Figure 39**, PAX has six carbons, and the end one has two sulfurs with an alternating single-double bond. Attached to one of the sulfur atoms is a sodium or potassium atom that breaks off in water, rendering the end of this compound anionic and ready to bond with a metal surface. The adjacent carbon to the end with the sulfurs has an oxygen bonded to it. There are three additional carbons in the chain of PAX compared to PEX, making PAX the more hydrophobic of the two collectors. This is because as bubbles are passed through a flotation system, the longer the hydrocarbon chain, the greater the chance of part of the chain adsorbing onto the surface of an air bubble and being pulled to the froth (Cytec, 2010).

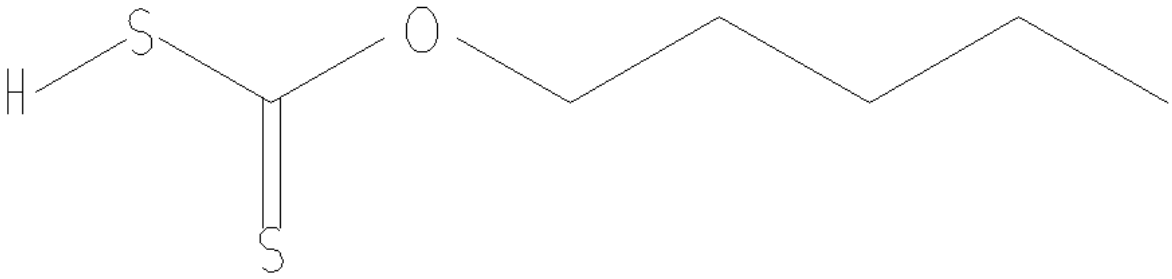

Figure 39: Potassium Amyl Xanthate (PAX) Structure

Appendix B: Voltammagrams and System Reactions

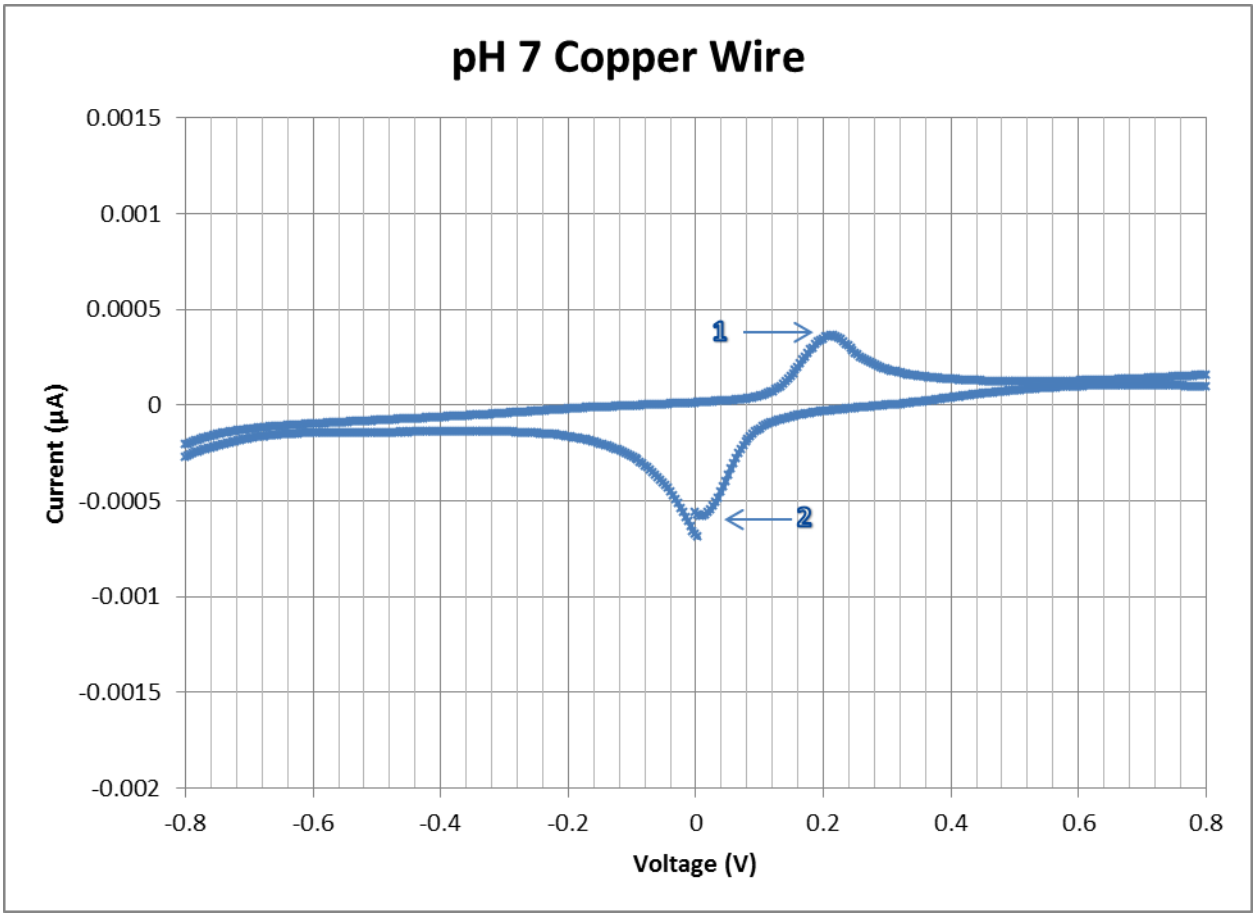

Figure 40: pH 7 Copper Wire Voltammagram

Table XXIV: pH 7 Copper Wire System Reactions

Peak	Eh Value	Reaction
1	0.04 to 0.27	$Cu° + H_2O + = CuOH + H^+ + e^-$
2	0.22 to -0.15	$CuOH + H^+ + e^- = Cu° + H_2O$

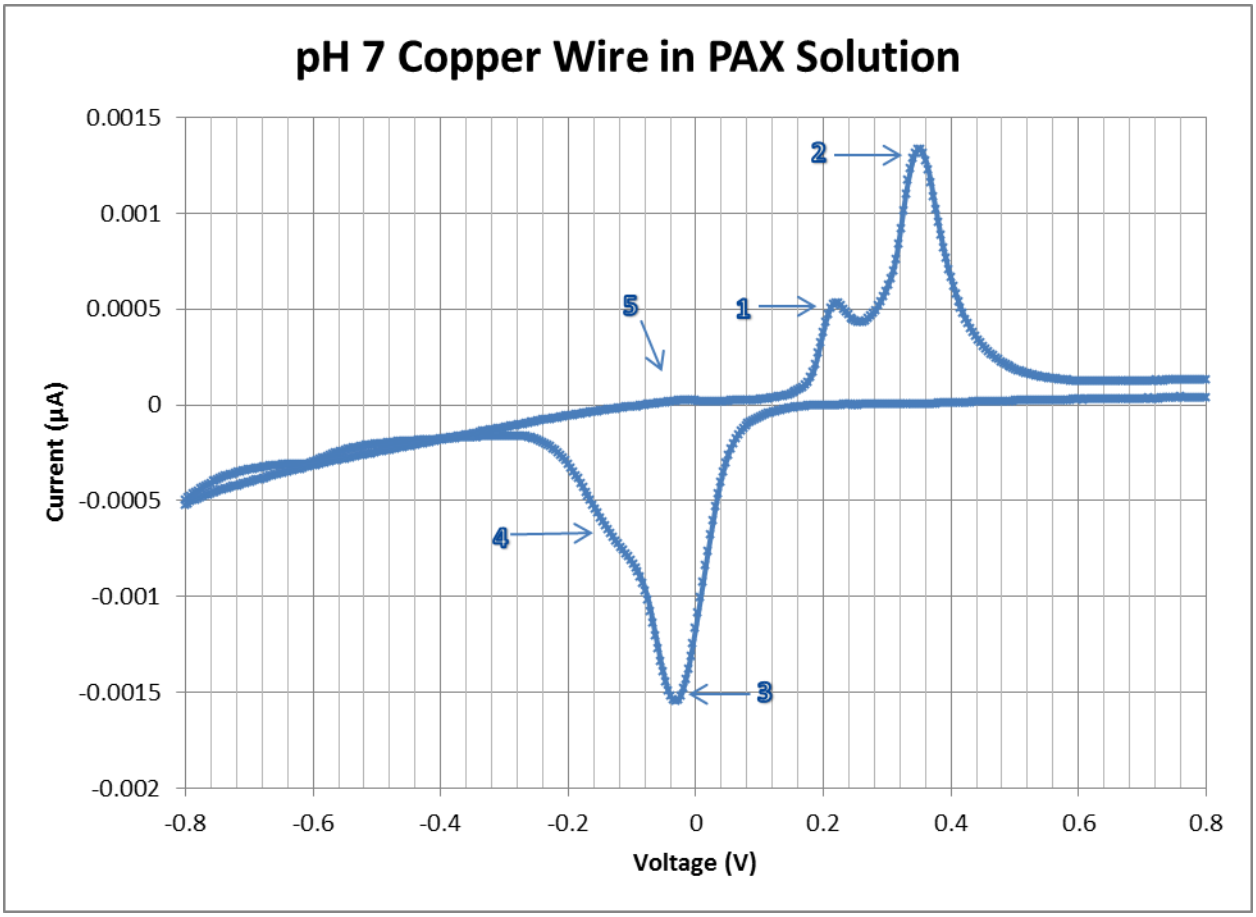

Figure 41: pH 7 Copper Wire in PAX Voltammagram

Table XXV: pH 7 Copper Wire in PAX Reactions

Peak	Eh Value (V)	Reaction
1	0.14 to 0.23	$Cu^{\circ} + X^{-} = CuX + e^{-}$
2	0.23 to 0.51	$CuX + 2OH^{-} = Cu(OH)_2 + 1/2X_2 + 2e^{-}$
3	0.09 to -0.14	$Cu(OH)_2 + 1/2X_2 + 2e^{-} = CuX + 2OH^{-}$
4	-0.18 to -0.22	$CuX + e^{-} = Cu^{\circ} + X^{-}$
5	-0.14 to 0.08	$X^{-} = X_{ads} + e^{-}$

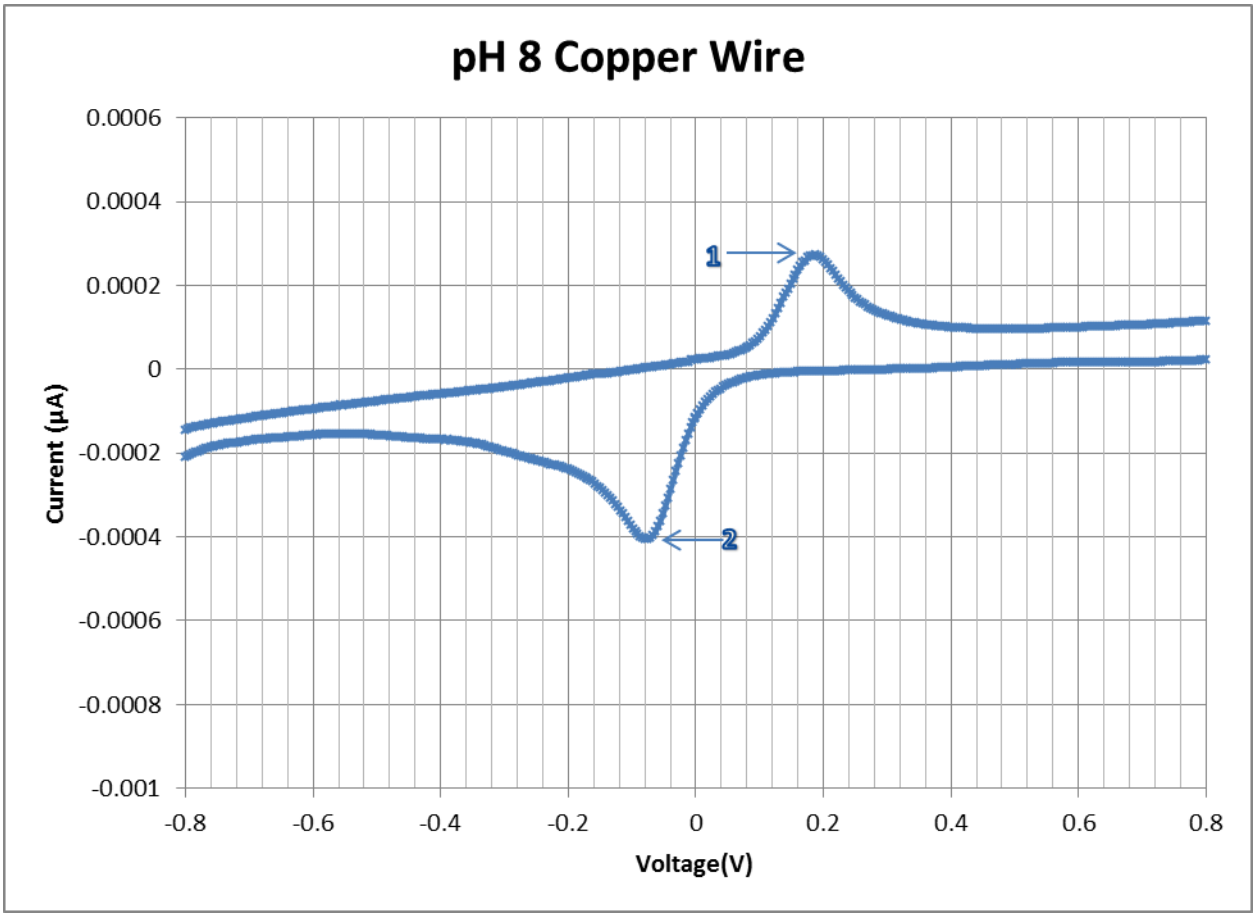

Figure 42: pH 8 Copper Wire Voltammagram

Table XXVI: pH 8 Copper Wire System Reactions

Peak	Eh Value	Reaction
1	0.03 to 0.3	$Cu° + H_2O + = CuOH + H^+ + e^-$
2	0.08 to -0.16	$CuOH + H^+ + e^- = Cu° + H_2O$

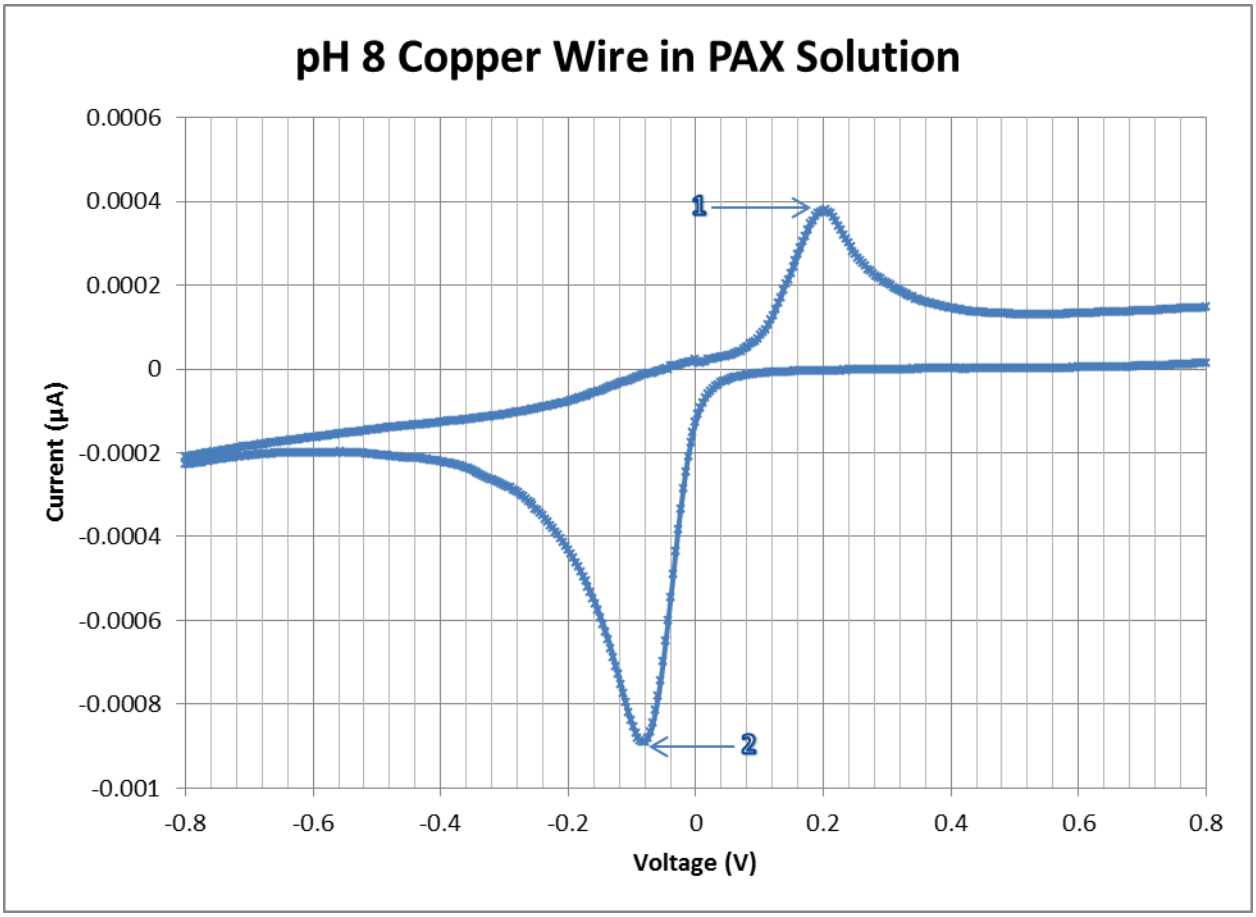

Figure 43: pH 8 Copper Wire in PAX Voltammagram

Table XXVII: pH 8 Copper Wire in PAX Reactions

Peak	Eh Value	Reaction
1	0.02 to 0.33	$Cu_2O + 2CuX + H_2O = 2CuO + 2CuX + 2H^+ + 2e^-$
2	0.06 to -0.28	$2CuO + CuX + 2H^+ + 2e^- = Cu_2O + CuX + H_2O$

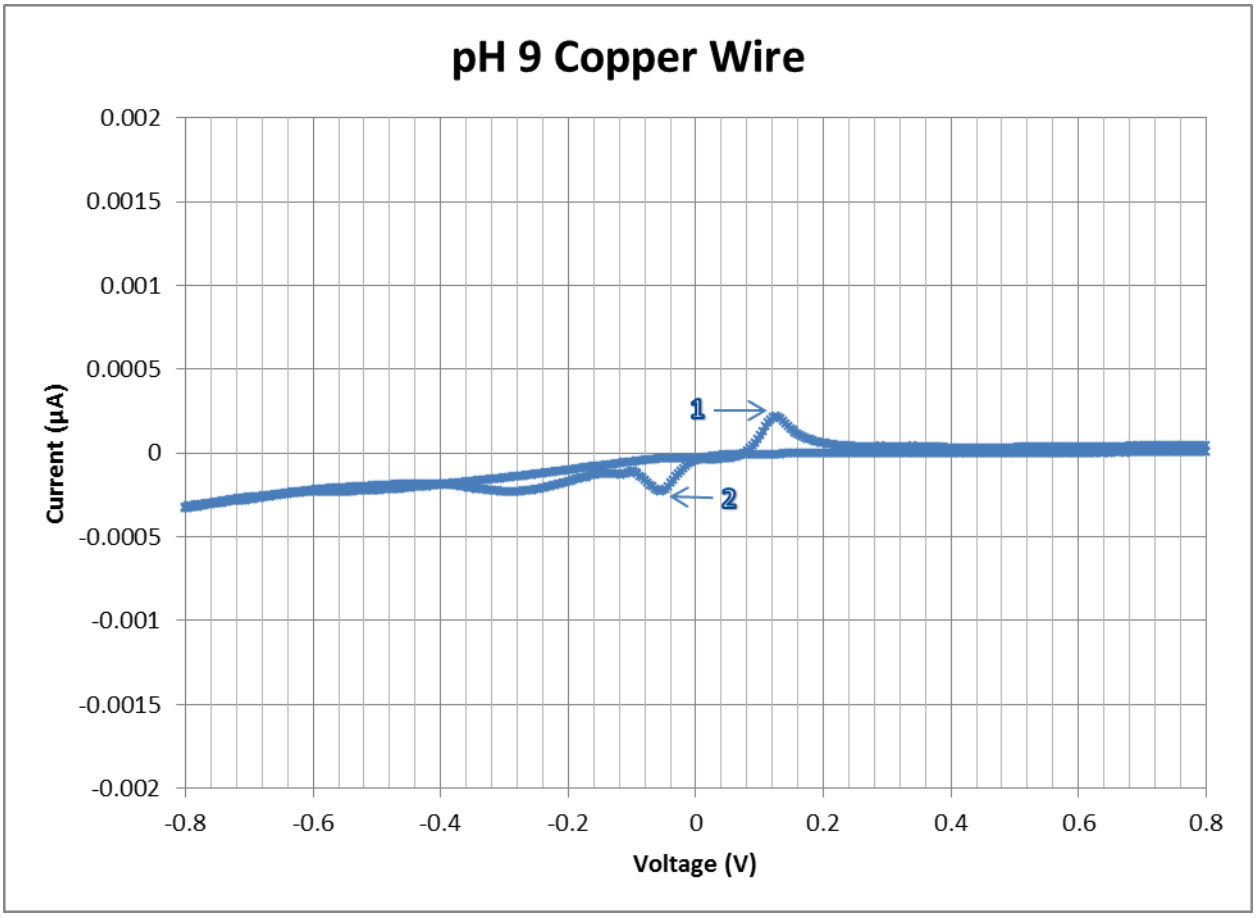

Figure 44: pH 9 Copper Wire Voltammagram

Table XXVIII: pH 9 Copper Wire System Reactions

Peak	Eh Value	Reaction
1	0.07 to 0.17	$Cu° + H_2O + = CuOH + H^+ + e^-$
2	-0.02 to -0.08	$CuOH + H^+ + e^- = Cu° + H_2O$

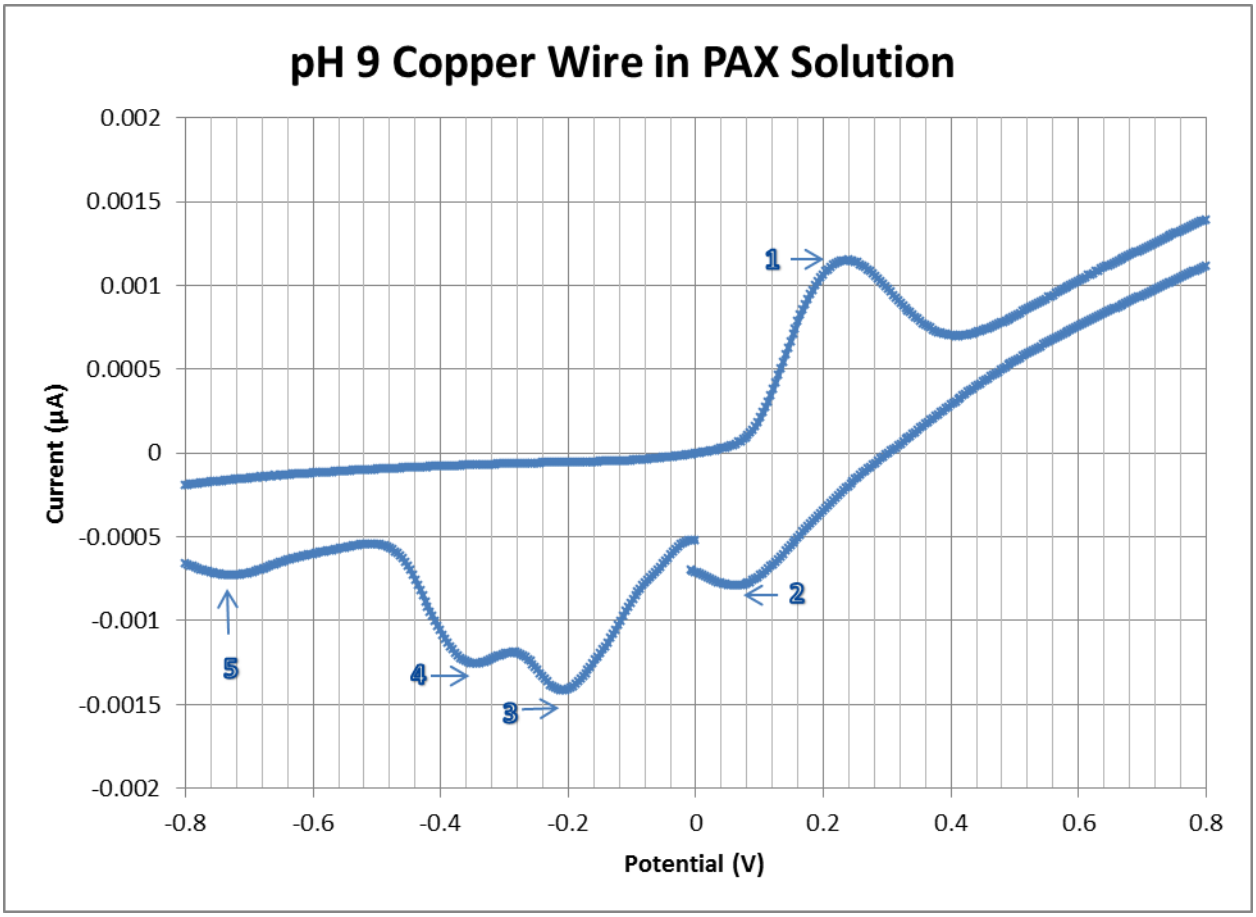

Figure 45: pH 9 Copper Wire in PAX Voltammagram

Table XXIX: pH 9 Copper Wire in PAX Reactions

Peak	Eh Value	Reaction
1	0.02 to 0.38	$3Cu_2O + CuX + 5X^- + 2H^+ = 2CuO + 5CuX + H_2O + 3e^-$
2	0.17 to -0.01	$2CuO + CuX + 4H^+ + 4e^- = Cu_2O + CuX + 2H_2O$
3	-0.12 to -0.25	$Cu_2O + CuX + 2H^+ + + 2e^- + = 2Cu^o + CuX + H_2O$
4	-0.25 to -0.45	$Cu^o + CuX + 2e^- = 2Cu^o + 2X^-$
5	-0.51 to -0.85	Hydrogen Formation

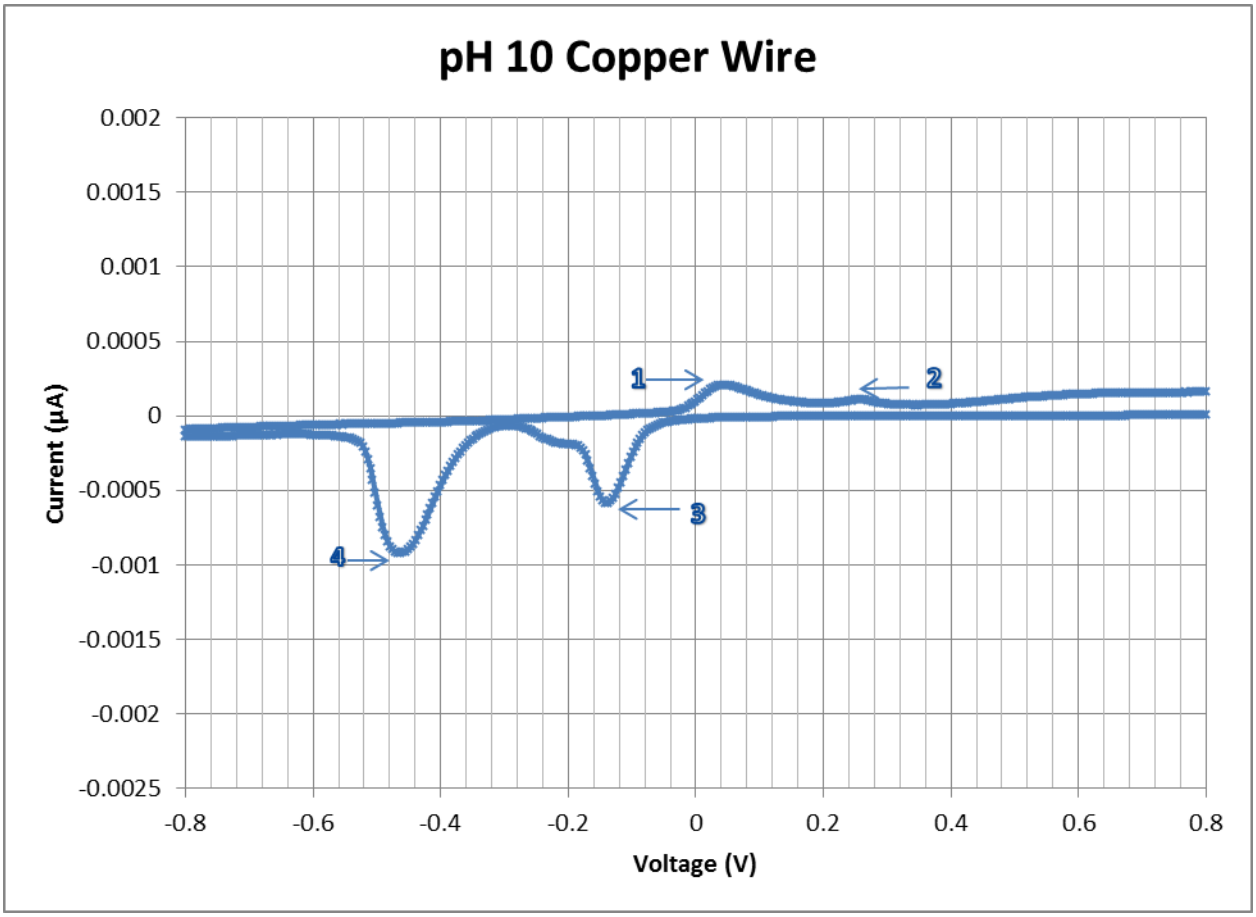

Figure 46: pH 10 Copper Wire Voltammagram

Table XXX: pH 10 Copper Wire System Reactions

Peak	Eh Value	Reaction
1	-0.03 to 0.11	$Cu° + H_2O + = CuOH + H^+ + e^-$
2	0.11 to 0.29	$CuOH + H_2O = Cu(OH)_2 + H^+ + e^-$
3	-0.03 to -0.26	$Cu(OH)_2 + H^+ + e^- = CuOH + H_2O$
4	-0.26 to -0.52	$CuOH + H^+ + e^- = Cu° + H_2O$

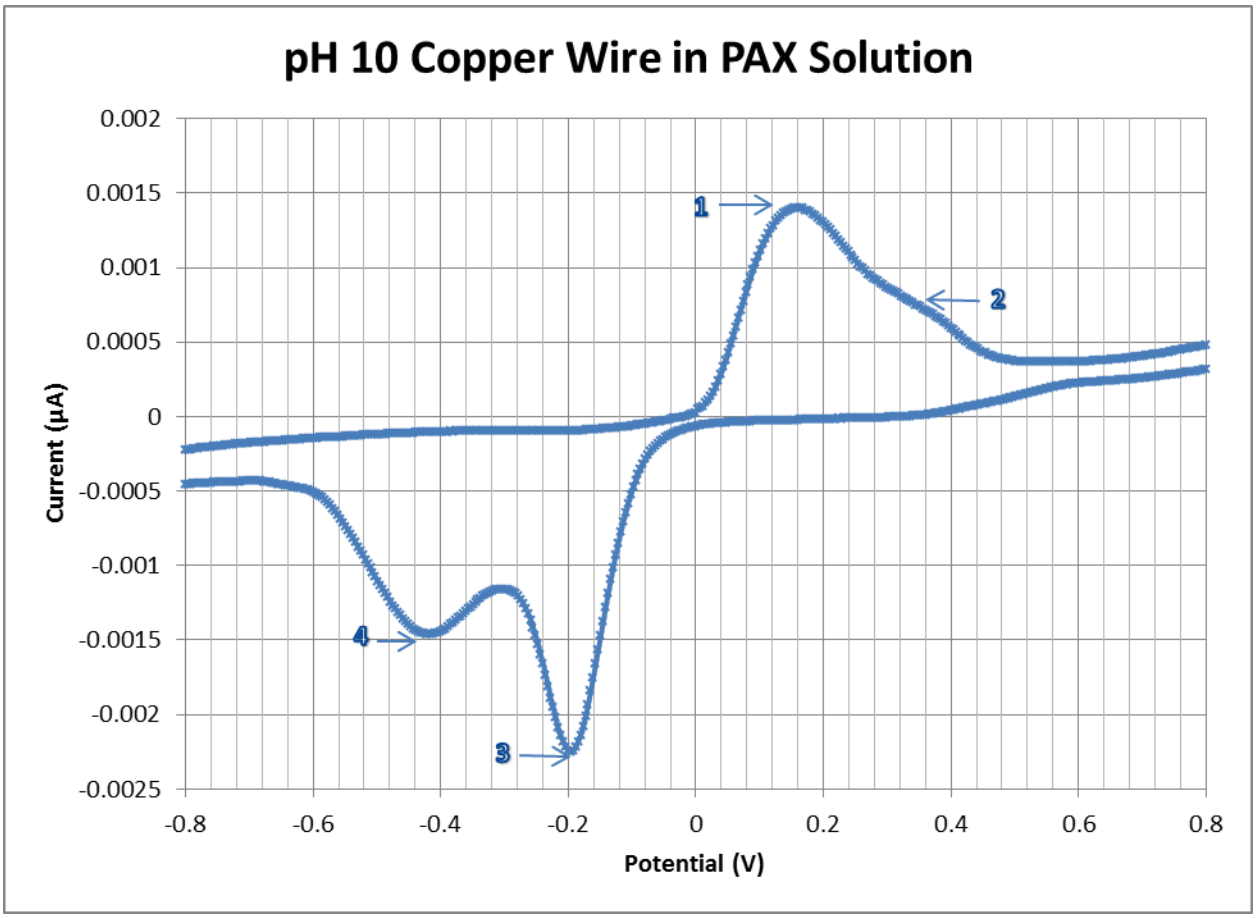

Figure 47: pH 10 Copper Wire in PAX Voltammagram

Table XXXI: pH 10 Copper Wire in PAX Reactions

Peak	Eh Value	Reaction
1	-0.01 to 0.28	$Cu^0 + X^- = CuX + e^-$
2	0.28 to 0.44	$CuX + 2OH^- = Cu(OH)_2 + 1/2X_2$
3	-0.06 to -0.27	$Cu(OH)_2 + 1/2X_2 = CuX + 2OH^-$
4	-0.27 to -0.56	$CuX + e^- = Cu^0 + X^-$

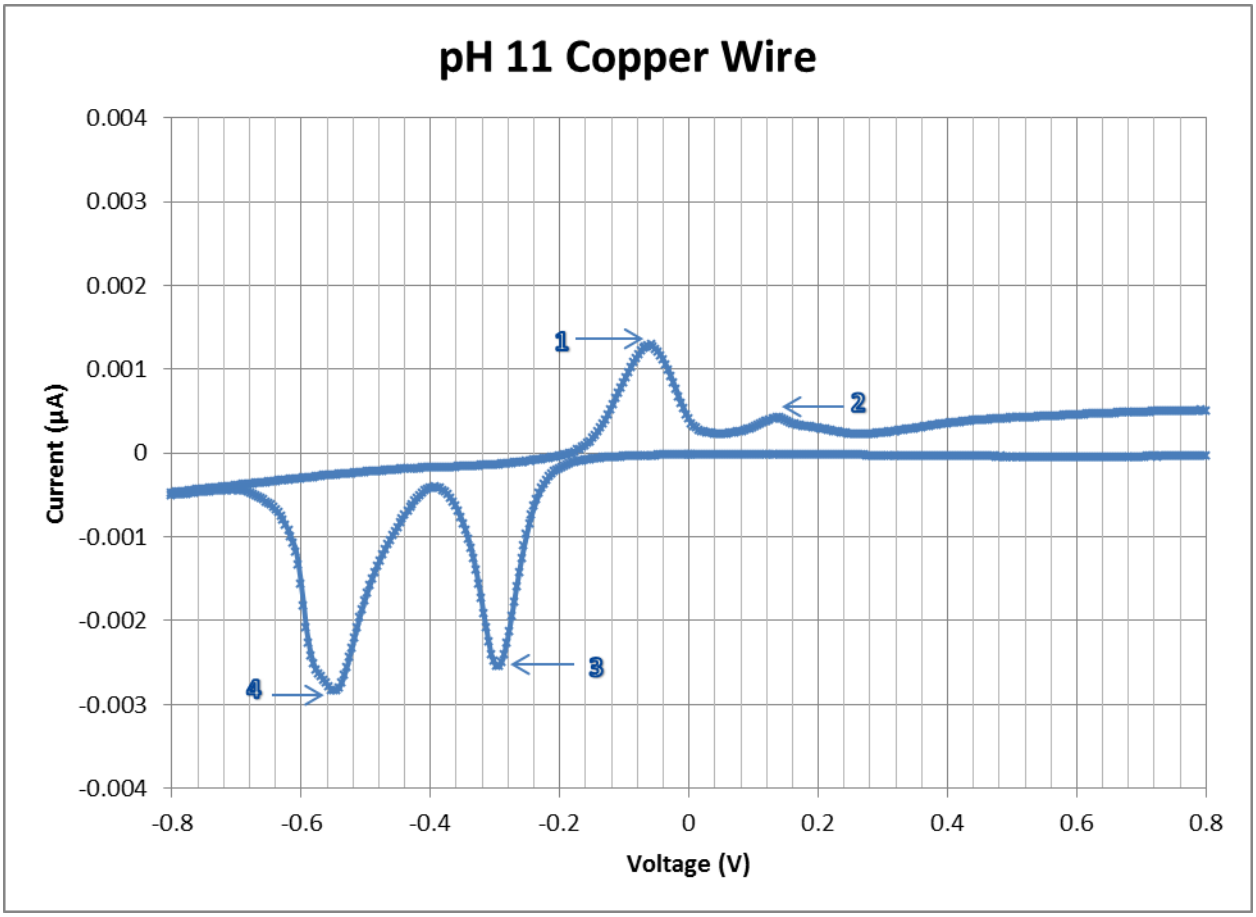

Figure 48: pH 11 Copper Wire Voltammagram

Table XXXII: pH 11 Copper Wire System Reactions

Peak	Eh Value	Reaction
1	-0.18 to 0.01	$Cu° + H_2O + = CuOH + H^+ + e^-$
2	0.01 to 0.03	$CuOH + H_2O = Cu(OH)_2 + H^+ + e^-$
3	-0.15 to -0.37	$Cu(OH)_2 + H^+ + e^- = CuOH + H_2O$
4	-0.37 to -0.68	$CuOH + H^+ + e^- = Cu° + H_2O$

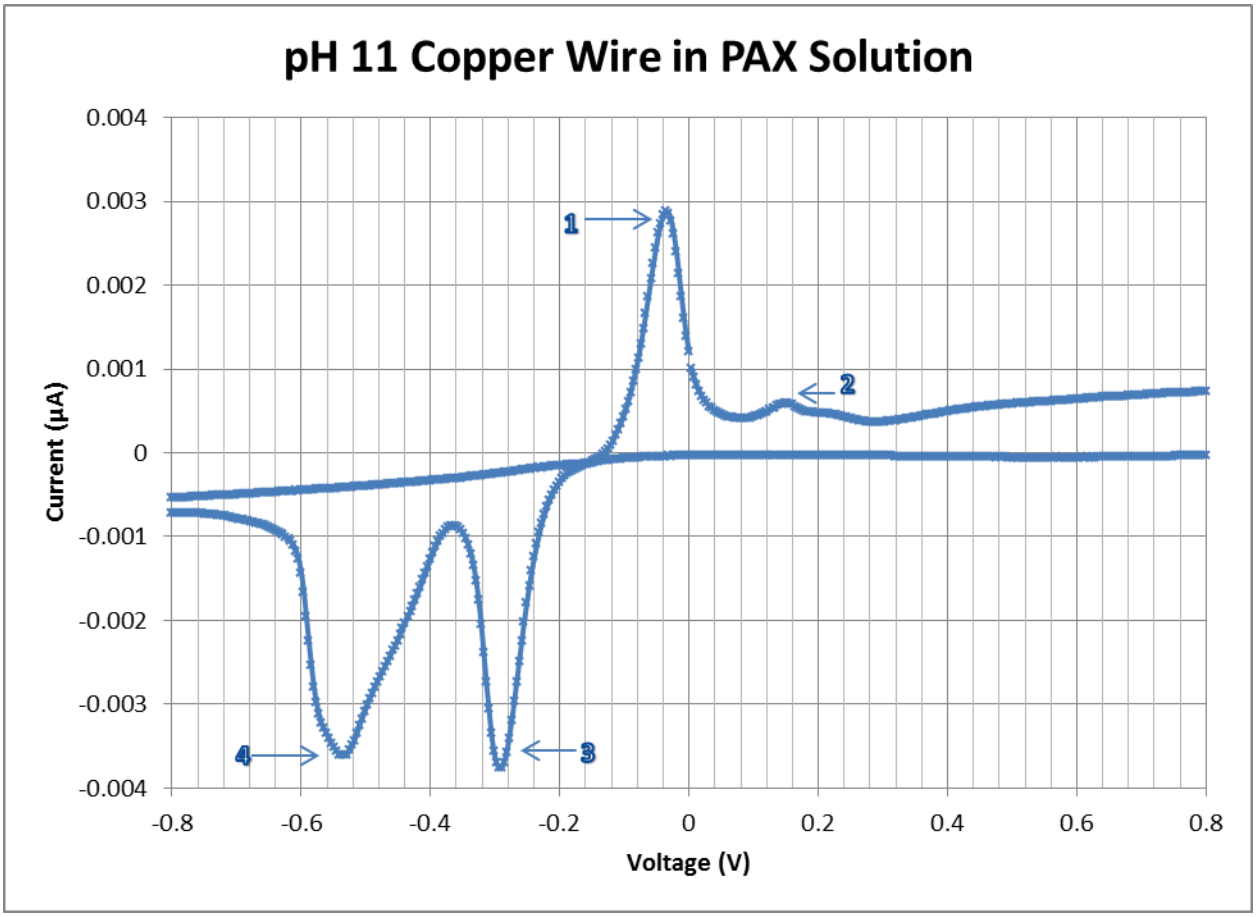

Figure 49: pH 11 Copper Wire in PAX Voltammagram

Table XXXIII: pH 11 Copper Wire in PAX Reactions

Peak	Eh Value	Reaction
1	-0.11 to 0.04	$Cu^0 + X^- = CuX + e^-$
2	0.04 to 0.24	$CuX + 2OH^- = Cu(OH)_2 + 1/2X_2$
3	-0.10 to -0.35	$Cu(OH)_2 + 1/2X_2 = CuX + 2OH^-$
4	-0.35 to -0.61	$CuX + e^- = Cu^0 + X^-$

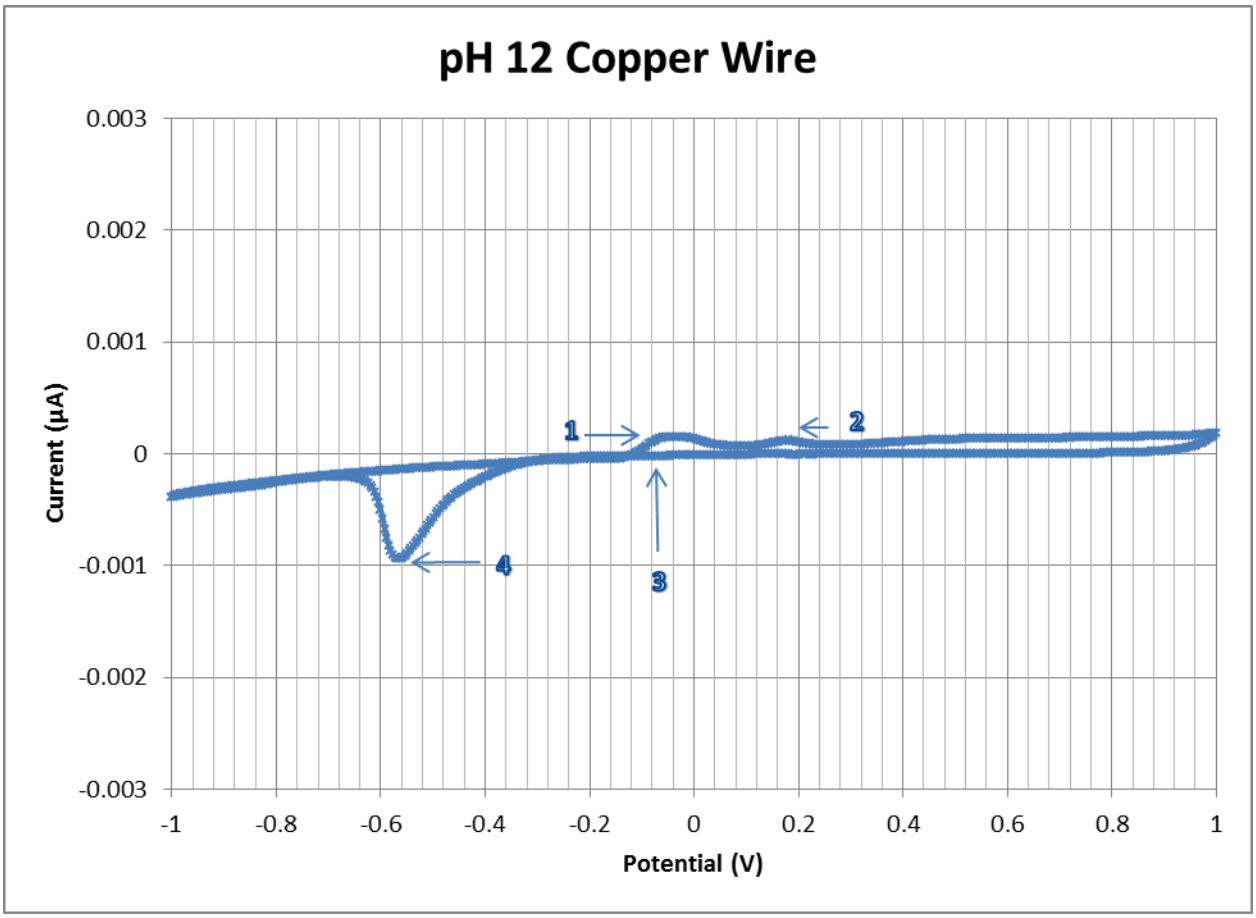

Figure 50: pH 12 Copper Wire Voltammagram

Table XXXIV: pH 12 Copper Wire System Reactions

Peak	Eh Value	Reaction
1	-0.10 to 0.07	$Cu° + H_2O + = CuOH + H^+ + e^-$
2	0.07 to 0.22	$CuOH + H_2O = Cu(OH)_2 + H^+ + e^-$
3	-0.11 to -0.15	$Cu(OH)_2 + H^+ + e^- = CuOH + H_2O$
4	- 0.36 to -0.61	$CuOH + H^+ + e^- = Cu° + H_2O$

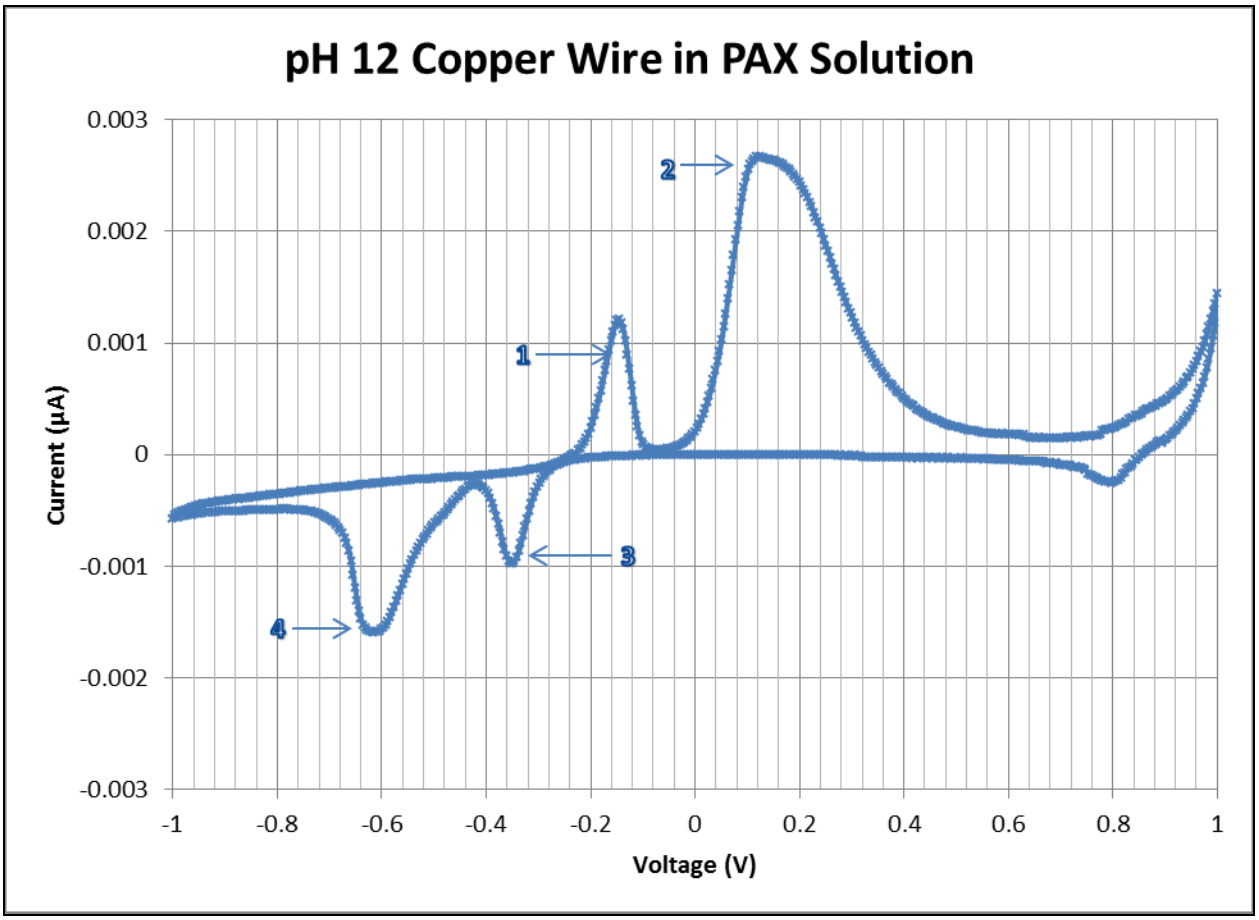

Figure 51: pH 12 Copper Wire in PAX Voltammagram

Table XXXV: pH 12 Copper Wire in PAX Reactions

Peak	E_H Value	Reaction
1	-0.23 to -0.03	$Cu^0 + X^- = CuX + e^-$
2	-0.03 to 0.55	$CuX + 2OH^- = Cu(OH)_2 + 1/2X_2$
3	-0.19 to -0.39	$Cu(OH)_2 + 1/2X_2 = CuX + 2OH^-$
4	-0.41 to -0.78	$CuX + e^- = Cu^0 + X^-$

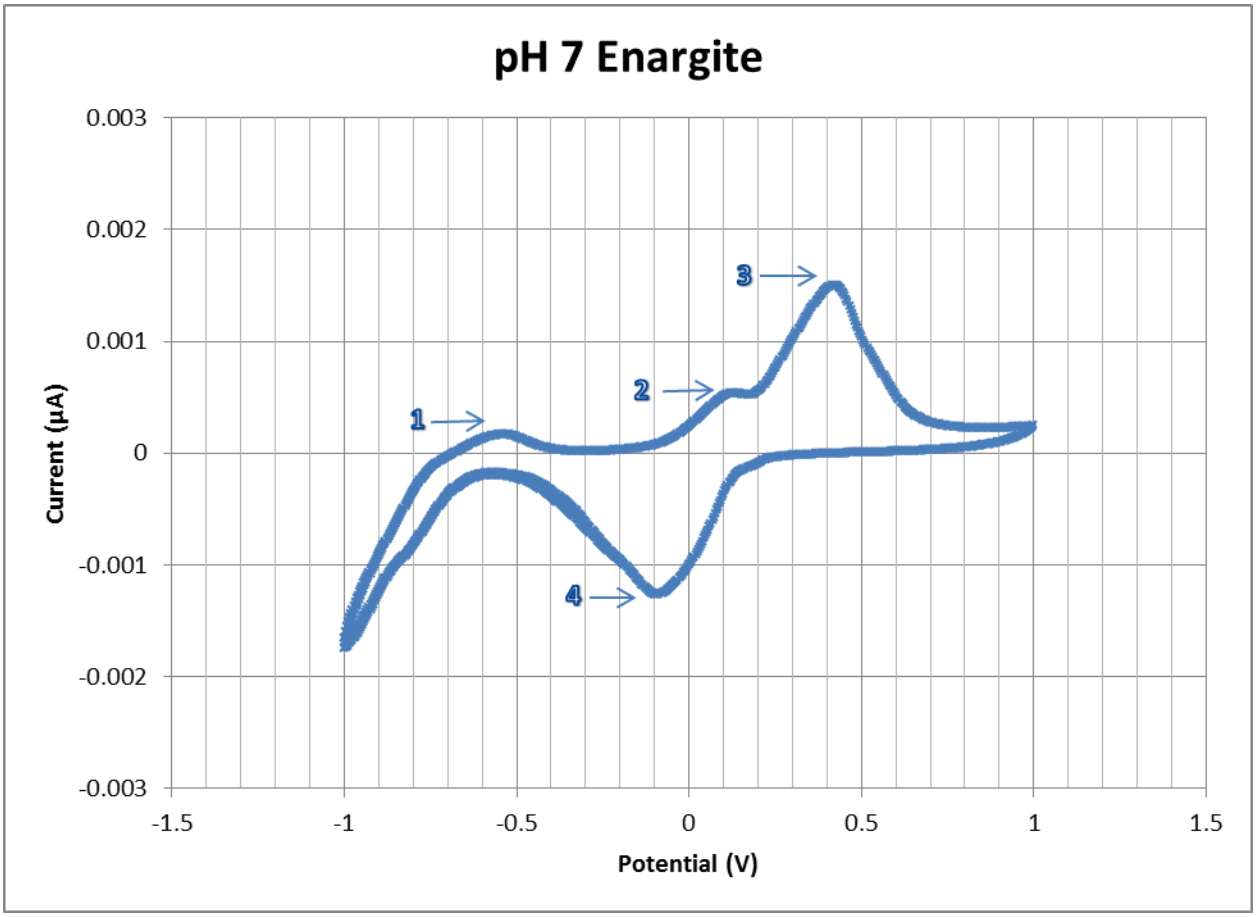

Figure 52: pH 7 Enargite Voltammagram

Table XXXVI : pH 7 Enargite Reactions

Peak	E_H Value (V)	Reaction
2	0.05 to 0.20	$Cu_3AsS_4 + 3H_2O = 3CuS + H_3AsO_3 + S^o + 3H^+ + 3e^-$
3	0.20 to 0.65	$2CuS + HAsO_4^{2-} + H_2O = Cu_2As_4OH + 2S^o + 2H^+ + 4e^-$
4	0.24 to 0.13	$Cu_2As_4OH + 2S^o + 2H^+ + 4e^- = 2CuS + HAsO_4^{2-} + H_2O$
5	0.13 to -0.45	$3CuS + H_3AsO_3 + S^o + 3H^+ + 3e^- = Cu_3AsS_4 + 3H_2O$
6	-0.74 to -0.87	$Cu_3AsS_4 = (Cu_{12}As_4S_2/Cu_6As_4S_9) = 3/2Cu_2S + As^o + 5/2HS^- + 5/2H^+ + 5e^-$
1	-0.60 to -0.40	$3/2Cu_2S + As^o + 5/2HS^- + 5/2H^+ + 5e^- = (Cu_{12}As_4S_2/Cu_6As_4S_9) = Cu_3AsS_4$

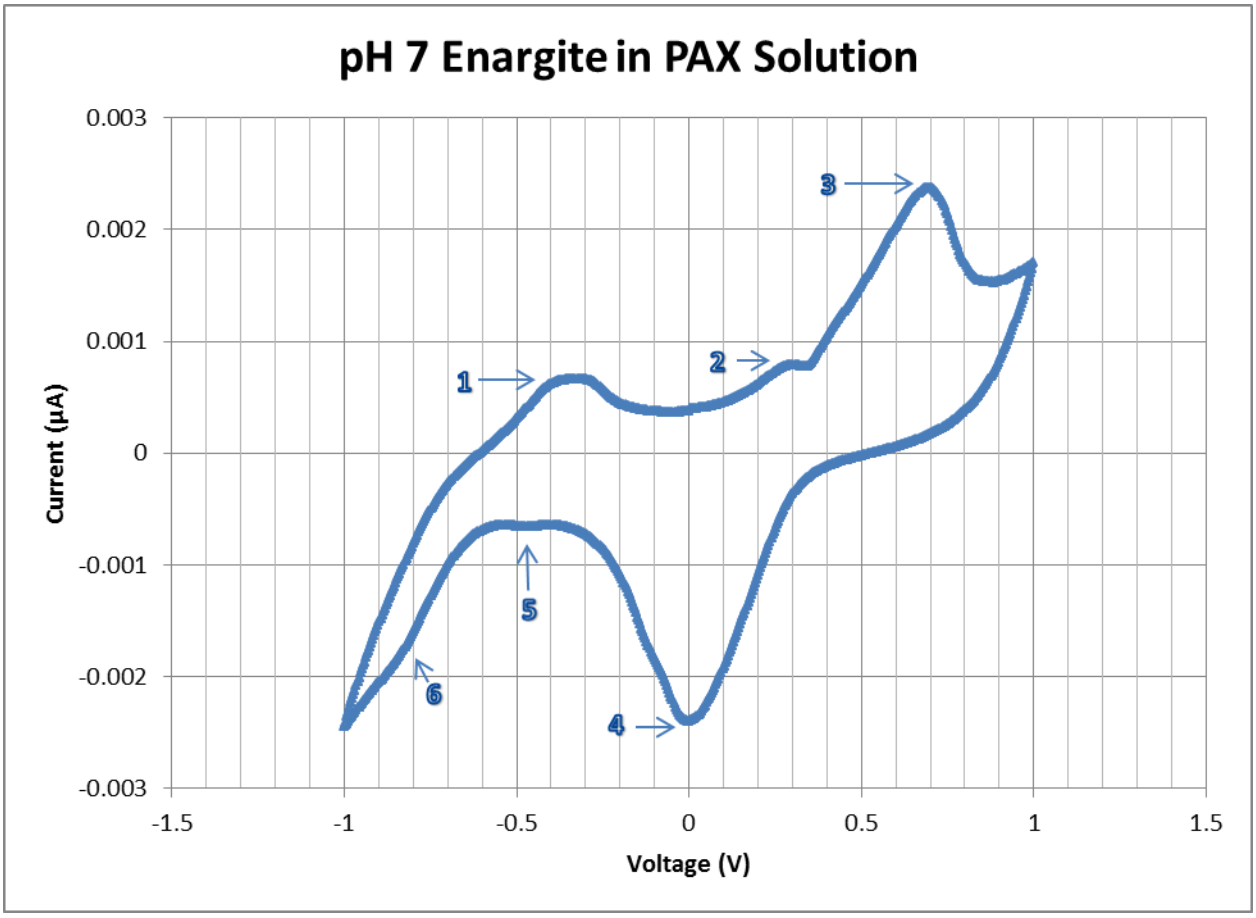

Figure 53: pH 7 Enargite in PAX Voltammagram

Table XXXVII: pH 7 Enargite in PAX Reactions

Peak	Eh Value	Reaction
2	0.00 to 0.33	$Cu_3AsS_4 + X^- + 3H_2O = CuX + 2CuS + H_3AsO_3 + 2S^o + 3H^+ + 4e^-$
3	0.33 to 0.75	$CuS + X^- = CuX + S^o + e^-$
4	0.50 to -0.30	$CuX + S^o + e^- = CuS + X^-$
5	-0.40 to -0.60	$CuX + 2CuS + H_3AsO_3 + 2S^o + 3H^+ + 4e^- = Cu_3AsS_4 + X^- + 3H_2O$
6	-0.70 to -0.90	$Cu_3AsS_4 = (Cu_{12}As_4S_2/Cu_6As_4S_9) = 3/2Cu_2S + As^o + 5/2HS^- + 5/2H^+ + 5e^-$
1	-0.60 to -0.15	$3/2Cu_2S + As^o + 5/2HS^- + 5/2H^+ + 5e^- = (Cu_{12}As_4S_2/Cu_6As_4S_9) = Cu_3AsS_4$

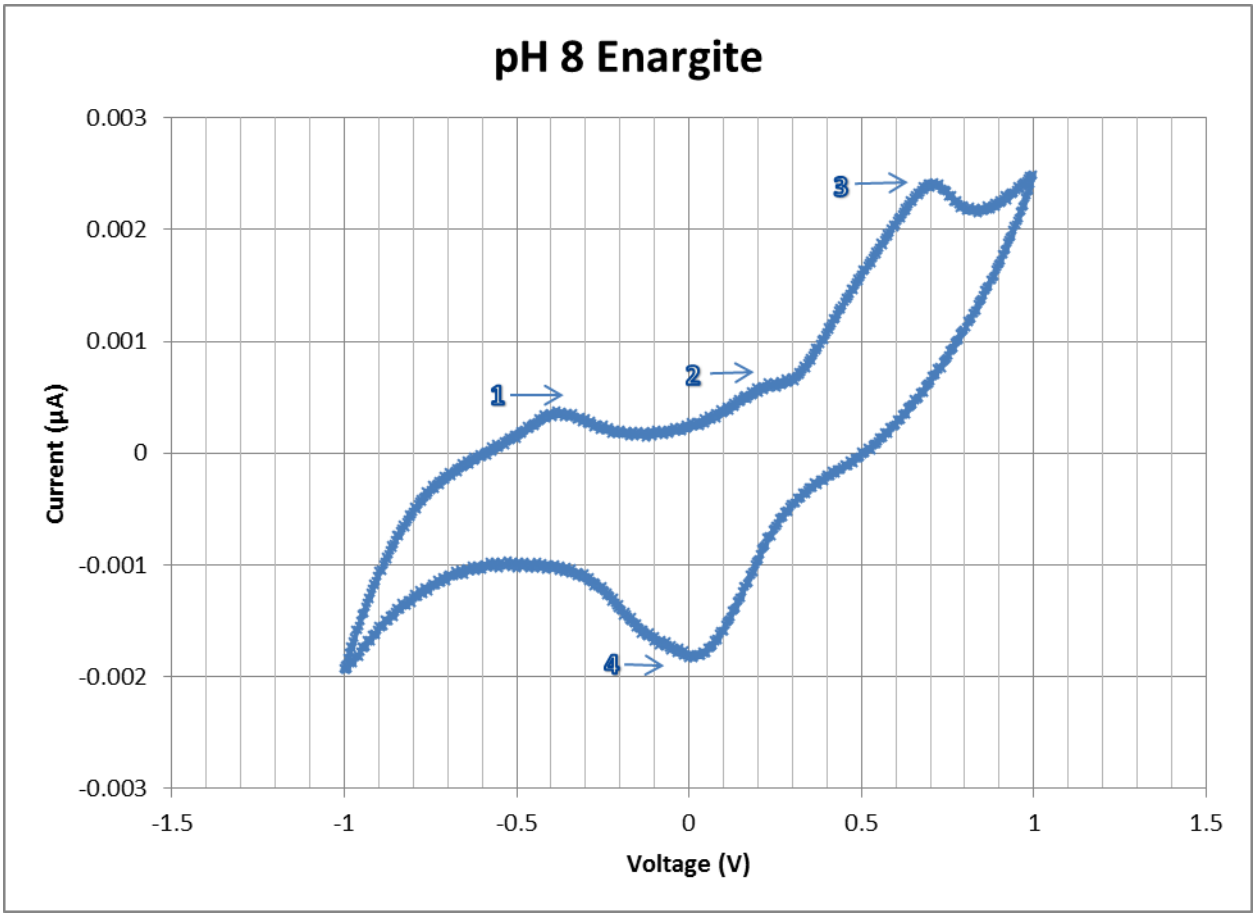

Figure 54: pH 8 Enargite Voltammagram

Table XXXVIII : pH 8 Enargite Reactions

Peak	E_H Value (V)	Reaction
2	0.00 to 0.30	$Cu_3AsS_4 + 3H_2O = 3CuS + H_3AsO_3 + S^o + 3H^+ + 3e^-$
3	0.30 to 0.75	$2CuS + HAsO_4^{2-} + H_2O = Cu_2AsO_4OH + 2S^o + 2H^+ + 4e^-$
4	0.30 to -0.50	$Cu_2AsO_4OH + 2S^o + 2H^+ + 4e^- = 2CuS + HAsO_4^{2-} + H_2O$ $3CuS + H_3AsO_3 + S^o + 3H^+ + 3e^- = Cu_3AsS_4 + 3H_2O$ $Cu_3AsS_4 = (Cu_{12}As_4S_2/Cu_6As_4S_9) = 3/2Cu_2S + As^o + 5/2HS^- + 5/2H^+ + 5e^-$
1	-0.60 to -0.10	$3/2Cu_2S + As^o + 5/2HS^- + 5/2H^+ + 5e^- = (Cu_{12}As_4S_2/Cu_6As_4S_9) = Cu_3AsS_4$

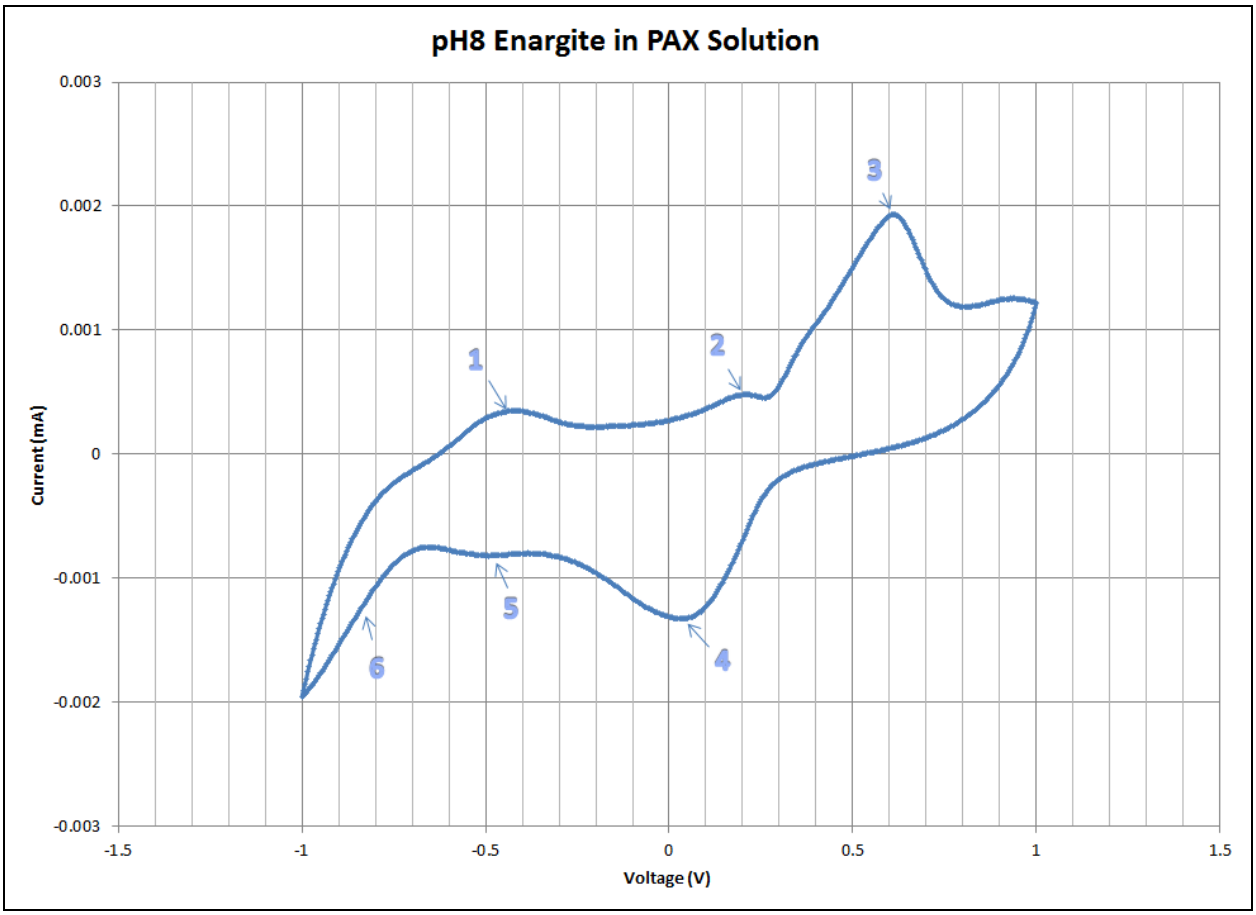

Figure 55: pH 8 Enargite in PAX Voltammagram

Table XXXIX: pH 8 Enargite in PAX Reactions

Peak	Eh Value	Reaction
2	-0.12 to 0.23	$Cu_3AsS_4 + X^- + 3H_2O = CuX + 2CuS + H_3AsO_3 + 2S^o + 3H^+ + 4e^-$
3	0.23 to 0.75	$CuS + X^- = CuX + S^o + e^-$
4	0.32 to -0.24	$CuX + S^o + e^- = CuS + X^-$
5	-0.31 to -0.61	$CuX + 2CuS + H_3AsO_3 + 2S^o + 3H^+ + 4e^- = Cu_3AsS_4 + X^- + 3H_2O$
6	-0.76 to -0.90	$Cu_3AsS_4 = (Cu_{12}As_4S_2/Cu_6As_4S_9) = 3/2Cu_2S + As^o + 5/2HS^- + 5/2H^+ + 5e^-$
1	-0.68 to -0.32	$3/2Cu_2S + As^o + 5/2HS^- + 5/2H^+ + 5e^- = (Cu_{12}As_4S_2/Cu_6As_4S_9) = Cu_3AsS_4$

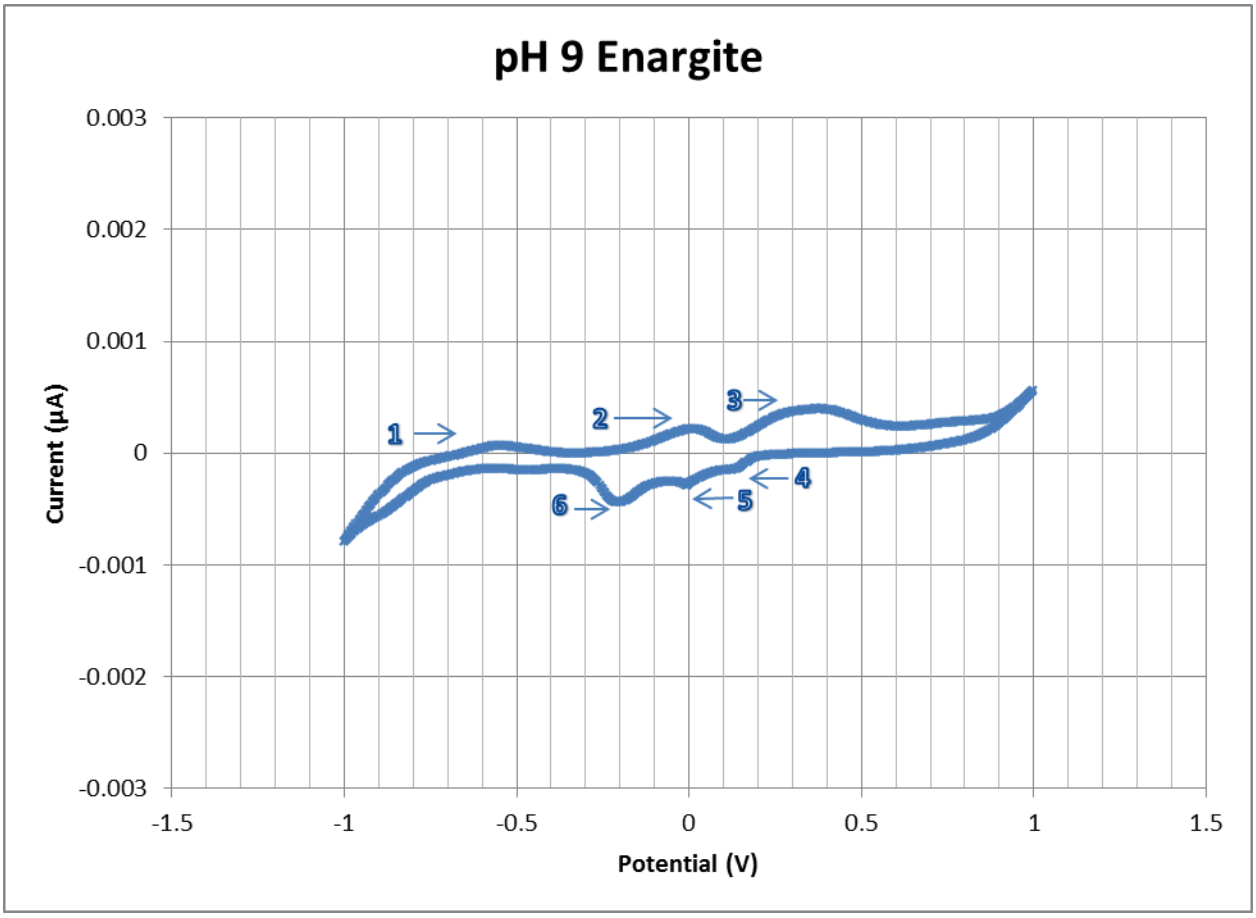

Figure 56: pH 9 Enargite Voltammagram

Table XL : pH 9 Enargite Reactions

Peak	E_H Value (V)	Reaction
2	-0.20 to 0.15	$Cu_3AsS_4 + 3H_2O = 3CuS + H_3AsO_3 + S^o + 3H^+ + 3e^-$
3	0.15 to 0.60	$2CuS + HAsO_4^{2-} + H_2O = Cu_2As_4OH + 2S^o + 2H^+ + 4e^-$
4	0.30 to 0.10	$Cu_2As_4OH + 2S^o + 2H^+ + 4e^- = 2CuS + HAsO_4^{2-} + H_2O$
5	0.05 to -0.15	$3CuS + H_3AsO_3 + S^o + 3H^+ + 3e^- = Cu_3AsS_4 + 3H_2O$
6	-0.15 to -0.46	$Cu_3AsS_4 = (Cu_{12}As_4S_2/Cu_6As_4S_9) = 3/2Cu_2S + As^o + 5/2HS^- + 5/2H^+ + 5e^-$
1	-0.70 to -0.40	$3/2Cu_2S + As^o + 5/2HS^- + 5/2H^+ + 5e^- = (Cu_{12}As_4S_2/Cu_6As_4S_9) = Cu_3AsS_4$

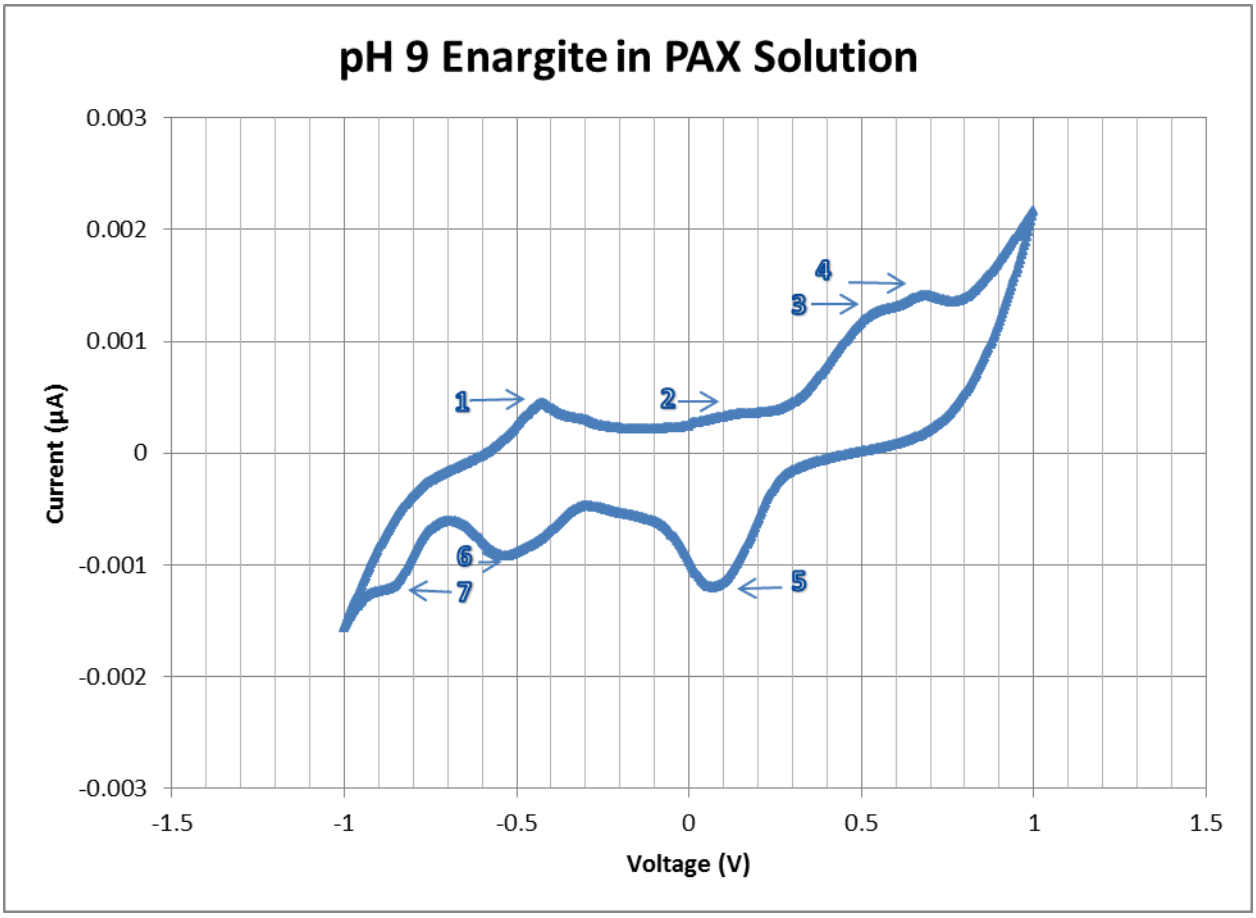

Figure 57: pH 9 Enargite in PAX Voltammagram

Table XLI: pH 9 Enargite in PAX Reactions

Peak	Eh Value	Reaction
1	-0.59 to -0.26	$Cu_3AsS_4 + X^- + 3H_2O = CuX + 2CuS + HAsO_4^{2-} + 2S^o + 5H^+ + 4e^-$
2	-0.07 to 0.24	$CuS + X^- = CuX + S^o + e^-$
3	0.24 to 0.68	$CuX + S^o + e^- = CuS + X^-$
4	0.68 to 0.74	$CuX + 2CuS + HAsO_4^{2-} + 2S^o + 7H^+ + 6e^- = Cu_3AsS_4 + X^- + 4H_2O$
5	0.31 to -0.07	$Cu_3AsS_4 = (Cu_{12}As_4S_2/Cu_6As_4S_9) = 3/2Cu_2S + As^o + 5/2HS^- + 5/2H^+ + 5e^-$
6	-0.26 to -0.68	$3/2Cu_2S + As^o + 5/2HS^- + 5/2H^+ + 5e^- = (Cu_{12}As_4S_2/Cu_6As_4S_9) = Cu_3AsS_4$
7	-0.68 to -0.85	$Cu_2S = 2Cu^o + S^o$

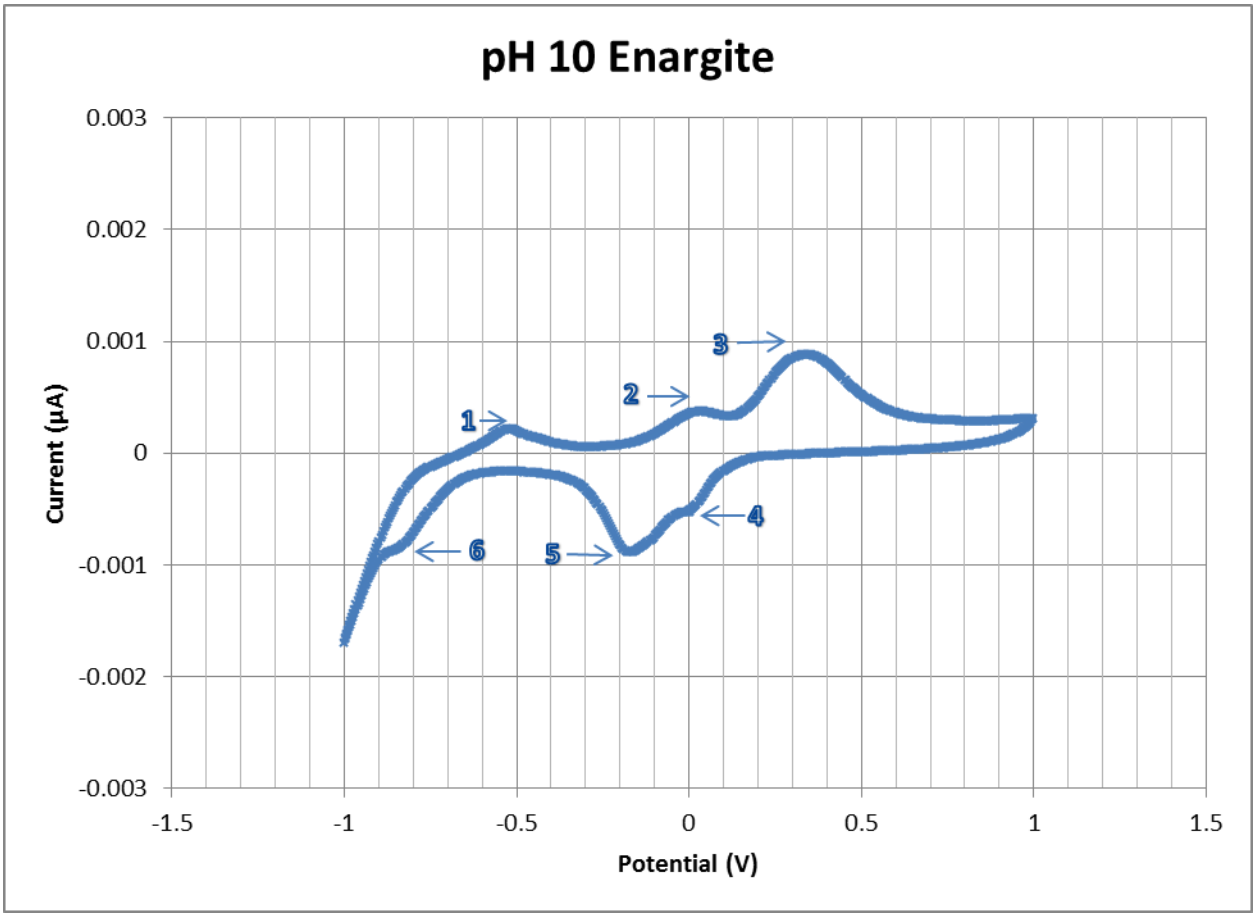

Figure 58: pH 10 Enargite Voltammagram

Table XLII : pH 10 Enargite Reactions

Peak	E_H Value (V)	Reaction
2	-0.15 to 0.15	$Cu_3AsS_4 + 3H_2O = 3CuS + HAsO_4^{2-} + S^o + 5H^+ + 3e^-$
3	0.15 to 0.60	$2CuS + HAsO_4^{2-} + H_2O = Cu_2As_4OH + 2S^o + 2H^+ + 4e^-$
4	0.35 to -0.05	$Cu_2AsO_4OH + 2S^o + 2H^+ + 4e^- = 2CuS + HAsO_4^{2-} + H_2O$
5	-0.05 to -0.40	$3CuS + HAsO_4^{2-} + S^o + 7H^+ + 5e^- = Cu_3AsS_4 + 4H_2O$
6	-0.70 to -0.85	$Cu_3AsS_4 = (Cu_{12}As_4S_2/Cu_6As_4S_9) = 3/2Cu_2S + As^o + 5/2HS^- + 5/2H^+ + 5e^-$
1	-0.65 to -0.40	$3/2Cu_2S + As^o + 5/2HS^- + 5/2H^+ + 5e^- = (Cu_{12}As_4S_2/Cu_6As_4S_9) = Cu_3AsS_4$

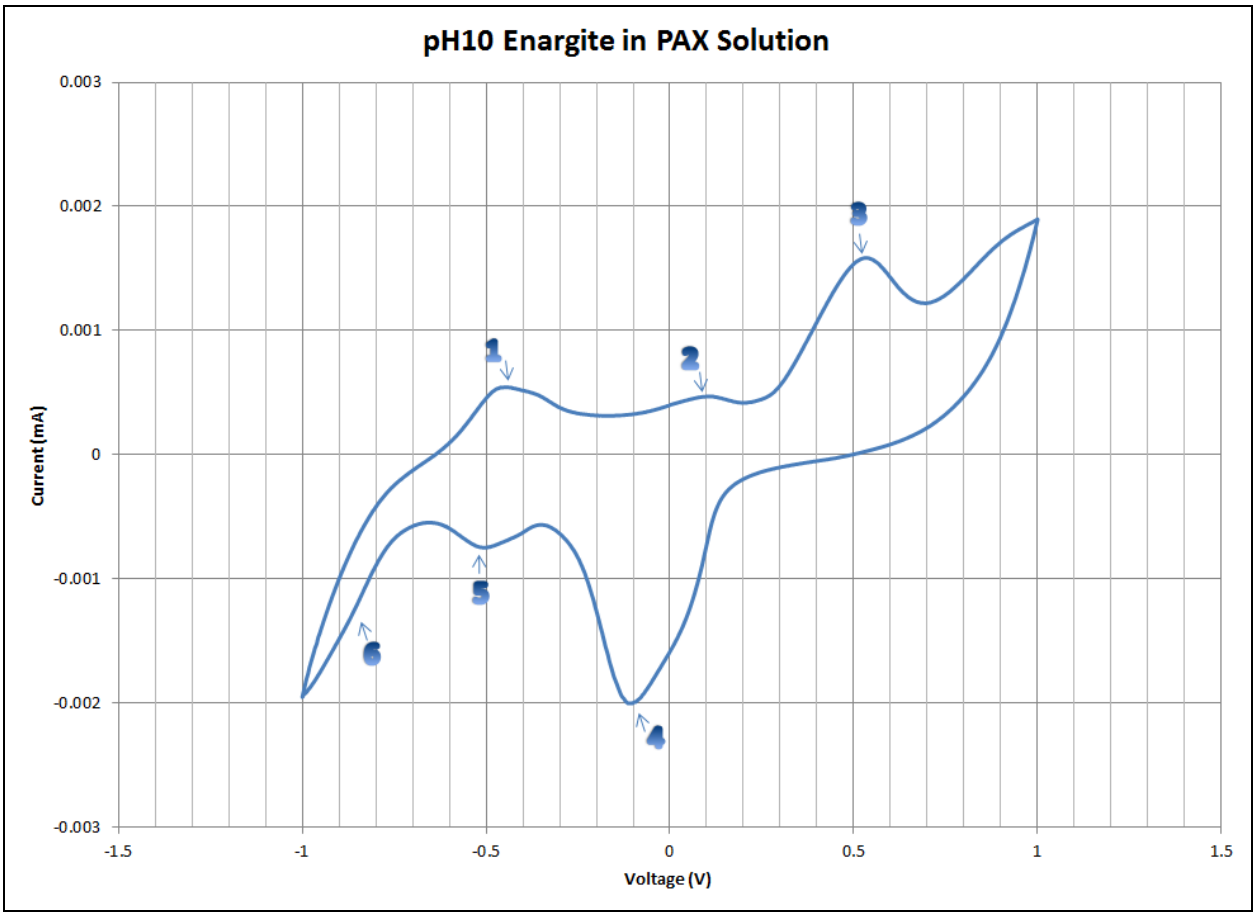

Figure 59: pH 10 Enargite in PAX Voltammagram

Table XLIII: pH 10 Enargite in PAX Reactions

Peak	Eh Value	Reaction
2	-0.07 to 0.15	$Cu_3AsS_4 + X^- + 3H_2O = CuX + 2CuS + HAsO_4^{2-} + 2S^o + 5H^+ + 4e^-$
3	0.21 to 0.66	$CuS + X^- = CuX + S^o + e^-$
4	0.20 to -0.31	$CuX + S^o + e^- = CuS + X^-$
5	-0.31 to -0.61	$CuX + 2CuS + HAsO_4^{2-} + 2S^o + 7H^+ + 6e^- = Cu_3AsS_4 + X^- + 4H_2O$
6	-0.75 to -0.90	$Cu_3AsS_4 = (Cu_{12}As_4S_2/Cu_6As_4S_9) = 3/2Cu_2S + As^o + 5/2HS^- + 5/2H^+ + 5e^-$
1	-0.65 to -0.35	$3/2Cu_2S + As^o + 5/2HS^- + 5/2H^+ + 5e^- = (Cu_{12}As_4S_2/Cu_6As_4S_9) = Cu_3AsS_4$

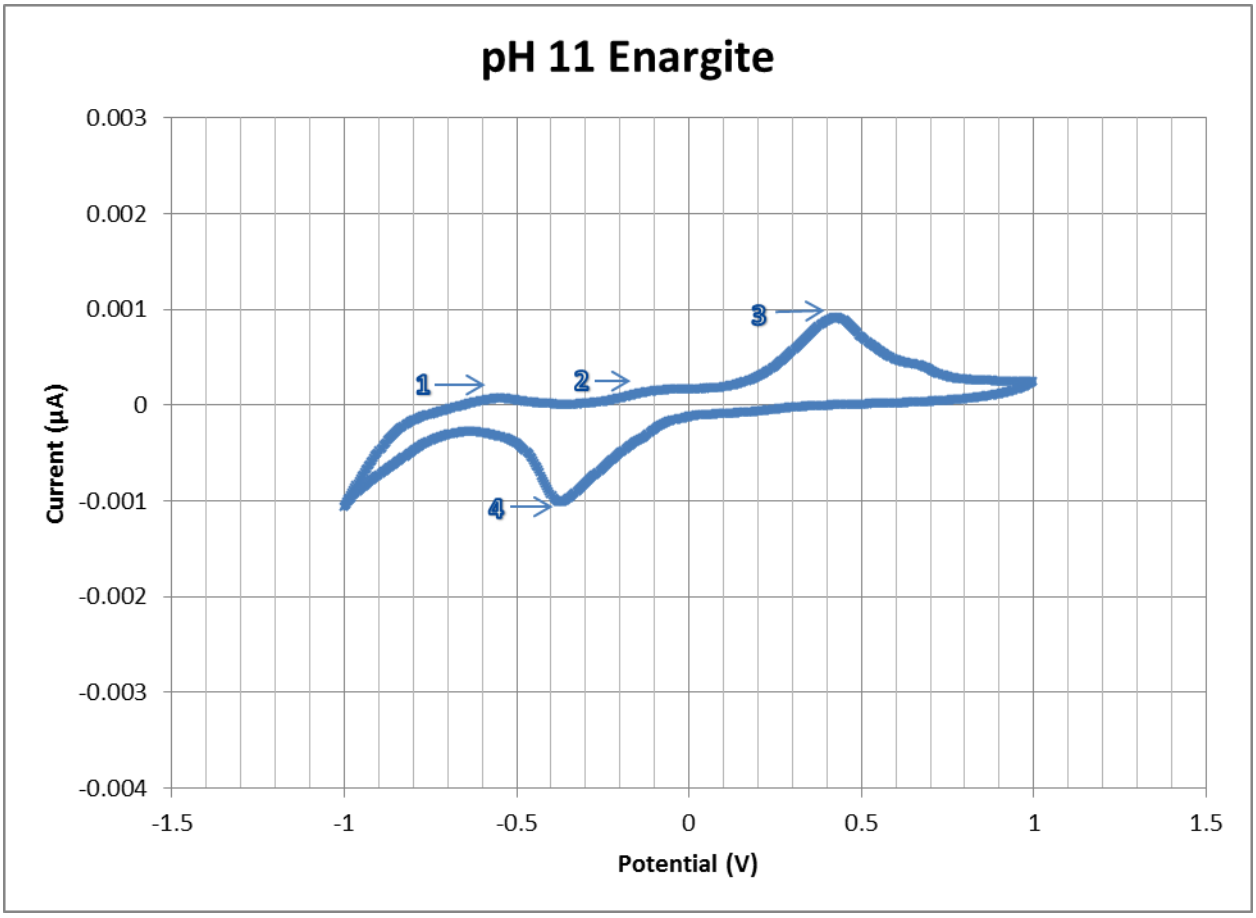

Figure 60: pH 11 Enargite Voltammagram

Table XLIV : pH 11 Enargite Reactions

Peak	E_H Value (V)	Reaction
2	-0.25 to 0.10	$Cu_2S + AsS_4^{3-} + 4H_2O = 2CuS + H_2AsO_4^{2-} + 3S^o + 7H^+ + 2e^-$
3	0.10 to 0.70	$CuS + 2H_2O = Cu(OH)_2 + S^o + 2H^+ + 2e^-$
4	-0.05 to -0.55	$CuS + HAsO_4^{2-} + 4S^o + 9H^+ + Cu(OH)_2 + 10e^- = Cu_2S + AsS_4^{3-} + 6H_2O$ $AsS_4^{3-} + 4H^+ + 5e^- = As^o + 4HS^-$
1	-0.70 to -0.40	$As^o + 4HS^- = AsS_4^{3-} + 4H^+ + 5e^-$

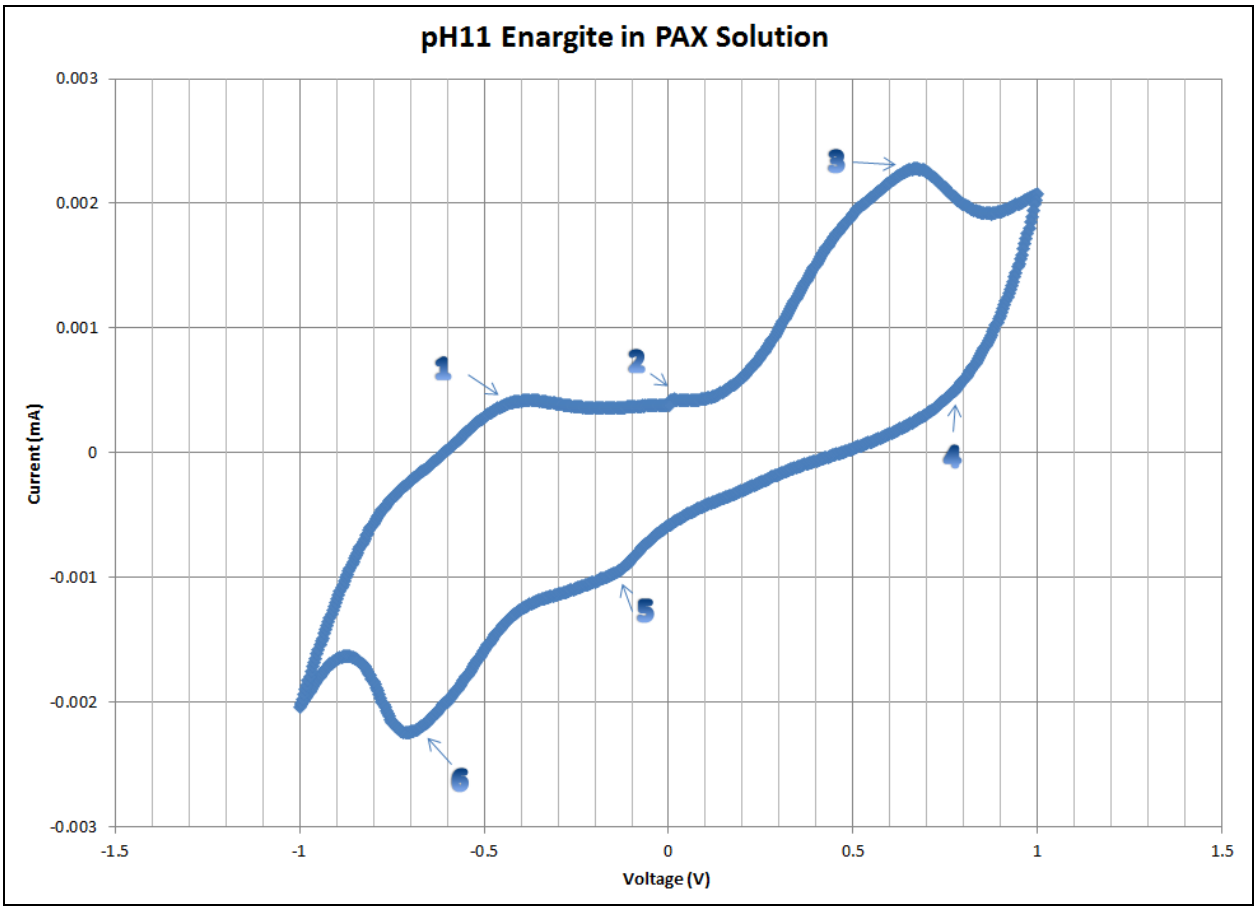

Figure 61: pH 11 Enargite in PAX Voltammagram

Table XLV: pH 11 Enargite in PAX Reactions

Peak	Eh Value	Reaction
2	-0.15 to 0.20	$Cu_2S + AsS_4^{3-} + 2H_2O = 2CuS + HAsO_4^{2-} + S^o + 3H^+ + 4e^-$
3	0.50 to 0.85	$CuS + X^- = CuX + S^o + e^-$
4	0.90 to 0.60	$CuX + 2OH^- = Cu(OH)_2 + X^- + e^-$
5	-0.07 to -0.45	$CuS + HAsO_4^{2-} + 4S^o + Cu(OH)_2 + 5H^+ + 6e^- = Cu_2S + AsS_4^{3-} + 4H_2O + 2OH^-$
6	-0.55 to -0.85	$AsS_4^{3-} + 4H^+ + 5e^- = As^o + 4HS^-$
1	-0.72 to -0.53	$As^o + 4HS^- = AsS_4^{3-} + 4H^+ + 5e^-$

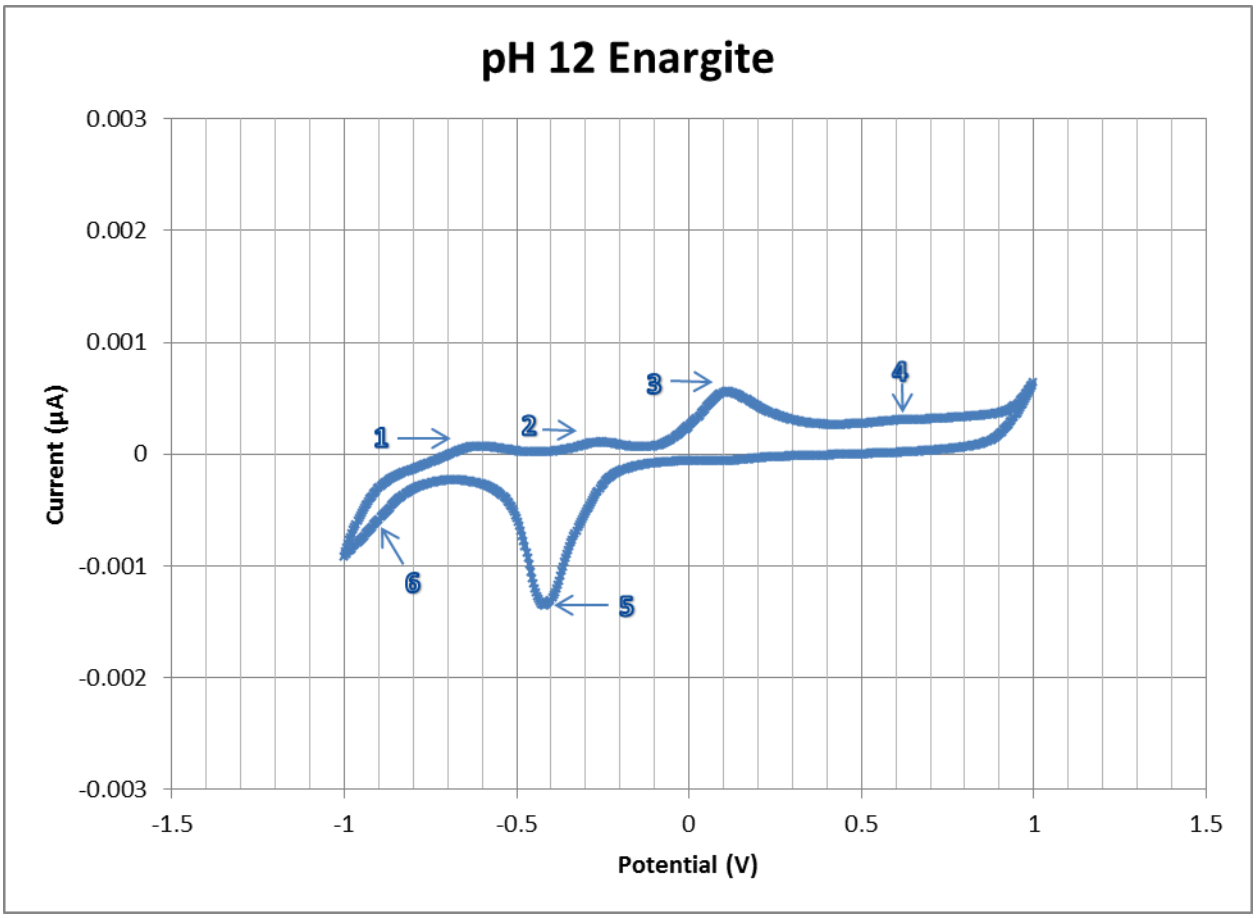

Figure 62: pH 12 Enargite Voltammagram

Table XLVI : pH 12 Enargite

Peak	E_H Value (V)	Reaction
2	-0.38 to -0.15	$Cu_2S + 1/2AsS_4^{3-} + 2H_2O = 2CuS + 1/2AsO_4^{3-} + S^o + 4H^+ + 4e^-$
3	-0.09 to 0.40	$AsS_4^{3-} + 4H_2O = AsO_4^{3-} + 4S^o + 8H^+ + 8e^-$
4	0.55 to 0.64	$CuS + 2H_2O = Cu(OH)_2 + S^o + 2H^+ + 2e^-$
5	-0.19 to -0.69	$CuS + 3/2AsO_4^{3-} + 6S^o + 14H^+ + Cu(OH)_2 + 14e^- = Cu_2S + 3/2AsS_4^{3-} + 8\ H_2O$
6	-0.85 to -0.95	$AsS_4^{3-} + 4H^+ + 5e^- = As^o + 4HS^-$
1	-0.70 to -0.50	$As^o + 4HS^- = AsS_4^{3-} + 4H^+ + 5e^-$

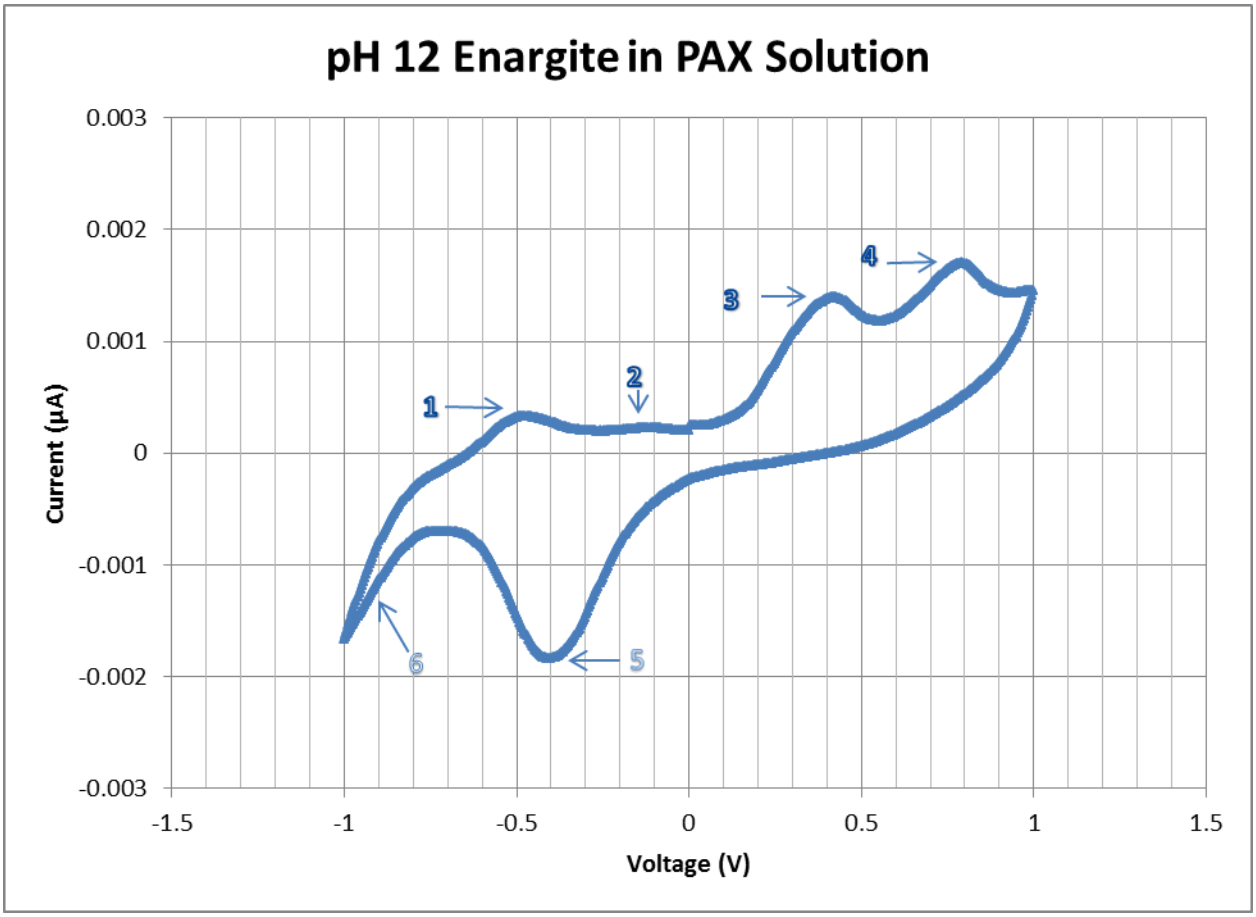

Figure 63: pH 12 Enargite in PAX Voltammagram

Table XLVII: pH 12 Enargite in PAX Reactions

Peak	Eh Value	Reaction
2	-0.21 to 0.00	$Cu_2S + 1/2AsS_4^{3-} + 2H_2O = 2CuS + 1/2AsO_4^{3-} + S^o + 4H^+ + 4e^-$
3	0.15 to 0.56	$CuS + X^- = CuX + S^o + e^-$
4	0.56 to 0.95	$CuX + 2OH^- = Cu(OH)_2 + X^- + e^-$
5	-0.05 to -0.65	$CuS + 1/2AsO_4^{3-} + 2S^o + Cu(OH)_2 + 4H^+ + 6e^- = Cu_2S + 1/2AsS_4^{3-} + 2H_2O + 2OH^-$
6	-0.85 to -0.95	$AsS_4^{3-} + 4H^+ + 5e^- = As^o + 4HS^-$
1	-0.60 to -0.25	$As^o + 4HS^- = AsS_4^{3-} + 4H^+ + 5e^-$

SIGNATURE PAGE

This is to certify that the thesis prepared by Tyler Broden entitled "Electrochemical Characterization of Xanthate Chemisorption on Copper and Enargite" has been examined and approved for acceptance by the Department of Metallurgical and Materials Engineering, Montana Tech of The University of Montana, on this 25th day of April, 2016

Courtney Young, PhD, Professor and Department Head
Department of Metallurgical And Materials Engineering
Chair, Examination Committee

William Gleason, PhD, Associate Professor
Department of Metallurgical And Materials Engineering
Member, Examination Committee

Jerome P. Downey, PhD, Professor
Department of Metallurgical And Materials Engineering
Member, Examination Committee

Rodney James, PhD, Professor Emeritus
Department of Environmental Engineering
Member, Examination Committee